
Non-ground state Bose condensates and spin-coupled compact localised states

Alexander Vivian Hugh McPhail

A thesis submitted in fulfilment of the requirements for the degree of
Doctor of Philosophy in Physics,
The University of Auckland, 2022.

Not Zen Haiku

A golden leaf falls,
a tear streaks down from my eye —
you must seize the day.

Dedication

For

Princess Diana

and

my wahine

Contents

CONTENTS	vii
LIST OF FIGURES	xi
ACRONYMS	xiii
PUBLICATIONS	xix
INTRODUCTION	1
BOSE-EINSTEIN CONDENSATION	3
Bosons and Fermions	3
Bose-Enhanced Growth	4
Condensation	5
Gross-Pitaevski Equation	6
The Miesner growth curve	8
Microscopic Theory	8
Truncated Wigner	11
Thermalisation	12
A BOSE-EINSTEIN CONDENSATE IS A BOSE CONDENSATE IN THE LABORATORY	
FRAME	13
Abstract	13
Introduction	14
Simple Harmonic Oscillator	15
Circular Motion	16
The Many Body Case	17
Quasi-particle Condensates	18

Conclusion	19
PHASE COHERENCE AND COLLECTIVE OSCILLATIONS	21
Introduction	21
The Na ⁺ /K ⁺ Pump	22
Stimulated Bose Hubbard Model	28
Quantum Phase	30
Phase Dependent Gross-Pitaevskii Equation	32
Conclusion	34
THEORY	35
Bose-Einstein Condensates	35
Optical Lattices	37
Spin-Orbit Coupling	39
Flat Bands and Compact Localised States	41
Discrete Model	44
METHODOLOGY	47
Experiment	47
New Apparatus	50
Further Experiments	50
SOC SIMULATIONS	51
Spinor GPE Model	52
Gligorić's Discrete GPE	55
CONCLUSION	59
APPENDICES	63
ELECTROMAGNETIC FIELDS	65
Lorentz Force Law	65
Zeeman Effect	68
Spin and Magnetic Fields	69
Multiple Electromagnetic Potentials	70
ANOMALOUS ZEEMAN EFFECT	71

<i>Contents</i>	ix
Spin-Momentum Hamiltonian	71
Counter-propagating beams	72
Comparison with Masson	77
Wigner-Eckhart Theorem	78
Group Theory	78
WORKS CITED	81

List of Figures

1	Two electron sheaths a distance a apart with an angle θ_{ij} between centre of masses, and distances $z_{i,j}$ from the membrane.	23
2	(a) mutual information of oscillators after initial burn-in, (b) mutual information at end of simulation, (c) time-series of oscillators for end of simulation, (d) position of oscillators at end of simulation.	25
3	Position of an oscillator node.	26
4	Phase portrait of an oscillator node.	27
5	Bose-Hubbard model parameters. See text for an explanation of the symbols. From Jaksch et al. (1998)	29
6	Lattice occupation number over time.	31
7	Phase of two populations of particles in a harmonic potential. The figures on the left are the mean phase and the figures on the right are the standard deviations of the phase. The first row is the standard spinor GPE with no interaction. The middle row shows the phase when the standard non-linear interaction is turned on. The third row shows the phase when phase differences are used.	33
8	A 2D optical lattice with an uneven distribution of atoms. This is the Bose-Einstein condensate (BEC) superfluid phase. From Lewenstein et al. (2007)	37
9	(a) Raman (kick) laser scheme. B_0 is the applied magnetic field, ω_l is the kick laser frequency and $\Delta\omega_l$ is the small detuning to give a momentum transfer. (b) Three-legged level diagram of the ^{87}Rb D2 transition with magnetic sublevels split by an applied magnetic field. Δ is the detuning from resonance, ω_z is the difference in frequency between the two Raman beams, δ is a small detuning. A lambda scheme is obtained when the magnetic field is large enough to induce the anomalous Zeeman effect in which case the $m_F = 1$ state is further separated and adiabatically eliminated. From Brown (2014).	40

10	Dispersion curve showing a flat band in the lowest energy state. From Morsch and Oberthaler (2006)	42
11	Diamond (rhombic) lattice showing different site labels. n is the unit cell. From Gligorić et al. (2016)	45
12	Diamond lattices with compact localised state (CLS)s identified as localised high density states. From Gligorić et al. (2016)	46
13	Scan of Raman detuning	49
14	Spin populations of full spinor spin-orbit coupling (SOC) Hamiltonian. The pump strength, Ω is 4 recoil units, the Zeeman splitting is 5.845 MHz, the radius of the wells is 0.8μ and the separation is $1.5 \mu\text{m}$. The spatial light modulator (SLM) can resolve $0.8 \mu\text{m}$	53
15	Spin populations of full spinor SOC Hamiltonian. The pump strength, Ω is 4 recoil units, the Zeeman splitting is 5.845 MHz, the radius of the wells is 0.8μ and the separation is $1.5 \mu\text{m}$. The SLM can resolve $0.8 \mu\text{m}$	54
16	Left panels show Dirichlet boundary conditions and Right panels show periodic boundary conditions. Top panels are all twenty nodes and bottom panels show the central nodes. Each unit cell has 6 nodes, 3 spin up and 3 spin down. From left to right, the node order is $a^+, a^-, b^+, b^-, c^+, c^-$	56
17	Time series of node 9 for $\lambda = 10$	57

Acronyms

BEC	Bose-Einstein condensate. xi , 7 , 35 , 37–39 , 42 , 44 , 46–48 , 50
BZ	Brillioun zone. 41 , 43
CLS	compact localised state. xii , 41 , 44 , 46 , 48 , 53–55 , 61 , 62
DMD	digital micro-mirror device. 49
FB	flat band. 41 , 43 , 44
GPE	Gross-Pitaevskii equation. 7 , 9 , 28 , 43 , 45
MOT	magneto-optical trap. 36 , 47 , 50
SLM	spatial light modulator. xii , 47–49 , 52–54
SOC	spin-orbit coupling. xii , 38 , 39 , 43 , 44 , 46–48 , 50–55
TOF	time of flight. 47

Acknowledgements

The idea to study flat band modes and compact localised states in 2D lattices of BECs was my supervisor's, Maarten Hoogerland.

Dylan has answered many questions about apparatus and theory and is good at diagnosing my apparatus failures and helping with fixes. Sam answered many questions about experiments, checked adapter plate design, and collaborated with me to get the new lab computer up and running. Thomas answered many questions about apparatus, helped with setting up experiments and the set up of the ultra high vacuum. Maarten is a good supervisor, helped in the lab when things went wrong, and provided good suggestions.

Gray Hunter wound Helmholtz coils. Ofri Adiv helped with experimental setup and conversed about room temperature BECs, topology, and spin statistics. Dominik Vogt was always willing to talk and was always helpful. Leo and I had interesting discussions, not necessarily about physics. Aonghas and I had chats about experimental physics and meditation. Mohammad Saghedi has always been a friendly face and I would like to thank Ira Mautner for countless conversations about physics and the state of the world. Joshua and Carey were always good to talk to, sometimes about consciousness and peace, sometimes about the rest of physics.

I would like to thank my co-supervisor, Scott Parkins, Howard Carmichael and the Quantum Optics group, Malcolm Grimson and Matthew Collett, Mark Conway, and Anna Yang, The research proposal committee, Nicola Gaston, Gilles Bellon, and Howard Carmichael, David, Brody and the technical Staff, the TA/GTA community and organisers, especially Anna Yang and Peter Wills, not just for teaching about *ako*, the professional staff, Maria, Sithra, Gen, Jeanette, Sue, the Heads of Department, Richard Easter and Jan Eldridge, the Proctor, Gillian Lewis, and Jemma Overmire.

The Dodd-Walls Centre for Photonic and Quantum Technologies and the University of Auckland for PhD Scholarships and Extensions.

The author(s) wish to acknowledge the use of New Zealand eScience Infrastructure (NeSI) high performance computing facilities, consulting support and/or training services

as part of this research. New Zealand's national facilities are provided by NeSI and funded jointly by NeSI's collaborator institutions and through the Ministry of Business, Innovation & Employment's Research Infrastructure programme. URL <https://www.nesi.org.nz>.

Brian Walsh, for over a decade of fortnightly dinners, over which we discussed philosophy, politics, and occasionally quantum mechanics. Also for the occasional financial contribution. My father, Hugh McPhail, for helping his son with finances throughout.

Know thyself.

Alexander Vivian Hugh McPhail

2022

Co-Authorship Form

This form is to accompany the submission of any PhD that contains published or unpublished co-authored work. **Please include one copy of this form for each co-authored work.** Completed forms should be included in all copies of your thesis submitted for examination and library deposit (including digital deposit), following your thesis Acknowledgements. Co-authored works may be included in a thesis if the candidate has written all or the majority of the text and had their contribution confirmed by all co-authors as not less than 65%.

Please indicate the chapter/section/pages of this thesis that are extracted from a co-authored work and give the title and publication details or details of submission of the co-authored work.		
Chapter: "A Bose-Einstein condensate is a Bose condensate in the laboratory ground state."		
Appears in Proceedings of the Royal Society A, doi: 10.1098/rspa.2021.0465		
Nature of contribution by PhD candidate	Wrote paper	
Extent of contribution by PhD candidate (%)	80	

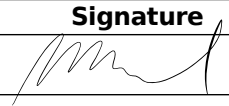
CO-AUTHORS

Name	Nature of Contribution
Maarten Dirk Hoogerland	Supervised, requested treatment of circular motion, edited

Certification by Co-Authors

The undersigned hereby certify that:

- ❖ the above statement correctly reflects the nature and extent of the PhD candidate's contribution to this work, and the nature of the contribution of each of the co-authors; and
- ❖ that the candidate wrote all or the majority of the text.

Name	Signature	Date
Maarten Dirk Hoogerland		

Publications

Brown, D. J., McPhail, A. V. H., White, D. H., Baillie, D., Ruddell, S. K., and Hoogerland, M. D. (2018). “Thermalization, condensate growth, and defect formation in an out-of-equilibrium Bose gas”. In: *Physical Review A* 98 (1), pp. 1–6. ISSN: 24699934. DOI: [10.1103/PhysRevA.98.013606](https://doi.org/10.1103/PhysRevA.98.013606)

McPhail, A. V. H. and Hoogerland, M. D. (Oct. 2021). “A Bose–Einstein condensate is a Bose condensate in the laboratory ground state”. In: *Proceedings of the Royal Society A: Mathematical, Physical and Engineering Sciences* 477 (2254). ISSN: 1364-5021. DOI: [10.1098/rspa.2021.0465](https://doi.org/10.1098/rspa.2021.0465). URL: <https://royalsocietypublishing.org/doi/abs/10.1098/rspa.2021.0465>

Abstract

Condensation is the phenomenon by which quantum particles near in phase space share a wavefunction and become a so-called mesoscopic quantum entity. We use experimental evidence we published to support our argument that condensates form through bosonic stimulation and can occur at non-ground state energies and at room temperature. We discuss the notion of phase coherence and collective oscillations, providing the Na^+/K^+ pump as a candidate mechanism for longitudinal collective modes as described by Fröhlich (1968b). We introduce the stimulated Bose-Hubbard model to account for number and phase dependencies in lattice models. We discuss an experimental test of Gligorić et al. (2016) that predicts the onset of compact localised states through engineered flat band modes. Compact localised states may well be useful in the manipulation of quantum state in quantum simulators. We mention a hypothesis that consciousness is related to condensation.

Introduction

#1

*My mind a still lake,
surface reflects sky and land —
breathing, what am I?*

The phenomenon of condensation was first introduced into the Western canon by Albert Einstein in 1925 (Einstein, [1925b](#)). Bose-Einstein condensation has been described as a situation in which multiple particles share a collective wave function, as formalised by Gross and Pitaevskii (Pitaevskii and Stringari, [2003](#)). Experimental evidence was achieved in 1995 by two groups, those of Cornell and Ketterle (M. H. Anderson et al., [1995a](#); K. B. Davis et al., [1995](#)). Since then, this mesoscopic quantum phenomenon has been found to be a versatile workbench for examination of quantum coherent dynamics (Ueda, [2010](#)). A similar non-linear equation is used in the field of optics, especially the examination of Kerr non-linearities and solitons, and analogies exist (New, [2011](#)).

Descartes ([1641](#)) proved mental existence, but separated it from the physical. Galen Strawson has argued for the mental reality of conscious experience (Strawson, [2010](#)). A proposal was put forward by Adam Cairns-Smith that in some way consciousness relies on quantum phenomena and Bose-Einstein condensates might be a phenomenon that can explain the gestalt (Cairns-Smith, [1998](#)). Immediate opposition to this hypothesis arose with the rejoinder that these phenomena only occur at ultracold temperatures, as asserted by Einstein. This is related to the general argument that quantum effects cannot occur at biological temperatures because of rapid phase decoherence brought about by environmental noise (McFadden and Al-Khalili, [2018](#)). Fröhlich ([1968b](#)) suggested a mechanism for condensation in biological systems but his candidate dipole oscillator, hydrogen bonds in carbon chains, requires energies in the microwave range, the energy of a photon for which is about 1 meV and does not seem to be able to be naturally generated. I have suggested a

different dipole oscillator, the transmembrane Na^+/K^+ pump, which I use to demonstrate phase synchronisation (McPhail, 2009).

This thesis arose from a desire to become further acquainted with the experimental and theoretical aspects of Bose-Einstein condensation as realised with ultracold Rubidium atoms in the same laboratory in which I had conducted dissertation research on Bragg diffracted condensates in a harmonic trap. My first goal was to gather more data for our thermalisation experiments (Brown et al., 2018) and then test a particular hypothesis about spin-orbit coupling and compact localised states (Gligorić et al., 2016). After the interference brought about by catastrophic equipment failure and the pandemic, the decision was made to abandon the experiment and concentrate on testing the hypothesis with simulations. The theory was that particular quasi-one-dimensional lattices, with the aid of spin dependent linear momentum, would give rise to a clumped and uneven distribution of atoms. Wanting to test whether a lateral force could arise from counter-propagating laser beams, I used a full spinor Gross-Pitaevskii simulation.

In this work, I bring together a brief theoretical development of condensation, prove that condensates can exist above the laboratory ground state and at room temperature, find phase coherence in a simulation of my dipole oscillator model, introduce the Stimulated Bose Hubbard model and a putative mechanism behind phase coherence, describe the intended experimental procedure and a new apparatus with greater optical access, and report the results of evaluating our intended test of Gligorić's hypothesis ¹.

¹all code can be accessed at <https://github.com/amcphail/phd>

Bose-Einstein Condensation

New Zealand

*Sunrise, sunset beach,
birthing, reviving — that's it.
Don't covet your zen.*

Bosons and Fermions

In quantum mechanics, particles are held to be identical and indistinguishable. Also, particles can have either half integer or integer spin. When we swap particles, $\mathbf{r}_1, \mathbf{r}_2$, in a two-particle system, $\Psi(\mathbf{r}_1, \mathbf{r}_2)$, the corresponding probability density, $|\Psi|^2$, should not change.

$$|\Psi(\mathbf{r}_1, \mathbf{r}_2)|^2 = |\Psi(\mathbf{r}_2, \mathbf{r}_1)|^2 \quad (2.1)$$

This can be achieved in two ways. The symmetric case, for integer spin particles, bosons,

$$\Psi(\mathbf{r}_1, \mathbf{r}_2) = \Psi(\mathbf{r}_2, \mathbf{r}_1), \quad (2.2)$$

and the antisymmetric case, for half-integer spin particles, fermions,

$$\Psi(\mathbf{r}_1, \mathbf{r}_2) = -\Psi(\mathbf{r}_2, \mathbf{r}_1). \quad (2.3)$$

The reason that fermions are antisymmetric and that bosons are symmetric under particle exchange is shown by the spin statistics theorem. In a Lorentzian treatment of spin statistics, integer-spin wave-functions transform in space-time as a tensor of odd-rank, and thus act as bosons, while half-integer-spin wave-functions transform as a tensor of even-rank, and thus satisfy the exclusion principle (Pauli, 1940). The formal requirement for a Lorentz transform is that there be an upper-bound on the speed with which a particle

can move to an adjacent point in space. If we consider time as the ordering of arrangements of matter and energy in space, and ignore the observer-centric premise of relativity, then we can look at the spinful particle propagator as having a finite range and every step the wave-function transforms, the odd and even rank tensors transform differently. A half-integer spin particle requires a $2 \cdot 2\pi$ rotation to return to its original state, whereas an integer spin particle requires a single 2π rotation.

If we solve the Schrödinger equation for a wave-function $\Phi(\mathbf{r}_1, \mathbf{r}_2)$ where the \mathbf{r}_i represent position and spin, in quantum mechanics, particles are treated as indistinguishable, we need to write a linear combination, or superposition, of candidate solutions, Φ_i

$$\Psi(\mathbf{r}_1, \mathbf{r}_2) = \frac{1}{\sqrt{2}} [\Phi(\mathbf{r}_1, \mathbf{r}_2) \pm \Phi(\mathbf{r}_2, \mathbf{r}_1)], \quad (2.4)$$

where the $+$ and $-$ are for bosons and fermions, respectively.

The joint probability of finding two particles at \mathbf{r}_1 and \mathbf{r}_2 is

$$|\Psi(\mathbf{r}_1, \mathbf{r}_2)|^2 = \frac{1}{2} \{ |\Phi(\mathbf{r}_1, \mathbf{r}_2)|^2 + |\Phi(\mathbf{r}_2, \mathbf{r}_1)|^2 \pm 2\Re[\Phi^*(\mathbf{r}_1, \mathbf{r}_2)\Phi(\mathbf{r}_2, \mathbf{r}_1)] \}. \quad (2.5)$$

The interference term, the \Re part, implies that the probability of finding two identical bosons at the same coordinate, $|\Psi(\mathbf{r}, \mathbf{r})|^2$, is twice that of $|\Phi(\mathbf{r}, \mathbf{r})|^2$, which is the corresponding probability for distinguishable particles. When the number of bosons, N , is large, the joint probability for finding all bosons in the same state is $N!$ larger than the distinguishable case. This is as a result of the number of possible permutations in the interference term. The constructive interference in this term only becomes significant when the wave-packets of the bosons overlap each other, which occurs when the de Broglie wavelength, λ_{DB} , approaches the interparticle spacing (see below). This is the quantum degeneracy condition. For fermions, the right hand side goes to zero, which shows that no two fermions can occupy exactly the same quantum state, the Pauli exclusion principle. Bosons do not obey this principle, and can aggregate in the same state (Ueda, 2010).

Bose-Enhanced Growth

Here we derive the basic mechanism for bosonic stimulation¹.

¹This treatment was provided by Professor John Close of the Australian National University at the Australian and New Zealand Summer School for Ultracold Physics at the University of Otago in 2019.

Target state empty For one possible state, we take the initial state, $|i\rangle = |S\rangle_1$, to be empty and the final state, $|f\rangle = |T\rangle_1$, to contain one boson. Then the Hamiltonian is

$$\hat{\mathcal{H}} = \alpha |i\rangle \langle f| + \text{h.c.} = \alpha |S\rangle_1 \langle T|_1 + \text{h.c.} \quad (2.6)$$

So the scattering rate is $|\langle i|\hat{\mathcal{H}}|f\rangle|^2 = \alpha^2$.

Target state contains one boson For two possible states, we take the initial state, $|i\rangle = \frac{1}{\sqrt{2}}[|S\rangle_1|T\rangle_2 + |T\rangle_1|S\rangle_2]$, a superposition, and the final state, $|f\rangle = |T\rangle_1|T\rangle_2$.

Then the Hamiltonian is

$$\hat{\mathcal{H}} = \alpha |i\rangle \langle f| + \text{h.c.} = \alpha |S\rangle_1 \langle T|_1 + \alpha |S\rangle_2 \langle T|_2 + \text{h.c.} \quad (2.7)$$

So the scattering rate is $2\alpha^2$ and in general the scattering rate is enhanced by $N+1$. This follows directly from the number of possible permutations of indistinguishable particles in the interference term, as mentioned above.

Condensation

Bose (1924) was thinking about the ultraviolet catastrophe, in which the classical theory of black-body radiation at thermal equilibrium predicted that the energy emitted would increase as frequency of the electromagnetic radiation increased, implying that a black-body would lose all its energy, when he found a distribution for the statistics of the spin 1 photon, a boson. He derived the expression for the occupancy expectation, \bar{n}_i of an energy state, i , as

$$\bar{n}_i = \frac{g_i}{e^{\epsilon_i/k_b T} - 1}, \quad (2.8)$$

where n_i is the number of particles in state i , g_i is the degeneracy of energy level i , ϵ_i is the energy of state i , k_b is Boltzmann's constant, and T is absolute temperature.

Bose sent his treatment to Einstein, who translated the work into German. The following year, Einstein contributed two papers to this field. One extended the treatment to interacting bosons

$$\bar{n}_i = \frac{g_i}{e^{(\epsilon_i - \mu)/k_b T} - 1}, \quad (2.9)$$

where μ is the chemical potential, the energy required to add one more particle to the system (Einstein, 1925a). This expression can be derived combinatorially from the grand

canonical ensemble without any approximations. The treatment allows exchange of energy and particles with a reservoir. Non-interacting photons do not have a chemical potential and disappear at absolute zero, but other bosons do interact, thus the need for μ . There is the condition that $\epsilon_i > \mu$, as negative particle numbers are forbidden.

In the other paper, Einstein (1925b) showed that below a critical temperature an ensemble of bosons will condense into the macroscopically occupied ground state². This is a quantum mechanical phase transition that occurs when the phase space density, $n\lambda_{DB}^3$, reaches a critical value, a density of approximately $n^{-1/3}$. Here $n = N/V$ is the density, where N is the particle number, and V is the volume. λ_{DB} is the de Broglie wavelength, defined as

$$\lambda_{DB} = \frac{h}{\sqrt{2\pi m k_B T}}, \quad (2.10)$$

where h is Planck's constant, m is the particle mass, k_B is Boltzmann's constant, and T absolute temperature. The critical temperature, T_c can be calculated as

$$T_c = \frac{2\pi}{[\zeta(3/2)]^{2/3}} \frac{\hbar^2}{m} \left(\frac{N}{V}\right)^{2/3}, \quad (2.11)$$

where ζ is the Riemann zeta function, and \hbar is the reduced Planck's constant. The condensed fraction can be calculated as

$$\frac{N_0}{N} = 1 - \left(\frac{T}{T_c}\right)^{3/2}. \quad (2.12)$$

The above quantities can be used to derive various properties of a condensed system (Ueda, 2010).

Gross-Pitaevski Equation

The effective interaction of two particles at low energies is generally limited to s -wave scattering, for which the interaction can be treated as a contact interaction

$$U(\mathbf{r}_i, \mathbf{r}_j) = U_0 \delta(\mathbf{r}_i - \mathbf{r}_j) = \frac{4\pi \hbar^2 a_s}{m} \delta(\mathbf{r}_i - \mathbf{r}_j), \quad (2.13)$$

²It is possible that his reasoning that led to the macroscopic occupation of the ground state was as a result of considering temperature and the degeneracy of energy levels. However, there is also the phenomenon of bosonic stimulation, as discussed above.

where a_s is the s -wave scattering length. Starting with an effective Hamiltonian

$$H = \sum_{i=1}^N \left[\frac{\mathbf{p}_i^2}{2m} + V_{ext}(\mathbf{r}_i) \right] + U_0 \sum_{i<j} \delta(\mathbf{r}_i - \mathbf{r}_j) \quad (2.14)$$

and using a Hartree mean-field approximation, a variational technique, and the method of Lagrange multipliers, we can derive the [Gross-Pitaevskii equation \(GPE\)](#)

$$\left[-\frac{\hbar^2}{2m} \nabla^2 + V_{ext}(\mathbf{r}) + U_0 |\psi(\mathbf{r})|^2 \right] \psi(\mathbf{r}) = \mu \psi(\mathbf{r}), \quad (2.15)$$

where μ is the chemical potential (Pethick and H. Smith, [2008](#)).

We require the normalisation condition

$$\int d\mathbf{r} |\psi(\mathbf{r})|^2 = N, \quad (2.16)$$

where N is the total particle number.

Pitaevskii and Stringari ([2003](#)) divide the wave-function into a condensate fraction, $\phi_0(\mathbf{r})$, and the remaining thermal fractions, $\phi_i(\mathbf{r})$, so that our overall wave-function is

$$\begin{aligned} \psi(\mathbf{r}) &= \phi_0(\mathbf{r}) + \sum_i \phi_i(\mathbf{r}) \\ &= \phi_0(\mathbf{r}) + \delta\phi(\mathbf{r}). \end{aligned}$$

At low temperatures and densities, they ignore the fluctuation term, $\delta\phi(\mathbf{r})$, and treat the condensate as a classical field, $\phi_0(\mathbf{r})$. This treatment assumes that the condensate will always occur in the zero-kinetic energy ground state, which we have shown to be a bad assumption³.

When the [BEC](#) particle number is sufficiently large and at low temperatures, the kinetic energy term in the Hamiltonian can be ignored and we have the Thomas-Fermi approximation, the solution of which is

$$|\psi(\mathbf{r})|^2 = \frac{\mu - V_{ext}(\mathbf{r})}{U_0}. \quad (2.17)$$

Note that $|\psi(\mathbf{r})|^2 = n(\mathbf{r})$, the probability density. The [BEC](#) will acquire the shape of the containing potential, thus, when the trap is harmonic, the density profile of the condensate will have an inverted parabolic shape and will have an accompanying thermal

³see Chapter [3](#)

cloud (Pethick and H. Smith, 2008). The temperature of the condensate can be measured by fitting a bosonic Gaussian to the thermal wings of a time-of-flight density map of the condensate (Ketterle, Durfee, and D. Stamper-Kurn, 1999).

The Miesner growth curve

Because of bosonic stimulation, a condensate fraction with initial particle number $N_{0,i}$, seeded by random fluctuations, will grow exponentially

$$\dot{N}_0 = \gamma N_0 \quad (2.18)$$

where γ is the initial growth rate. Since there are only a finite number of particles, the final condensate will reach the population carrying capacity, $N_{0,\text{eq}}$, which is modelled by the equation

$$\dot{N}_0 = \gamma N_0 \left[1 - \left(\frac{N_0}{N_{0,\text{eq}}} \right) \right]. \quad (2.19)$$

Gardiner, Zoller, et al. (1997) derive a master equation from quantum kinetic theory and find an exponential term, δ , in the differential equation which reflects the equilibration of the chemical potential between the condensate and surrounding thermal cloud. This treatment was used by Miesner (1998) to derive a growth curve that fit their experiment,

$$\dot{N}_0 = \gamma N_0 \left[1 - \left(\frac{N_0}{N_{0,\text{eq}}} \right)^\delta \right], \quad (2.20)$$

with solution

$$N(t) = N_{0,i} e^{\gamma t} \left[1 + \left(\frac{N_{0,i}}{N_{0,\text{eq}}} \right)^\delta (e^{\delta \gamma t} - 1) \right]^{-1/\delta}, \quad (2.21)$$

Where $N_{0,i}$ is the initial condensate size and δ was fixed to 2/5 in line with the quantum kinetic theory.

Microscopic Theory

Starting with Equation 2.14, we convert to using field operators for bosons, $\hat{\psi}^\dagger(\mathbf{r})$ and $\hat{\psi}(\mathbf{r})$,

$$\hat{H} = \int d\mathbf{r} \left[-\hat{\psi}^\dagger(\mathbf{r}) \frac{\hbar^2}{2m} \nabla^2 \hat{\psi}(\mathbf{r}) + V_{\text{ext}}(\mathbf{r}) \hat{\psi}^\dagger(\mathbf{r}) \hat{\psi}(\mathbf{r}) + \frac{U_0}{2} \hat{\psi}^\dagger(\mathbf{r}) \hat{\psi}^\dagger(\mathbf{r}) \hat{\psi}(\mathbf{r}) \hat{\psi}(\mathbf{r}) \right], \quad (2.22)$$

where the creation and annihilation operators satisfy the canonical commutation relations

$$\left[\hat{\psi}(\mathbf{r}), \hat{\psi}^\dagger(\mathbf{r}')\right] = \delta(\mathbf{r} - \mathbf{r}'), \left[\hat{\psi}(\mathbf{r}), \hat{\psi}(\mathbf{r}')\right] = 0, \left[\hat{\psi}^\dagger(\mathbf{r}), \hat{\psi}^\dagger(\mathbf{r}')\right] = 0. \quad (2.23)$$

We can substitute the Fourier expansion of the field operator

$$\hat{\psi}(\mathbf{r}) = \frac{1}{\sqrt{V}} \sum_{\mathbf{k}} \hat{a}_{\mathbf{k}} e^{i\mathbf{k}\mathbf{r}}, \quad (2.24)$$

where V is the volume of the system.

If we consider a uniform Bose gas, where the potential, V_{ext} , is zero, then we arrive at the Hamiltonian

$$\hat{H} = \sum_{\mathbf{k}} \epsilon_{\mathbf{k}}^0 \hat{a}_{\mathbf{k}}^\dagger \hat{a}_{\mathbf{k}} + \frac{U_0}{2V} \sum_{\mathbf{k}, \mathbf{k}', \mathbf{k}''} \hat{a}_{\mathbf{k}+\mathbf{k}'}^\dagger \hat{a}_{\mathbf{k}'-\mathbf{k}''}^\dagger \hat{a}_{\mathbf{k}'} \hat{a}_{\mathbf{k}}, \quad (2.25)$$

where $\epsilon_{\mathbf{k}}^0 = p^2/2m$. The bosonic creation and annihilation operators satisfy the commutation relations

$$\left[\hat{a}_{\mathbf{k}}, \hat{a}_{\mathbf{k}'}^\dagger\right] = \delta_{\mathbf{k}, \mathbf{k}'}, \left[\hat{a}_{\mathbf{k}}, \hat{a}_{\mathbf{k}'}\right] = 0, \left[\hat{a}_{\mathbf{k}}^\dagger, \hat{a}_{\mathbf{k}'}^\dagger\right] = 0. \quad (2.26)$$

If we consider the fluctuations, $\delta\phi(\mathbf{r})$, are small, and retain only terms which have at least two powers of $\psi(\mathbf{r})$ and $\psi^*(\mathbf{r})$, we reach the Bogoliubov approximation. The fluctuations represent occupation of modes that are not the classical field of the [GPE](#) and in this approximation represent quasi-particles of equal and opposite momenta. This approximation only includes two-body interactions, which is the reason for omitting higher-order terms.

$$\hat{H} = \frac{N_0^2 U_0}{2V} + \sum_{\mathbf{k}, \mathbf{k} \neq 0} (\epsilon_{\mathbf{k}}^0 + n_0 U_0) \hat{a}_{\mathbf{k}}^\dagger \hat{a}_{\mathbf{k}} + \frac{n_0 U_0}{2} \sum_{\mathbf{k}, \mathbf{k} \neq 0} (\hat{a}_{\mathbf{k}}^\dagger \hat{a}_{-\mathbf{k}}^\dagger + \hat{a}_{\mathbf{k}} \hat{a}_{-\mathbf{k}}), \quad (2.27)$$

where $n_0 = N_0/V$, the density of particles in the zero-momentum state. We can recast the Hamiltonian to reflect its simple structure of a sum of independent terms

$$\hat{h} = \epsilon_0 (\hat{a}^\dagger \hat{a} + \hat{b}^\dagger \hat{b}) + \epsilon_1 (\hat{a}^\dagger \hat{b}^\dagger + \hat{b} \hat{a}), \quad (2.28)$$

where ϵ_i are c -numbers and the \hat{a} bosonic operators act on the state with momentum \mathbf{k} and the \hat{b} bosonic operators act on the state with momentum $-\mathbf{k}$. This Hamiltonian can be solved for its eigenvectors and eigenvalues using a Bogoliubov transformation. Simply,

we introduce operators $\hat{\alpha}$ and $\hat{\beta}$ such that the Hamiltonian only has terms proportional to $\hat{\alpha}^\dagger \hat{\alpha}$ and $\hat{\beta}^\dagger \hat{\beta}$. The new operators satisfy the transformation

$$\hat{\alpha} = u\hat{a} + v\hat{b}^\dagger, \hat{\beta} = u\hat{b} + v\hat{a}^\dagger, \quad (2.29)$$

with bosonic commutation relations

$$[\hat{\alpha}, \hat{\alpha}^\dagger] = [\hat{\beta}, \hat{\beta}^\dagger] = 1, [\hat{\alpha}, \hat{\beta}^\dagger] = [\hat{\beta}, \hat{\alpha}^\dagger] = [\hat{\alpha}, \hat{\beta}] = [\hat{\alpha}^\dagger, \hat{\beta}^\dagger] = 0. \quad (2.30)$$

We can take u and v to be real because their phases are arbitrary, also we find that

$$u^2 = v^2 = 1 \quad (2.31)$$

from the transformation and the commutation relations. We then find that

$$u = \cosh t, v = \sinh t \quad (2.32)$$

and, with

$$\epsilon = \sqrt{\epsilon_0^2 - \epsilon_1^2} \quad (2.33)$$

we arrive at the Hamiltonian

$$\hat{h} = \epsilon(\hat{\alpha}^\dagger \hat{\alpha} + \hat{\beta}^\dagger \hat{\beta}) + \epsilon - \epsilon_0, \quad (2.34)$$

in which two kinds of quasi-particle bosons can be created and destroyed (Pethick and H. Smith, 2008).

Reintroducing momentum indexes, where $\hat{a} \rightarrow \hat{a}_{\mathbf{k}}$, $\hat{b} \rightarrow \hat{a}_{-\mathbf{k}}$, $\hat{\alpha} \rightarrow \hat{\alpha}_{\mathbf{k}}$, and $\hat{\beta} \rightarrow \hat{\alpha}_{-\mathbf{k}}$, we arrive at the Hamiltonian

$$\hat{H} = \frac{N^2 U_0}{2W} + \sum_{\mathbf{k}, \mathbf{k} \neq 0} \epsilon_{\mathbf{k}} \hat{\alpha}_{\mathbf{k}}^\dagger \hat{\alpha}_{\mathbf{k}} - \frac{1}{2} \sum_{\mathbf{k}, \mathbf{k} \neq 0} (\epsilon_{\mathbf{k}}^0 + n_0 U_0 - \epsilon_{\mathbf{k}}) \quad (2.35)$$

with

$$\epsilon_{\mathbf{k}} = \sqrt{(\epsilon_{\mathbf{k}}^0)^2 + 2\epsilon_{\mathbf{k}}^0 n_0 U_0}. \quad (2.36)$$

The operators given by

$$\hat{\alpha}_{\mathbf{k}}^\dagger = u_{\mathbf{k}} \hat{a}_{\mathbf{k}}^\dagger + v_{\mathbf{k}} \hat{a}_{-\mathbf{k}} \quad (2.37)$$

create and destroy elementary excitations. Thus the system acts as a collection of non-interacting bosons in which there can be quasi-particle excitations. The velocity of these quasi-particle excitations is the speed of sound in the condensate. Up until this point we have treated the condensate as occupying the ground state of the system, with the introduction of quasi-particles as perturbations to this ground state.

Truncated Wigner

What is not included in any of the previous treatments is the notion of quantum noise. These can be fluctuations in the vacuum at the outset of an experiment and there may be noise during the evolution of the system. Using a technique from quantum optics, we can express noise in a multimode expansion using a Truncated Wigner function. The Wigner function is an example of a quasi-distribution function in phase space. A quasi-distribution function is unlike a probability distribution in that it can have negative values at some points. These negative regions are associated with the notions of superposition and entanglement, and thus any analysis which assumes the Wigner function is positive, as is normally assumed, will leave these quantum mechanical properties out. By sampling the Wigner function for initial conditions and then evolving the system deterministically, the Truncated Wigner approach mimics experimental noise by including it in the initial conditions, half a quantum of energy in each mode.

In the Truncated Wigner derivation, we start with a master equation and map onto a system of stochastic partial differential equations, Fokker-Planck-like equations. A mapping is derived from combinations of density matrix and annihilation and creation operators to expressions which are functions of the c-numbers that the SPDEs evolve. We cut off many-body interactions and limit ourselves to terms quadratic in interaction, which prevents infinite squeezing (Steel et al., 1998). The Truncated Wigner treatment starts by not assuming the coherent state as the ground-state, but instead uses the Hamiltonian

$$\hat{H} = K + \frac{\alpha}{2} P^2 + \sum_j E_j \hat{b}_j^\dagger \hat{b}_j, \quad (2.38)$$

where K is a constant, \hat{b}_j is the annihilation for the quasiparticle excitation of energy E_j , and the mean-field satisfies the GPE. This is a Bogoliubov Hamiltonian.

The Truncated Wigner approximation includes a greater number of modes than merely the condensate ground state, which was the omitted $\delta\phi(\mathbf{r})$ term in the GPE. In most of the literature, these additional terms are viewed as modes in which there are a particular

number of quasi-particle excitations, slightly increasing the energy of the mode, and thus requiring an extension to the GPE, but not significantly altering the premise that BECs occur in the zero-kinetic energy state.

Thermalisation

With the Truncated Wigner approximation we successfully modelled bosonic stimulation in a non-ground state Bose condensate without further enhancing the theoretical underpinnings of the model (Brown et al., 2018). In this case, the additional modes were not the modes of quasi-particle excitations, but higher-momentum modes of a condensate.

Extensions have been made to the Truncated Wigner approximation in the form of the stochastic GPE (Gardiner, Anglin, and Fudge, 2002; Gardiner and M. J. Davis, 2003), which divide the analysis of the gas into a condensate region and a thermal region. Depending upon the assumptions as to how these two regions interact, various numerical efficiencies can be achieved. These treatments all rely on a phase-space quasi-distribution representation of a master equation, which for many experimental realisations is adequate, however, there are some cases for which a field approximation is no longer workable, for example, while Fock states are representable, a superposition of Fock states is not (Blakie et al., 2008).

A Bose-Einstein condensate is a Bose condensate in the laboratory frame

#18: The post-war dream

Golf and coach rugby;

Read, think, and write; cricket too

Where shall we eat, dears?

Abstract

Bose-Einstein condensates of weakly interacting, ultra-cold atoms have become a workhorse for exploring quantum effects on atomic motion, but does this condensate need to be in the ground state of the system? Researchers often perform transformations so that their Hamiltonians are easier to analyse. However, changing Hamiltonians can require an energy shift. We show that transforming into a rotating or oscillating frame of reference of a Bose condensate does not then satisfy Einstein's requirement that a condensate exists in the zero kinetic energy state. We show that Bose condensation can occur above the ground state and at room temperature, referring to recent literature.

I assert that in this case a steadily growing number of molecules compared to the total density will go over into the 1st quantum state (state without kinetic energy), while the remainder of the molecules will distribute themselves according to the parameter value $\lambda = 1 \dots \dots$ one part "condenses," the rest remains a saturated ideal gas. (Einstein, 2015, p. 418)

Introduction

D. M. Stamper-Kurn et al. (1998) found hydrodynamic excitations and co-oscillations between a Bose-Einstein condensate and the accompanying thermal cloud. Rotating a Bose condensate, which looks stationary in a rotating reference frame, can create excited vortices (Chevy, Madison, and Dalibard, 2000; Haljan et al., 2001). The dynamics of fractional vortices were explained by Ji et al. (2008).

Matter waves, such as dark (Denschlag, 2000) and bright (Strecker et al., 2002) solitons, and rogue waves (Wen et al., 2011), described as metastable states, are evidence of non-ground state configurations, but these are treated as perturbations to an underlying ground state (Z. X. Liang, Z. D. Zhang, and W. M. Liu, 2005). Fabbri et al. (2009) found excitation resonances on one-dimensional lattices.

In Brown et al. (2018) we showed that an entire Bose condensate formed in a non-zero momentum state, as opposed to some components being in a metastable state as in the experiments with solitons and vortices. We used a Bragg pulse to excite 50% of a population of Rubidium-87 atoms in the ground state of an approximately harmonic trap into the $|2\hbar k\rangle$ momentum state. The higher momentum state oscillated in the trap at the trap frequency and collided with the zero momentum state, scattering atoms. These atoms then coalesced back into a condensate at the average momentum, the centre of mass, state, $|1\hbar k\rangle$, through bosonic stimulation (Miesner, 1998). This centre of mass state was originally empty. We showed that the temperature of this state was higher than the ground state, but still remained below the critical temperature, T_c . We also found that the new condensate was sometimes multiply seeded, which caused gray solitons through the Kibble-Zurek mechanism. This is evidence that condensates can occur above the ground state energy level.

In the literature, a Bose-Einstein condensate is described as an ensemble of interacting bosons that macroscopically occupy the *ground state* of a system. Here we demonstrate that the transformation from the $|0\hbar k\rangle$ momentum state of a simple harmonic oscillator into the $|1\hbar k\rangle$ momentum state is an energy-requiring transformation that shows that our Bose condensate was not in the ground state of the system. It is also not an inertial frame of reference. After that, we contrast an oscillating frame with transformations in a system of circular rotations. These too require energy, but the frames of reference remain inertial. We then point out that the laboratory ground state still has non-zero kinetic energy. Finally, we justify the existence of quasi-particle Bose condensates at room temperature.

Simple Harmonic Oscillator

Starting from a simple harmonic oscillator reference frame centred at the $|0\hbar k\rangle$ state, we shall show that transforming into the frame oscillating at the $|1\hbar k\rangle$ rate requires energy. Then we show that the frame of reference is not inertial.

Transformation to $|1\hbar k\rangle$ momentum state

The $|1\hbar k\rangle$ state has some energy, $E_1 = \hbar\omega$, which can be determined by finding the energy eigenvalues of the Hamiltonian. We want to transform into the frame of reference where the $|1\hbar k\rangle$ state is stationary.

From the simple harmonic oscillator, in action-angle coordinates, we know that

$$P = \frac{E}{\omega} = \frac{\hbar n\omega}{\omega} \quad (3.1)$$

$$Q = \omega t + \alpha \quad (3.2)$$

and we want to transform into a new frame of reference

$$P' = P - \frac{E_1}{\omega} \quad (3.3)$$

$$Q' = Q. \quad (3.4)$$

The old and new Hamiltonians are

$$\hat{H} = \omega P \quad (3.5)$$

$$\hat{H}' = \omega P' \quad (3.6)$$

$$= \omega P - \omega \frac{E_1}{\omega}. \quad (3.7)$$

The difference between the Hamiltonians is

$$H' - H = -E_1, \quad (3.8)$$

which is non-zero and thus shifts the energy of the Hamiltonian. In the oscillating reference frame, the system appears to have $E_1 = \hbar\omega$ less energy than when we consider the oscillation. The ground state still has less energy than the $|1\hbar k\rangle$ state, even though the higher energy state appears stationary in a transformed picture.

Frames of Reference

A Galilean, or inertial, frame of reference is one in which the reference frame is not accelerating. A Galilean transform is a transformation between coordinate systems that can be achieved through a combination of uniform motion, translations, and rotations. These are all linear operations that can be written as a matrix algebra.

The canonical transformation into the $|1\hbar k\rangle$ state is not a linear transformation. In the oscillating frame of reference there is a non-zero acceleration, thus the frame of reference is not inertial.

We can rewrite the oscillator Hamiltonian in terms of kinetic and potential energy,

$$\hat{H} = \frac{p^2}{2m} + V(q), \quad (3.9)$$

where $V(q) = \frac{m\omega^2}{2}q^2$. Since this is a conservative field, we can calculate the force at position q as $F(q) = -m\omega^2q$, and from Newton's second law we have $a = -\omega^2q$. Thus there is a non-zero acceleration, the value of which depends on the particle's position. Clearly, this is not an inertial frame of reference.

Circular Motion

Contrast an oscillating body, which acquires and loses potential energy, with circular motion. In quantum mechanics, considering only orbital angular momentum, we can generate a time-dependent rotation about an axis, z , with the rotation operator,

$$R(z, \omega) = \exp(i\omega t L_z). \quad (3.10)$$

Our transformed wave function is

$$\psi'(t) = \exp(i\omega t L_z)\psi(t), \quad (3.11)$$

and the Schrödinger equation is

$$i\frac{d}{dt}\psi'(t) = (\omega L_z \exp(-i\omega t L_z) + \exp(i\omega t L_z)H(t)\exp(-i\omega t L_z))\psi'(t). \quad (3.12)$$

The transformed Hamiltonian is

$$H'(t) = \omega L_z \exp(-i\omega t L_z) + \exp(i\omega t L_z)H(t)\exp(-i\omega t L_z). \quad (3.13)$$

If we look at a half period of rotation, from $t : 0 \rightarrow \pi$, the exponentials will equal 1 and -1 , and thus, in a conservative field with rotational symmetry, we have the energy difference between the Hamiltonians,

$$H'(t) - H(t) = -2\omega L_z, \quad (3.14)$$

which is non-zero and thus shifts the energy of the Hamiltonian. In the rotating reference frame, the system appears to have $2\omega L_z$ less energy than when we consider the rotation.

The shift to the rotating frame of reference is an energy requiring transformation. This implies that the lowest energy state of a trapping system in a laboratory frame rotating about the Earth actually has kinetic energy. Also, a condensate rotating in the laboratory frame will have non-zero kinetic energy. Becker *et al.* (Becker et al., 2018), using an experiment aboard a rocket, performed condensation and interferometry tests during launch and generated a condensate in Earth orbit, which involves a non-inertial frame of reference during launch and non-zero kinetic energy with respect to the Earth's frame of reference during their six minutes of microgravity. So while a Bose-Einstein condensate might have kinetic energy, it is non-the-less in a ground state. The difference between circular motion and oscillatory motion is that the rotating frame of reference is inertial, whereas the oscillating frame of reference has non-zero acceleration. Thus we have supported the experimental evidence that Bose condensates can form in non-ground states and in non-inertial frames of reference.

The Many Body Case

In the treatment of circular motion, we can already extend to the many body case, as the rotation operator simply acts upon each particle. The oscillator Hamiltonian was constructed for the single particle case. In the case of many interacting particles, the treatment still holds. It is true that a many particle system will have interaction terms in the Hamiltonian, such as the probability density term in the Gross-Pitaevskii equation, however we can use a canonical transform between Hamiltonians, and a legal transform will operate on the interaction terms suitably. The interactions are dependent on the relative positions of particles rather than their centre of mass motion, so that in a non-relativistic setting, will not be affected by a transformation. A many body Hamiltonian, transformed to a new frame of reference, will still be subject to the same energetic requirements.

Perturbations to an underlying ground state, such as with solitons, vortices, and rogue waves, arise because in experiments the atoms have non-zero interaction strengths. These

non-zero couplings imply that there will be some non-zero energy as a result of the non-vanishing proximity of adjacent particles. This uneven distribution of energy has been analysed both hydrodynamically and as quasi-particle excitations (Pitaevskii and Stringari, 2003). In a theoretical analysis of condensates with attractive interactions, it was found that a build-up of energy at the core of the condensate was dissipated as a rogue wave. An example of a collective oscillation that arises from the phase coherence brought about by interparticle interaction. The presence of these couplings greatly affects the condensate regime (Zinner and Thøgersen, 2009). If there is a phase matching requirement for transitions between adjacent points in phase space, a collective oscillation might enhance the occupancy rate of a mesoscopic state.

Another level of complication comes about when different species of particle are introduced, such as with spinor condensates, metastable states of which can theoretically give rise to solitons (Li et al., 2005). While these features are evidence of non-zero kinetic energy, they can be treated as perturbations to the potential ground state. The experiment we have described is an observation of the formation of an entire condensate in a higher momentum state.

Quasi-particle Condensates

We have shown that Bose condensates can form in a state with kinetic energy. Miesner *et al.* (Miesner, 1998) found a rate equation encapsulating bosonic stimulation derivable from spin statistics (Pauli, 1940). Fröhlich Fröhlich (1968a) conjectured that Bose condensation could occur in biological systems, but he may not have identified the correct dipole molecules (Fröhlich, 1968b). This form of condensation might be relevant to quantum biology (McFadden and Al-Khalili, 2018). Fröhlich's treatment used an effective ground state to find a small frequency range of longitudinal energy storage. His rate equations were subsequently shown to be equivalent to a second quantised form (T. M. Wu and Austin, 1981) that is like three-wave mixing in non-linear optics.

Recalling that mass and temperature are two proportional factors in the de Broglie wave equation,

$$\lambda_{DB} = \frac{h}{\sqrt{2\pi mk_B T}}, \quad (3.15)$$

so that for Rubidium-87 of mass about 10^{-27} kg with a critical temperature of, say, 10^{-7} K, the ratio is about 10^{-34} . Thus, for the de Broglie wavelength to be the same at room

temperature (300 K), we require a mass less than about 10^{-37} kg. Also, a further decrease in mass of the quasi-particle by 10^6 will increase the de Broglie wavelength by 10^3 . Small effective mass quasi-particles, like magnons (Giamarchi, Rüegg, and Tchernyshyov, 2008), photon-dye interactions in a cavity (Klaers et al., 2010), and non-linear photon interactions in an erbium-ytterbium co-doped fibre cavity (Weill et al., 2019), Bose condense at room temperature. This helps explain high temperature superconductivity (Ramírez and Wang, 2009), a maximum temperature for which might be calculated from the effective mass of Cooper pairs and the lattice spacing. While lasers are coherent, photons in a vacuum cannot interact and condense. This requires the intermediary non-linear matter interaction that overcomes dispersive forces, such as that in a laser cavity.

Conclusion

We have shown that the transformation into the oscillating $|1\hbar k\rangle$ reference frame requires energy and thus there is the formation of a Bose condensate that is not in the ground state of the trapping system. We have also shown that transforming into a rotating frame of reference requires energy and so an apparatus ground state can still have overall kinetic energy. Thus we have justified that Bose condensates can be created in non-ground states and non-inertial reference frames. Bose condensates attract particles into a macroscopically occupied state, not necessarily the ground state, through bosonic stimulation. From the perspective of quasi-particles, we have shown that Bose condensation can occur at room temperature.

Phase Coherence and Collective Oscillations

A no surprise surprise

*Ch'an is not buddhism,
And if not zen is zen then —
Basement impresses.*

Introduction

Fröhlich conjectured that oscillatory bodies in biological systems could excite long range energy storage through longitudinal electric modes that would then condense in a manner analagous to Bose condensation (Fröhlich, 1968b; Fröhlich, 1968a). His three requirements were that (i) there are oscillating dipole units, (ii) they are in a heat bath, and (iii) there is an external energy source coupled to the oscillating units. While he conjectured that perhaps hydrogen bonds in carbon chains could oscillate, the energy and frequency of these would be in the microwave range and not observable naturally in biological systems.

First we introduce a candidate dipole oscillator, the Na^+/K^+ pump, that meets Fröhlich's three criteria. We then examine a network of these oscillators and discuss collective oscillations and phase coherence. A network of identical oscillators can lead to the formation of various patterns (Alexander, 1986). The Kuramoto model has been able to capture the phenomenon of collective oscillations, the key feature being a phase shift based on the phase difference between two oscillators (Kuramoto and Nakao, 2019).

We then discuss a similar model, that of bosons on a tilted optical lattice. Expressed in action-angle coordinates this model's Hamiltonian looks similar to the Bose-Hubbard, but with two additional factors, one that is proportional to the number difference, and one

that is proportional to the phase difference. We discuss the impact of these factors and how they relate to Bose condensation, arguing that Bogoliubov quasi-particles can be thought of as buffering the random phase of a viscous, thermal region, from the phase coherent region of superfluidity.

Phase has been imprinted on a condensate cloud to induce vortices (Matthews et al., 1999) and the phase gradient determines the velocity field of a condensate. An excitatory applied force has been shown to induce collective excitations that persist longer in the phase coherent state (Jin et al., 1996), thus phase coherence has an impact on the time evolution of a system. Then we relate this phase coherence to the collective oscillations seen in a network of our dipole oscillators and discuss the notions of energy and information transfer.

The Na^+/K^+ Pump

For a nerve cell to pass an electrochemical message, there has to be maintained across the cellular membrane a voltage potential difference, so that sufficient depolarisation, often at the post-synaptic membrane, causes a wave of depolarisations as the signal travels across the neuron.

Excitable membranes, such as those of nerve cells, which transmit action potentials to register, process, and react to stimuli, must maintain a potential difference across the phospholipid bilayer in order for membrane depolarisation to be triggered. This electrochemical difference is maintained by the Na^+/K^+ transmembrane ATPase (ATP-catalysing enzyme) pump that dephosphorylates one ATP molecule to power the transfer of three extracellular K^+ ions for two intracellular Na^+ ions. The membrane spanning protein has an accompanying valence shell electron cloud. We propose that this electron cloud be treated as a dipole oscillator, as the transfer of energy from the phosphorylation will quantum mechanically perturb, albeit slightly, the electron shell from a resting position. The restoring force provided by the positively charged ions of the protein acts as the mechanism of oscillation. Thus this pump meets the three requirements of Fröhlich, (i) the oscillatory unit is the Na^+/K^+ pump, (ii) the heat bath is the direct environment of the cellular membrane, at 300 K, and (iii) the external energy source is provided by the ATP phosphorylation.

If the positively charged ion core is modelled as a hollow cylinder with an infinitely thin negatively charged electron sheath and there is a Coulomb interaction between each

unit of the core and sheath, each of height a centred about the origin, and if we only allow displacement in the long axis, z , then the restoring force, F_R is

$$F_R(z) = -\operatorname{arcsinh} \frac{z+a}{a} - \operatorname{arcsinh} \frac{z-a}{a} + 2 \operatorname{arcsinh} \frac{z}{a}. \quad (4.1)$$

The ATP phosphorylation is modelled as a dead-time Poisson process that can only fire when the electron shell is on the interior of the membrane. This is implemented as a steadily decaying memory variable that allows a firing event once below a threshold, with a given probability. Should the firing event occur, the memory variable is reset, and a pumping force, $F_P(z)$ is applied to the electron sheath. The energy input of the phosphorylation is matched by interaction with the energy bath, which is thermally noisy. This provides a damping force, $F_D(\dot{z})$, which can simply be written as a constant factor, b , of the velocity. Thus we can write an ordinary differential equation for the oscillator as

$$\frac{d^2}{dt^2} z + b \frac{d}{dt} z + F_R(z) = F_P(z) \quad (4.2)$$

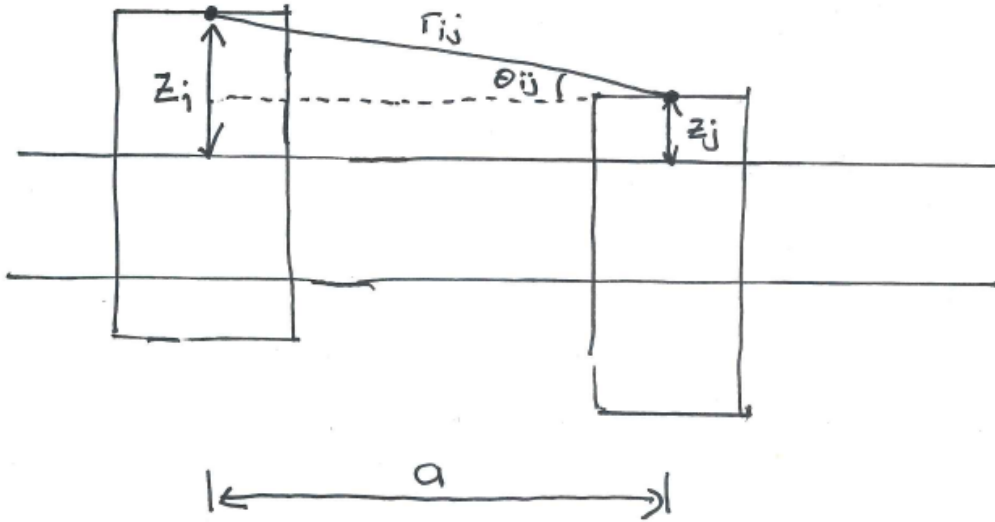


Figure 1: Two electron sheaths a distance a apart with an angle θ_{ij} between centre of masses, and distances $z_{i,j}$ from the membrane.

The restoring force is linear for the region of interest, so our model is simply a damped, forced harmonic oscillator. When the forcing frequency approaches the natural frequency

of the oscillator, resonance will occur. We then consider a lattice of oscillators, where the interaction is a negative Coulomb force between adjacent electron sheaths. The interaction force is

$$F_I(z_i) = -k \sum_j K_{ij} \frac{z_i - z_j}{a^2 + (z_i - z_j)^2}, \quad (4.3)$$

where k is the force constant, K_{ij} is the adjacency matrix element between nodes i and j , and a is the distance between adjacent nodes. The adjacency matrix is a matrix of size $N \times N$ where N is the number of nodes in the lattice. When an entry in the i th row and j th column is non-zero, that is the strength of the interaction from the j th node on the i th node. Figure 1 shows the vertical force exerted by an oscillator upon its neighbour.

The interaction force equation can be recast as

$$F_I(r_{ij}, \theta_{ij}) = -k \sum_j K_{ij} \frac{1}{r_{ij}^2} r_{ij} \sin \theta_{ij}, \quad (4.4)$$

where θ_{ij} is the angle between two electron sheaths and r_{ij} is the distance between them. This is consistent with an inverse square law.

Simulating this system where the adjacency matrix is a one dimensional chain and using relatively arbitrary parameters shows the development of collective oscillations. In Figure 2 we show the results of the simulation. Subplots (a) and (b) show the pairwise mutual information of oscillator nodes. Initially there is little coordination between the positions of the oscillators, but by the end of the simulation we can see that there is correlation between all nodes, even though the interactions are limited to nearest neighbour. Subplot (c) shows the positions of the oscillators for the last time period of the simulation, it can be seen that collective oscillations have been established. Subplot (d) shows the final positions of the oscillators. Neighbouring nodes are in anti-phase, which is a result of the negative interaction force between adjacent nodes.

The turn-over rate of the Na^+/K^+ pump is about 25 to 100 Hz in cultured cells (Hootman and Ernst, 1988; M. Liang et al., 2007), and thus, if this is near the resonance frequency of the membrane lattice oscillators, could account for the gamma oscillations viewed in EEG signals, and explain extracellular currents (Buzsáki, Anastassiou, and Koch, 2012). The collective oscillations would have a lower frequency, and thus could explain such EEG evidence. It is impossible for an amplitude envelope to oscillate faster than the actual oscillator node, therefore any collective oscillation, manifest as synchrony or that envelope, will have a frequency lower than the frequency of the individual oscillator. That there are

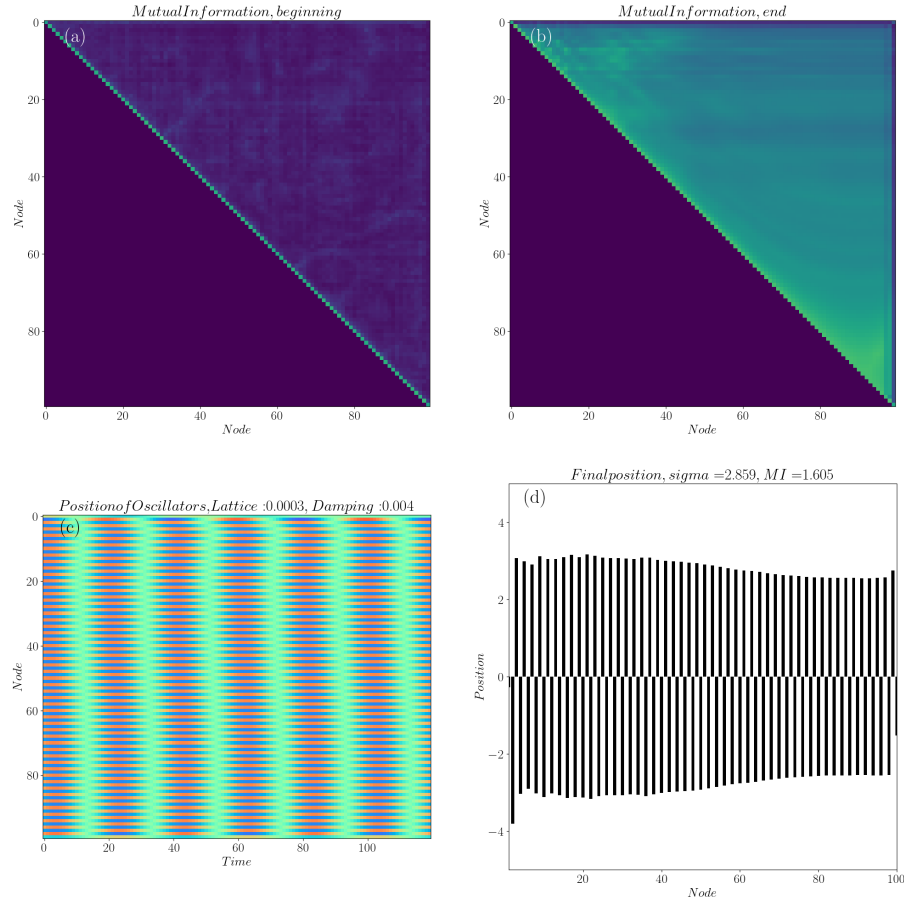


Figure 2: (a) mutual information of oscillators after initial burn-in, (b) mutual information at end of simulation, (c) time-series of oscillators for end of simulation, (d) position of oscillators at end of simulation.

collective oscillations at a low frequency is consistent with Bloch's theorem in solid state physics, in which a lattice of static potentials can be expressed as the product of a plane wave and a matching periodic potential. In a lattice of N nodes, there are $N!/(N-M)!M!$ M node subgroups. This gives us the total number of collective modes, but given the number of small subgroups commensurate with the phase of large subgroups, the amplitude of the larger, lower frequency, lower energy subgroups will be larger.

From Figure 3, we can see that the oscillations of the node are bounded by a slower

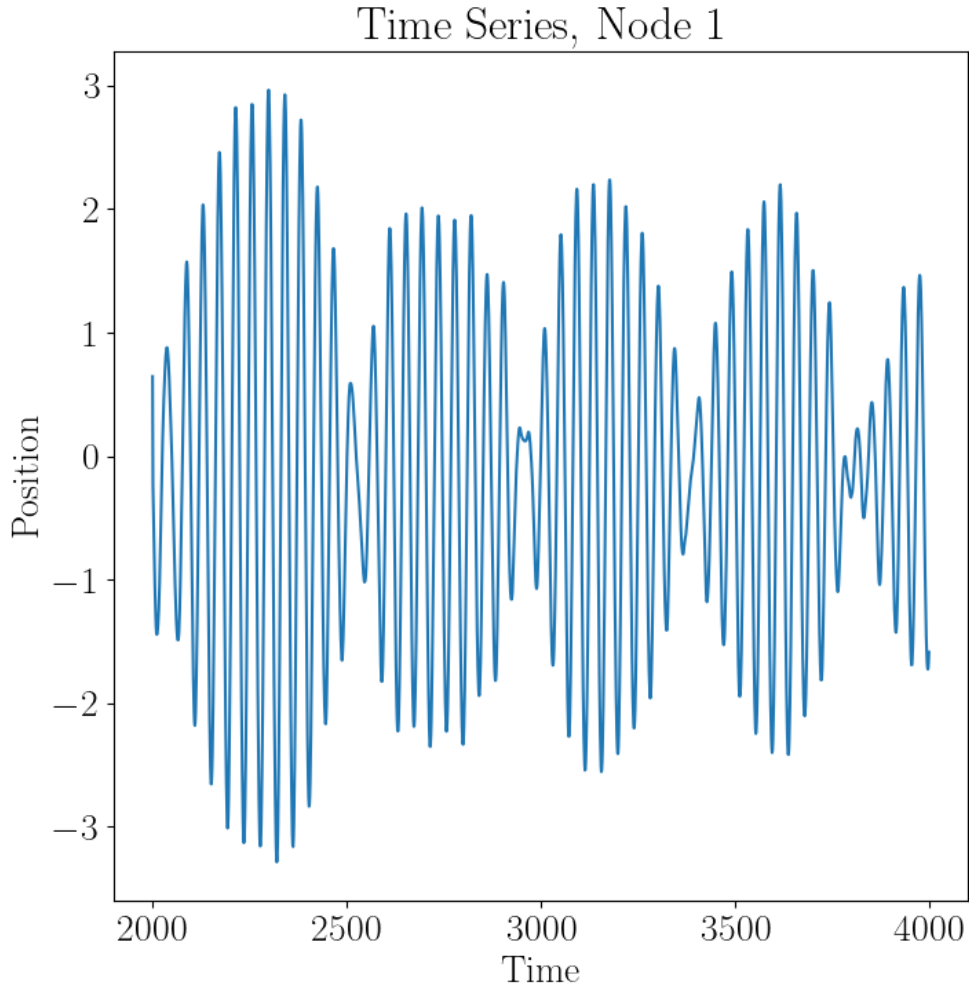


Figure 3: Position of an oscillator node.

frequency envelope. Recalling figure 2(c), this envelope is synchronised across the lattice. Figure 4 shows a plot of the position versus velocity of an oscillator. It can be seen that the amplitude varies and occasionally receives a small perturbation, which is the result of the stochastic kick. Small perturbations, such as that of the random kick, have been shown not to qualitatively affect overall dynamics (Gopalsamy and Rai, 1988). We can assign a phase as the angle swept out by the oscillator.

Phase reduction techniques have been used to analyse networks of oscillators (Nakao, 2016). The canonical model of phase synchronisation is the Kuramoto model. Each oscilla-

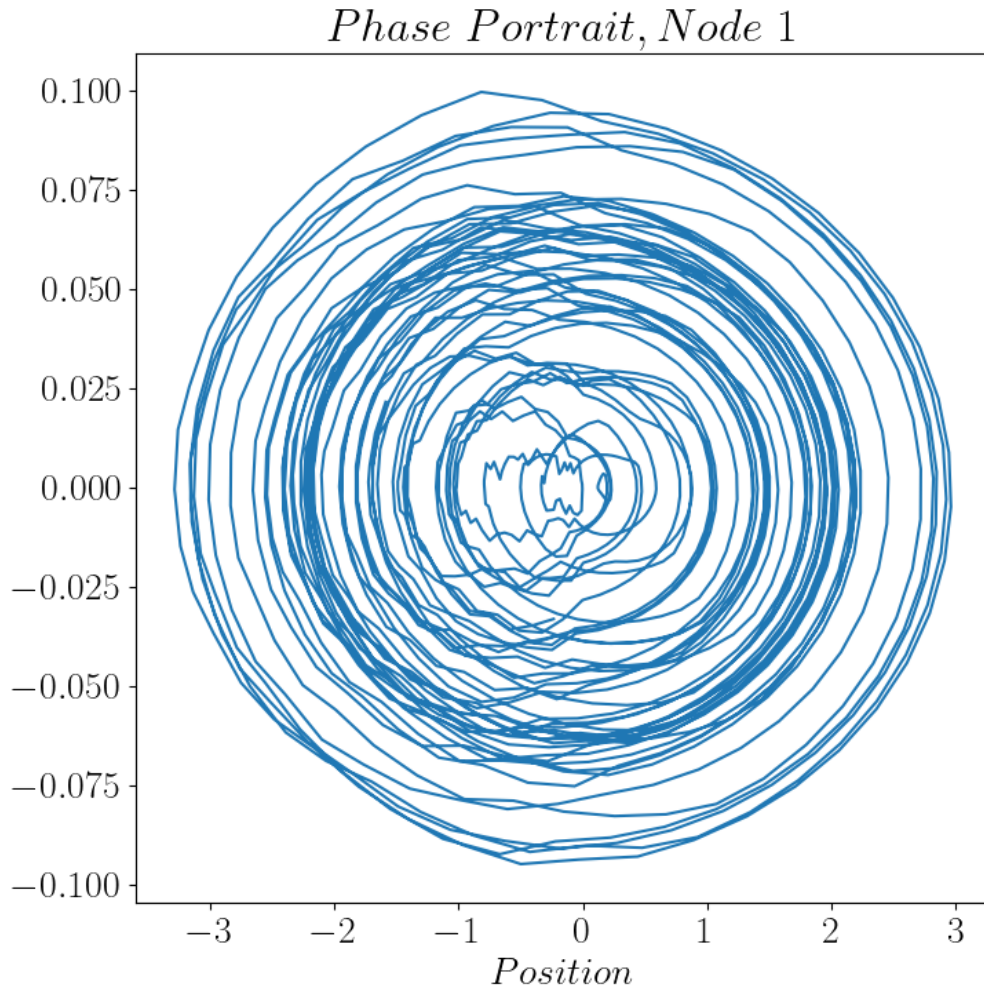


Figure 4: Phase portrait of an oscillator node.

tor is reduced to a single variable, its phase, φ . The ansatz is to hypothesize that a phase difference between connected nodes would retard or advance respective phases.

$$\dot{\varphi}_i = \omega_i - J \sum_j K_{ij} \cos(\varphi_i - \varphi_j), \quad (4.5)$$

where i and j range over lattice node indices, ω_i is the natural frequency of the oscillator, J is the interaction strength, and K_{ij} is the adjacency matrix. The adjacency matrix has a non-zero entry in the i row and j th column when there is a coupling between node i

and node j . Next in the analysis is to calculate an order parameter, the mean phase, and express the model in terms of this overall parameter,

$$\dot{\varphi}_i = \omega_i - J \cos(\bar{\varphi} - \varphi_i). \quad (4.6)$$

This order parameter is reminiscent of the classical field variable representing a condensate in the [GPE](#) equation, and each oscillator state is expressed as a perturbation from this mean value. In a fully connected model, a phase transition was found between incoherent oscillations and phase synchrony, based on the tuning of the interaction strength. Various network topologies have uncovered a range of behaviours, ranging from full synchronisation, to patchworks of synchrony, to random phases. Unfortunately, our simulation parameters did not yield a constant amplitude envelope and thus it is not directly amenable to phase reduction techniques that lead to the Kuramoto model.

Stimulated Bose Hubbard Model

The Bose-Hubbard Hamiltonian models spinless bosons on a lattice,

$$H = \sum_i \epsilon_i \hat{n}_i + \frac{U}{2} \sum_i \hat{n}_i(\hat{n}_i - 1) - J \sum_{\langle i,j \rangle} b_i^\dagger b_j. \quad (4.7)$$

The sum with $\langle i, j \rangle$ denotes enumeration over nearest neighbour sites, b_i^\dagger (b_i) are the annihilation (creation) operators for bosons and satisfy the usual commutation relations $[b_i, b_j^\dagger] = \delta_{ij}$, \hat{n}_i is the number operator, ϵ_i describes the energy offset of each lattice site, and U is the onsite interaction energy ($U > 0$ is repulsive). These various components are illustrated in [Fig. 5](#). Neglected are the next-nearest neighbour interactions and the nearest-neighbour repulsions, which are typically two orders of magnitude smaller than the included interactions ([Jaksch et al., 1998](#)).

Bose-Einstein condensation has been examined on a tilted optical lattice, where each lattice site provides a harmonic potential and the tilting introduces a force between each lattice site. This system is similar to our oscillator model above. Starting from the one dimensional Gross-Pitaevskii equation, and converting to action-angle coordinates ([Witthaut and Timme, 2014](#)), the Hamiltonian is

$$\hat{H} = \epsilon_i \sum_i I_i + \frac{U}{2} \sum_i I_i^2 - J \sum_{ij} K_{ij} \sqrt{I_j} \sqrt{I_i} (I_j - I_i) \sin(\varphi_j - \varphi_i). \quad (4.8)$$

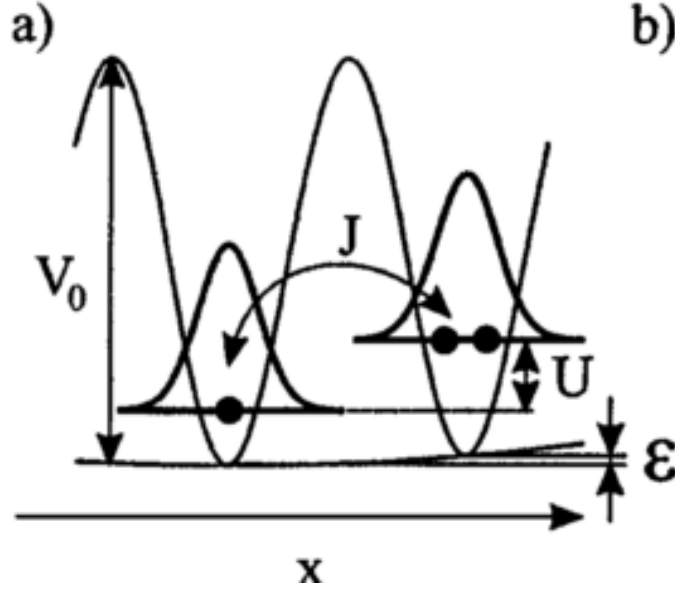


Figure 5: Bose-Hubbard model parameters. See text for an explanation of the symbols. From Jaksch et al. (1998)

Where I_i is the action of the i th node. This Hamiltonian, for some parameter space, shows chaotic behaviour as a result of dephasing between lattice sites. Coherence requires the matching of the lattice depth, the lattice spacing, and the interaction force. This matching is required so that a region of parameter space that is commensurate with coherence is reached. The lattice depth will determine the natural frequency, and if interaction strength and lattice spacing do not induce the correct phase shifts, then dephasing will occur.

The action is the square root of the energy, if we compare this Hamiltonian to the second-quantised Bose Hubbard model, we see a direct similarity, with the addition of a number dependent term and a phase dependent term. We make the analogy and write down the Hamiltonian:

$$\hat{H} = -\epsilon \sum_i \hat{n}_i + \frac{U}{2} \sum_i \hat{n}_i (\hat{n}_i - \hat{1}) - J \sum_{i,j} K_{ij} \hat{b}_i^\dagger \hat{b}_j (\hat{n}_i - \hat{n}_j + \hat{1}) \hat{s}_i(\hat{\varphi}_i - \hat{\varphi}_j + \phi) \cos(\hat{\varphi}_i - \hat{\varphi}_j + \phi) \quad (4.9)$$

Where $\hat{b}_i^\dagger, (\hat{b}_i)$ is the bosonic creation (annihilation) operator on node i , \hat{n}_i is the number operator, $\hat{b}_i^\dagger \hat{b}_i, \hat{\varphi}_i$ is the phase operator, $\hat{s}_i(\theta)$ is the phase shift operator, ϵ is the chemical potential, ϕ is the phase interaction offset, ($|\phi|^2 < \frac{\pi}{2}$ is attractive), and all else is as above.

The Bose Hubbard model has been used to model the phase transition between Mott insulator and superfluid states (Fisher et al., 1989a; Greiner et al., 2002). In the insulating state, bosons are localised to individual lattice sites and there is no phase coherence between adjacent bosons. In the superfluid state there is phase coherence and the wave functions of the individual bosons are spread across lattice sites. This model bears the name Bose because it allows multiple occupation of the same quantum state, which distinguishes it from a fermionic system. What is not included in the model is bosonic stimulation (Miesner, 1998). The introduction of a number dependent term will lead to the multiple occupation of lattice sites in the broadened transition between the insulating and superfluid states. Figure 6 shows the expected occupancy number in a simulation of the stimulated Bose Hubbard model for various parameters (Kramer et al., 2018). This transition can explain the region of number dependence found in a photonic model of the insulator-superfluid transition (Greentree et al., 2006).

Quantum Phase

The issue of a variable such as phase has been vexing in the study of quantum mechanics because of its multivalued nature. The solution is to rely on the cosine and sine operators to act as conjugate to the number operator, in this way we have smooth, well behaved variables (Susskind and Glogower, 1964; Pegg and Barnett, 1989; Kastrup, 2006). In action-angle coordinates, the angle variable is actually a linearly increasing function of time, the problem arises when switching to a circular phase, which jumps by 2π every round trip. Also, just as in practice the number operator is given an arbitrary roof, the infinite dimensional Hilbert space is truncated for the phase variable. If, as mentioned in Chapter 1, time is a label on arrangements, then the only sensible treatment of time is as intervals, or differences, and the problem of an infinite dimensional Hilbert space for time, angle, or energy (action) is obviated.

A number state has a random phase, for phase coherence to occur, as in superfluidity, there must be a mechanism by which neighbouring particles' phase synchronise. Most theoretical treatments limit the interaction between particles to a hard shell contact interaction based on the two body s -wave scattering length. This is introduced in the Gross-Pitaevski equation as an interaction parameter multiplied by the density operator. In no way is phase

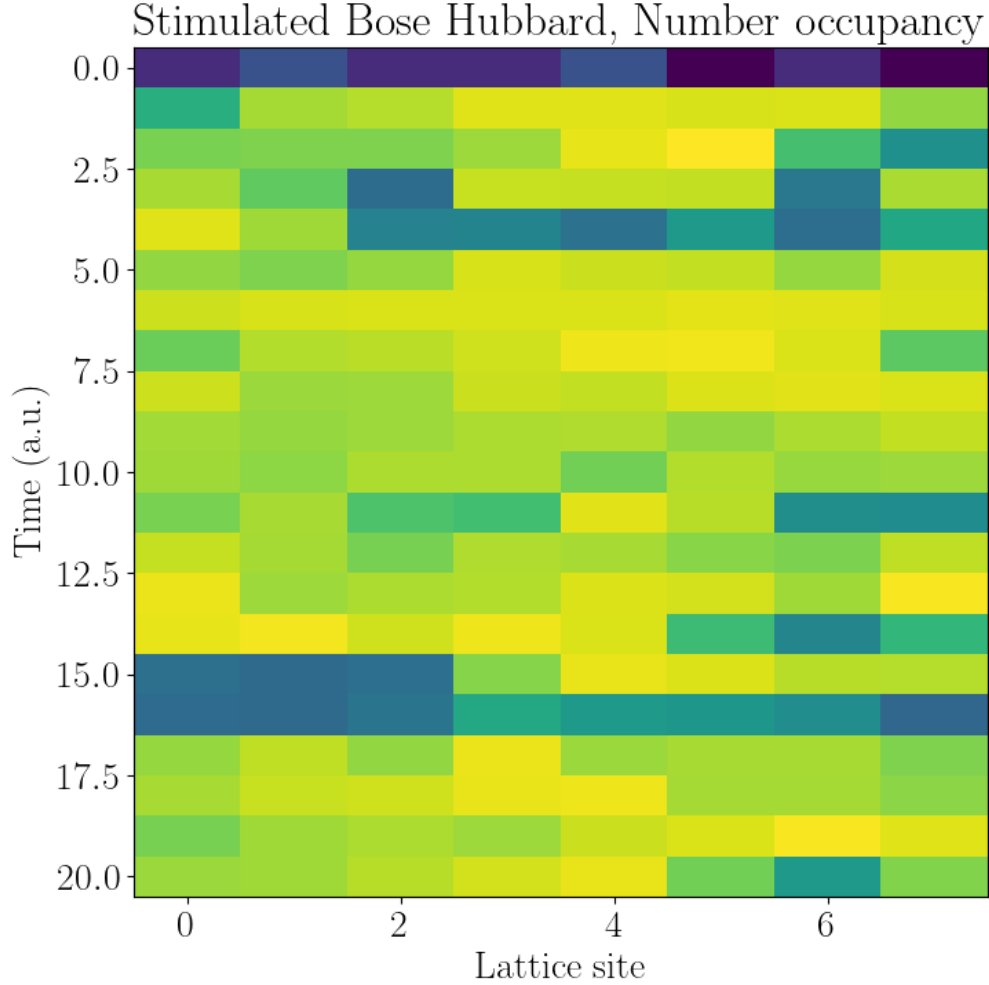


Figure 6: Lattice occupation number over time.

taken into account. A condensate occurs when the interparticle spacing approaches the de Broglie wavelength, thus we choose to model the phase interaction as a soft interaction. The phase shift introduced by a direct linear s -wave elastic collision is ka_0 , where k is the wavenumber and a_0 is the s -wave scattering length (Walraven, 2019). As we are starting with phase incoherent particles, their phases will not be synchronised, which is implicitly assumed in most theoretical treatments, where, for example, the time-evolution of the

annihilation operator being $e^{i\omega t + \phi}$, it is ignored. Thus we model the phase interaction as

$$\frac{d\varphi}{dt} = \sum_i \omega_i - J \sum_{i,j} K_{ij} \exp(\cos(\varphi_i - \varphi_j + k_i a_0 + \phi) \cdot \pi). \quad (4.10)$$

Where the variables are defined as above and we can expand the cosine term in appropriate sum and difference identities. If we require phase-matching for a particle to join a condensate, which is supported by the observation of a healing length, then we can see that an ensemble of particles with commensurate phases will occupy a smaller region of configuration (phase, in a different sense) space. This proximity further enhances Bose stimulated growth. An exponent of $2/5$ was found to be required in the Miesner growth curve (Miesner, 1998), which can be explained when taking an expectation value of interacting phases.

Phase Dependent Gross-Pitaevskii Equation

We have modelled the interaction of two populations of particles with our above phase shift operator acting on the density operator. Implementation of this operator in position-momentum space requires the comparison of neighbouring points in the truncated Hilbert space and thus loses the flavour of the mean-field contact interaction GP equation, however, it is required to explain the phenomenon of phase coherence. Figure 7 shows two populations in a ground state. Without interactions the two populations follow a steady phase evolution. When density interactions are turned on, there is a complicated phase relationship and when phase interactions are turned on, this relationship remains. While we have been unable to provide evidence, I hypothesize that when the phase interaction strength matches the simulation grid spacing appropriately, phase coherence between the two populations can be achieved.

A condensate cannot have a specific number of particles to remain coherent and condensates always are surrounded by a thermal cloud. A thermal cloud is a collection of particles with random phase and in order for a particle to join the condensate it must match the condensate's phase. In the Bogoliubov model, quasi-particles can travel through the condensate at the speed of sound, a function of phase coherence, and in a superfluid form in the region between viscous flow and the superfluid. These buffering particles must carry phase, which is reasonable, as the quasi-particle excitations are equivalent to phonons but are carried by the electromagnetic field and thus have phase. A condensate is a coherent matter wave, and the evidence of a healing length means that there is an effective force

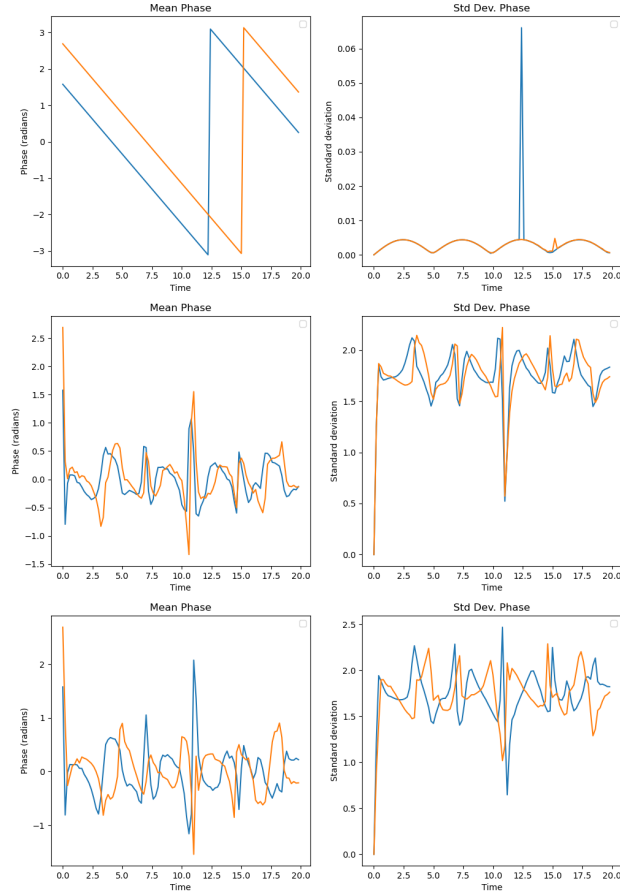


Figure 7: Phase of two populations of particles in a harmonic potential. The figures on the left are the mean phase and the figures on the right are the standard deviations of the phase. The first row is the standard spinor GPE with no interaction. The middle row shows the phase when the standard non-linear interaction is turned on. The third row shows the phase when phase differences are used.

restoring the phases of the constituent particles to be aligned with the phases of neighbouring particles. This is reminiscent of the Ising spin model and the ferromagnetic transition, the effective field created by aligned phases repairs disturbances to phase coherence.

As we have mentioned, for a contact interaction, and remaining limited to the s-wave regime, the phase shift induced by a head-on collision is fixed. In many treatments, the hard shell approximation is softened. If we allow the wavefunction to spread and also allow

glancing collisions, then not all collisions between two particles will induce the full phase shift. Indeed if two particles are travelling in almost parallel, such as in a superfluid, then a weak approach will induce a small phase shift. Given the correct conditions, these small phase shifts can act as correcting forces that maintain the superfluidity and protect against turbulence.

Conclusion

A phase coherent wave can transmit energy and thus information much more rapidly than a disordered medium. Relating the phase coherence of a condensate to the phase coherence of the oscillator model, we can see that once phase coherence is established, energy can be transmitted by that collective mode. Collective modes are one way of expressing the dynamics of system that is useful if we can find mechanisms that can transfer a collective quantum of energy. For the condensation of collective excitations in a biological setting to be of any relevance, there needs to be a mechanism by which those quanta can be transferred to do useful work, otherwise the energy storage may be of little significance. Synchronisation can lead to useful work, especially if there is an energy barrier that cannot be overcome by a single unit.

Theory

Communication and Cooperation

*Cooperation,
without, sounds — prerequisite for
communication.*

Bose-Einstein Condensates

BECs were first reported experimentally in 1995 by M. H. Anderson et al. (1995b) working with ^{87}Rb and K. B. Davis et al. (1995) working with ^{23}Na , for which the Nobel prize in Physics was awarded in 2001. Since the first creation of **BECs** in the laboratory, the field has undergone an explosion in theoretical and experimental reports (Inguscio, Stringari, and Wieman, 1998; Dalfovo et al., 1998; Leggett, 2001; Pitaevskii and Stringari, 2003; Pethick and H. Smith, 2008). **BECs** are ideal tools for exploring analogies to other physical systems, including condensed matter and particle physics systems, because of the easily tunable system parameters and cleanness of the experimental configuration. In the realm of condensed matter physics, topological properties of lattice structures can provide insight into the superfluid-Mott insulator transition (Greiner et al., 2002), topological insulators (Hasan and Kane, 2010), and other quantum Hall effects (Sørensen, Demler, and Lukin, 2005; Goldman, Kubasiak, et al., 2009), among others. **BEC** systems can be used to realise Feynman’s dream of targeted quantum simulators (Feynman, 1982; Buluta and Nori, 2009; Bloch, Dalibard, and Nascimbène, 2012).

From elementary atomic physics, we know that the positive nucleus, which carries most of the mass of an atom, is orbited by negative electrons. Solutions to the Schrödinger equation yield differently shaped electron orbitals with various energy levels. Alkali atoms,

those in the first column of the periodic table, have one valence electron and are thus simpler to study and manipulate than atoms with multiple interacting valence electrons. The outer electron can occupy various energy levels and the transitions between these energy levels have specific values, or frequencies. The quantum numbers, n , ℓ , and m , determine the fine structure of an atom. This is the level-splitting achieved without considering relativistic or spin effects. Hyperfine splitting is determined by the interaction of the nuclear moments with the electrons and there can also be splitting of spin states by an (effective) magnetic field. Rb atoms have transitions in the near-infrared range and are thus easily accessible to inexpensive laser light. When an atom is illuminated by electromagnetic radiation of a frequency that matches the energy of the atomic transition, or is on resonance, the valence electron will absorb a photon and increase in energy. After the typical life-time of the transition the electron emits a photon and drops back down in energy levels. While there are many energy levels, some of them degenerate, there are selection rules which govern which transitions occur. Transitions must conserve angular momentum.

Atoms are cooled using a [magneto-optical trap \(MOT\)](#), in which a pair of magnetic coils in the anti-Helmoltz configuration generate a linearly varying magnetic field with a zero at the centre of the trap. Counter-propagating laser beams that are red-detuned from resonance are used to cool the atoms. The magnetic field induces Zeeman splitting, meaning that the further from the centre of the trap an atom is, the greater the energy shift. When a polarised atom moves away from the mid-point it approaches resonance with the laser, it then absorbs a photon and receives a momentum kick back towards the centre. The atom then spontaneously emits a photon in a random direction. After many iterations, cool atoms collect in the centre of the trap where the Zeeman shift is zero and the atoms are dark. Temperatures in the microkelvin range can be reached in this manner.

Initial attempts to cool atoms achieved temperatures lower than expected and some theoretical work had to be undertaken to uncover polarisation gradient cooling (Cohen-Tannoudji, 1998). The counterpropagating beams of the [MOT](#), when correctly polarised, will create alternating regions of polarised light. As the light polarisation alternates, light shifts are induced in the energy of the atom. Once it reaches a peak of the Zeeman shift, a photon is emitted and the atom loses energy.

The final stage in the creation of a Bose-Einstein condensate is classical evaporative cooling, in which the power of a laser trap, different from the [MOT](#) lasers and normally a harmonic potential, is slowly ramped down. The most energetic atoms will no longer be held by the trap and the remaining atoms are given an opportunity to rethermalise. This process is repeated until only ultracold atoms remain. When the critical temperature is

reached, atoms coalesce into a condensate. As we showed in Chapter 3, Bose condensates need not be in the ground state of the trap and form through Bose stimulation.

Optical Lattices

Optical lattices, normally created by the interference of multiple laser beams, are periodic microscopic potentials for atoms induced by the AC Stark effect and were studied in the context of laser cooling of atoms, before the first realisation of BEC (Fig. 8) (Verkerk et al., 1992; Jessen et al., 1992; T. W. Hemmerich, 1993). The wave function of the atoms can

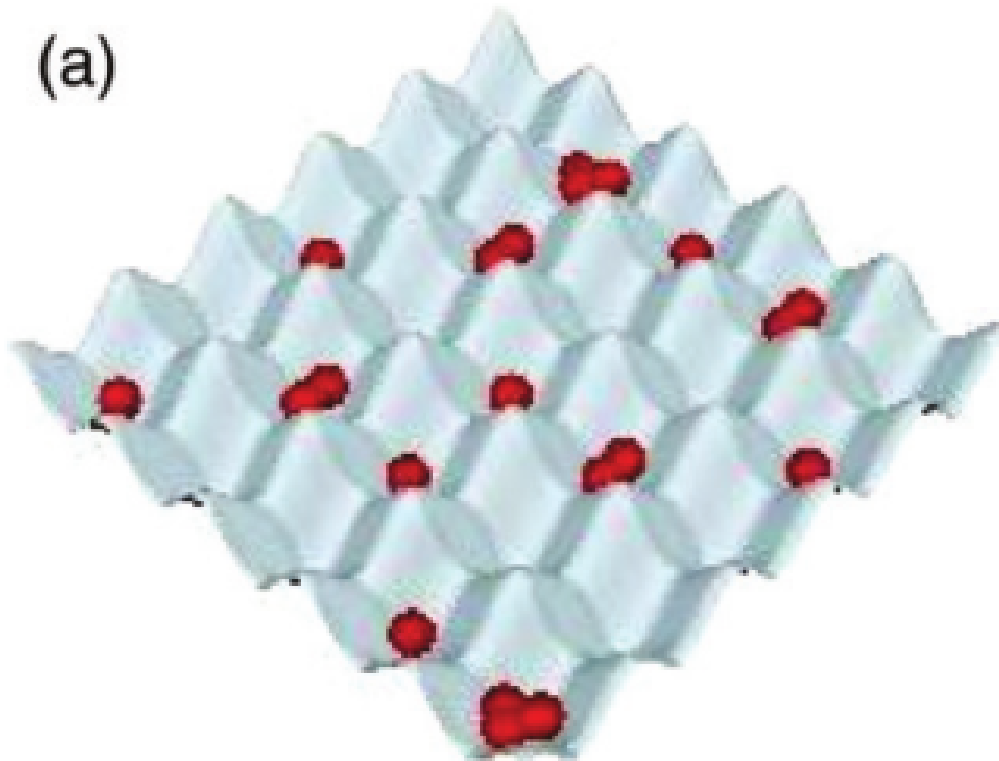


Figure 8: A 2D optical lattice with an uneven distribution of atoms. This is the BEC superfluid phase. From Lewenstein et al. (2007)

be described by a periodic Bloch function, $\Psi(\mathbf{r}) = e^{i\mathbf{k}\cdot\mathbf{r}}u(\mathbf{r})$ with $u(\mathbf{r}) = u(\mathbf{r} + \mathbf{a})$ and \mathbf{k} the wave vector of the Brillouin zone, where \mathbf{a} is the lattice constant. This wavefunction extends over the entirety of the lattice. A transformation to orthonormal localised

eigenstates, or Wannier functions, can be made. The AC Stark effect is the shifting and splitting of spectral lines by an electric field as a result of the electric field interacting with the induced polarisation of the atoms. These optical lattices are without defects and are dissipationless so are an ideal model for analysing condensed matter systems, which normally do have these deviations. The interfering laser beams are far-detuned from resonance, which reduces spontaneous emission, and create attractive (red-detuned) or repulsive (blue-detuned) potentials. Atoms loaded into these periodic potentials have vibrational motion and can tunnel between the potential wells. The energy of the atoms in the lattice can be described as a band structure, like electrons in a metal lattice (Raithel et al., 1997). The lowest energy band can be populated by loading from a BEC. Tunneling between adjacent sites in a vertical lattice was realised by B. P. Anderson and Kasevich (1998).

The hopping parameter, J , can be tuned by adjusting the intensity of the lattice potential laser beam. There is a transition from the normal superfluid state, with high tunneling probability, to a Mott insulator, or crystal, state in which a band gap is introduced between the ground state and higher excited states. This transition occurs when the intensity of the laser field is increased so as to essentially eliminate hopping between sites (Fisher et al., 1989b). The Mott insulator state can not be treated via the Gross-Pitaevskii equation as there is not a single macroscopic wavefunction such as in a BEC (Greiner et al., 2002). BECs in optical lattices lead to interesting nonlinear effects and can be used not only to model condensed matter systems but also as quantum simulators (Morsch and Oberthaler, 2006; Lewenstein et al., 2007). Superlattices are superpositions of basic lattices with multiple, different frequencies and thus lattice constants, and can be used to generate complicated structures, including disordered lattices, which are achieved using incommensurate frequencies. Various lattice configurations have been proposed and implemented, including Kagome (Ruostekoski, 2009; G.-B. Jo et al., 2011), one dimensional sawtooth and zigzag (T. Zhang and G. B. Jo, 2015), and Lieb (Taie et al., 2015; Slot et al., 2017) lattices. Sawtooth lattices have been shown to have nearly flat first excited state bands (See below).

SOC can be applied to BECs in optical lattices, giving rise to many interesting effects. SOC couplings cause degeneracies in the energy dispersions. Around these degeneracies the dispersions are linear (Larson et al., 2010). A number of theoretical papers have treated the question of SOC on lattices, some of which have predicted the onset of topological insulators (Beugeling, Goldman, and C. M. Smith, 2012; Struck et al., 2012; Kartashov et al., 2016; Pan et al., 2016; Grusdt et al., 2017). Experimental realisation of one-dimensional

lattices with [SOC](#) was reported in 2014 (Atala et al., [2014](#)) and of two-dimensional lattices with [SOC](#) in 2016 (Z. Wu et al., [2016](#)).

Spin-Orbit Coupling

Atoms used in [BEC](#) studies are neutral atoms and are thus not subject to electromagnetic forces in the same way as charged particles. This can initially be seen to be an impediment to the modelling of structures such as metals and ferromagnets. However, artificial gauge fields can be used to simulate electronic and spintronic effects (Lin, Compton, et al., [2011](#); Goldman, Juzeliunas, et al., [2014](#)). A gauge field is a field included in a system's equations of motion to ensure that the equations of motion are invariant under local transformations allowed by degrees of freedom in that equation of motion. The symmetries involved mean that transformations of the gauge fields do not affect the underlying physics and thus conserve quantities. [SOC](#), in which the spin of a particle is coupled to its centre of mass momentum, is an example of a gauge field used to induce behaviours similar to those of charged particles. A number of proposals have been put forward to induce [SOC](#) in ultracold atoms. Initially these involved all the magnetic sublevels of a hyperfine state (Osterloh et al., [2005](#); Ruseckas et al., [2005](#); Stanescu, C. Zhang, and Galitski, [2007](#); Spielman, [2009](#)). Following this, pseudo-spin-1/2 boson systems, in which all but two magnetic sublevels are eliminated, were then suggested (Stanescu, B. Anderson, and Galitski, [2008](#); X. J. Liu et al., [2009](#)). The pioneering work of Lin, Jiménez-García, and Spielman ([2011](#)) opened the door to experimental realisation of [SOC](#), which implemented one-dimensional [SOC](#) of pseudo-spin-1/2 bosons. [SOC](#) is typically a combination of the Rashba (R) (Bychkov and Rashba, [1984](#)) and Dresselhaus (D) (Dresselhaus, [1955](#)) forms, where the Hamiltonian component is

$$H_{R,D} = \alpha_{R,D}(\hat{\sigma}^x k_y \mp \hat{\sigma}^y k_x), \quad (5.1)$$

with α the coupling strength, σ^i the Pauli matrices, and k_i the wave vectors.

[SOC](#) in ultracold Bose gases is achieved through the use of two-photon Raman paired laser pulses (Fig. [9\(a\)](#)). In this situation a photon of one wavelength from one beam with a particular polarisation is absorbed by the atom and then is ejected by stimulated emission of another photon at a different wavelength by the other beam, again with a specific polarisation. This gives the atom a momentum transfer proportional to the wavevector of the interfering laser beams. The polarisation is chosen to match the quantum transition rules for the particular transition desired.

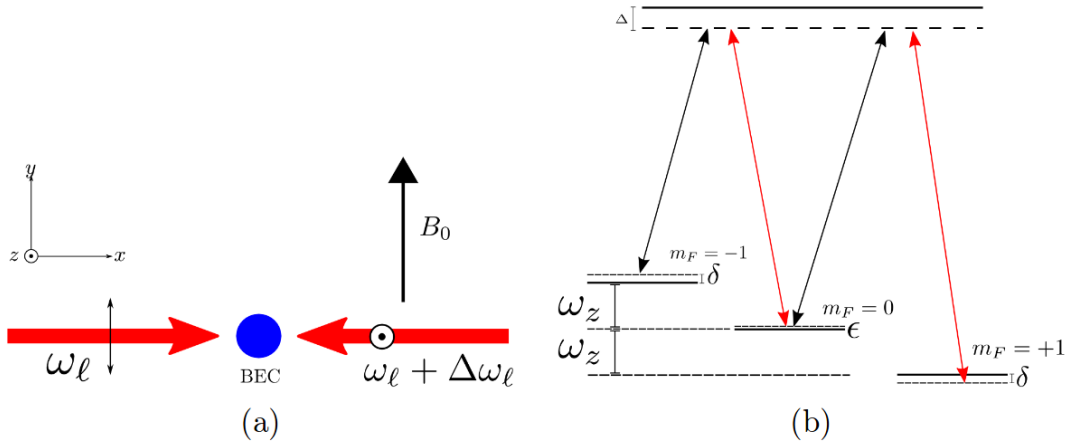


Figure 9: (a) Raman (kick) laser scheme. B_0 is the applied magnetic field, ω_l is the kick laser frequency and $\Delta\omega_l$ is the small detuning to give a momentum transfer. (b) Three-legged level diagram of the ^{87}Rb D2 transition with magnetic sublevels split by an applied magnetic field. Δ is the detuning from resonance, ω_z is the difference in frequency between the two Raman beams, δ is a small detuning. A lambda scheme is obtained when the magnetic field is large enough to induce the anomalous Zeeman effect in which case the $m_F = 1$ state is further separated and adiabatically eliminated. From Brown (2014).

In the $5^2S_{1/2}$ hyperfine state of an atom there are three ground state magnetic sublevels, $|F = 1, m_F = -1\rangle$, $|F = 1, m_F = 0\rangle$, and $|F = 1, m_F = 1\rangle$. Fig. 9(b) shows the three magnetic sublevels transitioning to the higher excited state, $F = 2$. Energy is on the vertical axis. It can be seen that the three magnetic sublevels have different energies, which are a result of the applied magnetic field. In the original proposal, a three-legged scheme linking the $F = 2$ excited state to the three lower sublevels was envisaged. These sublevels are degenerate but the degeneracy can be removed by introducing a magnetic field, which splits the sublevels into different energy states through the linear Zeeman effect. This requires a pair of Raman beams for each transition between magnetic sublevels.

With a sufficiently strong magnetic field, the anomalous Zeeman effect comes into play and can be used to adiabatically eliminate one of the sublevels. This leaves a Lambda scheme in which two of the magnetic sublevels can transition to the higher hyperfine state. These two remaining sublevels are an example of a pseudo-spin-1/2 system in which one of the states can be labelled spin up, $|\uparrow\rangle$, and the other spin down, $|\downarrow\rangle$. Now only one pair of Raman beams is required. One of these beams must be circularly polarised to change the m_F quantum number and the other can be linearly polarised. The Raman beams are set to the wavelength of the $5^2S_{1/2} \rightarrow 5^2P_{3/2}$ transition with a detuning, Δ , to reduce

spontaneous emission, which is the emission of a photon when an electron just raised to an excited state transitions back down to the ground state. The detuning means that the electron has a reduced chance of being raised to the excited state. This means that the excited state becomes a virtual state and there remains a Rabi frequency, Ω , between the two magnetic substates, which is the two-photon Raman coupling, proportional to the difference in wavelength between the two laser beams.

Because there is a momentum change, the atoms are not at rest in the laboratory frame and so there is a small detuning, δ , from the magnetic field induced energy levels of the two m_F substates.

Flat Bands and Compact Localised States

A dispersion curve is a relationship between the wavevector of a particle and its energy on a lattice structure. The energy normally varies with wavevector. Flat band modes are dispersionless bands for which the energy is constant as the wavevector varies. Flat bands can give rise to a **CLS** in which the particles in question are not uniformly distributed across the lattice but instead occupy a small subset of lattice sites. Examples of **CLSs** are solitons, wavepackets that maintain their shape, and discrete breathers, periodically oscillating wavepackets that do not disperse. These have been predicted theoretically to be achievable with particular two dimensional lattice structures and spin-orbit coupling. **CLSs** could find application in the field of quantum computation as they can provide a basis for qubits. These qubits could be manipulated by dynamic modification of the surrounding lattice and laser pumps.

A perfect lattice with infinite extent, according to Bloch's theorem, will give rise to energy eigenstates that extend to infinity periodically across the lattice. On a lattice, the momentum space reciprocal lattice of the unit cell is called the **Brillouin zone (BZ)**. A dispersion curve relates the particle energy to its wave-vector across the **BZ**. Dispersionless **flat band (FB)** are curves for which the energy does not change with changes in wave vector (Fig. 10).

FBs can give rise to localised states. They were introduced by Sutherland (1986) and Lieb (1989) and then expounded upon by Mielke (1991) and Tasaki (1992). These localised states can be used to transmit or localise information on specific sites of a lattice, which could lead to advances in quantum computation. The term **CLS** was coined by Aoki, Ando, and Matsumura (1996) to refer to a localised Wannier function constructed from a superposition of degenerate Bloch waves.

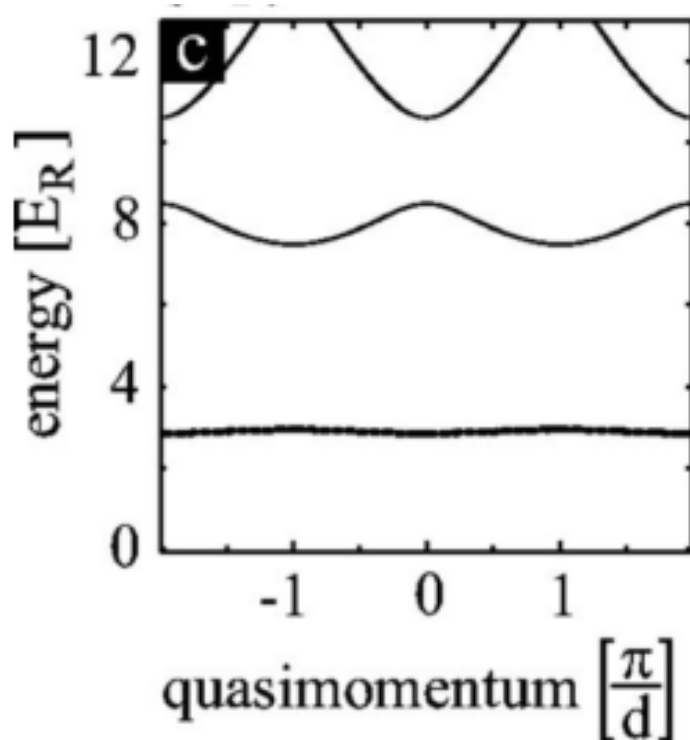


Figure 10: Dispersion curve showing a flat band in the lowest energy state. From Morsch and Oberthaler (2006)

Anderson localisation occurs in a disordered system and is manifest by the localisation of particles due to frustrated transport through the system. This is a quantum mechanical effect as the particles are treated as following all possible paths, with constructive and destructive interference of multiple paths through the disorder leading to localisation (P. W. Anderson, 1958). Spatially localised modes in crystals were predicted to occur in the presence of anharmonicity as opposed to the previously understood localisation due to defects and disorder (Sievers and Takeno, 1988). BECs on lattices are expected to give rise to an atomic band-gap structure, in analogy with photonic crystals. This band-gap structure, in combination with the nonlinear effects of a BEC, were predicted to give rise to localised bright gap solitons in 2D lattices (Ostrovskaya and Kivshar, 2003). A soliton is a shape-preserving wave that is reliant on non-linear effects to counteract normal dispersion. Intrinsic localised modes, including solitons and discrete breathers, are the result of intrinsic nonlinear effects rather than disorder or impurities (Campbell, Flach, and Kivshar, 2004). A discrete breather is similar to a soliton but the wavefunction periodically oscillates between a number of configurations.

The lowest energy band of the 2D honeycomb lattice, such as that of graphene, was found to be completely flat over the entire BZ (C. Wu et al., 2007). The flatness of the band arises from the frustration of bosons' kinetic energy by the particular lattice structure and was found to occur in sawtooth and Kagome lattices. The flat band occurs in these cases for a specific ratio between the hopping matrix elements of the different edges in these triangular geometries. Localised eigenstates of the kinetic energy will arise in flat bands. These compact localised states are wavefunctions that extend over only a subset of lattice sites (Huber and Altman, 2010).

The Hall effect occurs in a current-carrying conductor exposed to a perpendicular magnetic field. In this case the electrons build up on one side of the conductor due to the magnetic field, thus creating an electric field perpendicular to both the original electric field and the magnetic field. The quantum Hall effect occurs in 2D electron systems at cold temperatures and is typified by integer levels of current. The fractional quantum Hall effect is more complicated and relies on composite fermionic quasiparticles, resulting in fractional jumps of the the observed voltage (Parameswaran, Roy, and Sondhi, 2013). FBs in a non-trivial topology are expected to allow the realisation of fractional topological states similar to the fractional quantum Hall effect (Sun et al., 2011). These authors suggest a method to produce models which allow a nonzero bandwidth of the FB but still require the bandwidth to be much smaller than the band gap. They find that such models can arise even without long range interactions, relying only on nearest-neighbour interactions. These models rely on time-reversal symmetry as well as lattice symmetries and a non-trivial topology. When time-reversal symmetry is broken, band gaps with nonzero Chern numbers can open up. The Chern number is the integral of the Berry curvature over a closed manifold. The Berry curvature is a local gauge field associated with the Berry phase, which is a phase difference acquired over the course of a cycle, which is the hopping of atoms around a plaquette. Thus, the Chern number is a measure of the topology of a lattice energy band and a non-zero Chern number implies a non-trivial topology. Yao et al. (2012) propose a system for producing nontrivial Chern numbers in the band structure which result in FBs. Their treatment relies on artificial gauge fields which interact with the spin of hard-core bosons. Y. Zhang and C. Zhang (2013) examined SOC with bosons on lattices and show that the instability of Bloch waves leads to the breakdown of superfluidity. The nonlinear interaction of the GPE reduces the flatness of the dispersion curves but does not fully eliminate it. SOC was first experimentally realised for fermions on an optical lattice in 2012 (Cheuk et al., 2012).

Leykam et al. (2013) introduce the quasi-one-dimensional diamond lattice and study the interaction of the FBs with disorder, finding many interesting topological states. CLSs generate FBs through perfect destructive interference. Disorder will expel all states from the FB mode and also allow for fine-tuning of the FB singularities (Bodyfelt et al., 2014). Experimental demonstration of FBs (without SOC) on a two dimensional Lieb lattice showed the appearance of localised states (Taie et al., 2015). In the same year Mukherjee, Spracklen, et al. (2015), Mukherjee and Thomson (2015), and Vicencio et al. (2015) reported the experimental realisation (without SOC) of a FB state in an array of optical waveguides in Lieb and rhombic diagonal lattices. A theoretical framework for computing flat-band generators where the CLS occupy two unit cells was provided by Maimaiti et al. (2017). Röntgen, Morfonios, and Schmelcher (2018) developed a method for subdividing the lattice Hamiltonian based on local symmetry partitioning.

Beličev et al. (2015) provide a theoretical treatment of SOC on 1D lattices with two-component (spinor) BECs, which are BECs with two different spin states. They find the existence of localised states and a miscible/immiscible transition between the binary spinor species. Zeng, Zhu, and Sheng (2017) examine the theory of Hall effects in two-component particle systems on a lattice.

So far much work has been done on BECs and BECs in lattices. Experiments have recently realised SOC on lattices and some experiments have identified localisation on these lattices. What has not been accomplished yet is the systematic generation of FBs and CLSs on a lattice with BEC and SOC. CLSs can be used in quantum computation to store and manipulate information. A better understanding of the behaviour of ultracold atoms in optical lattices will lead to the realisation of exotic states of matter such as topological insulators. Ultracold atoms on a lattice provide a framework for quantum simulation. The ability to model condensed matter systems will assist in the design of materials suitable for quantum simulation and quantum computation.

Discrete Model

The phenomenon to be examined in this proposal is laid out theoretically by Gligorić et al. (2016). They propose a rhombic (diamond) lattice configuration of binary BECs exposed to SOC (Fig. 11).

The unit cell has a three nodes a, b, c . Nodes a and c , which are colinear in the direction perpendicular to the quasi-one dimensional axis and offset from that axis, are connected

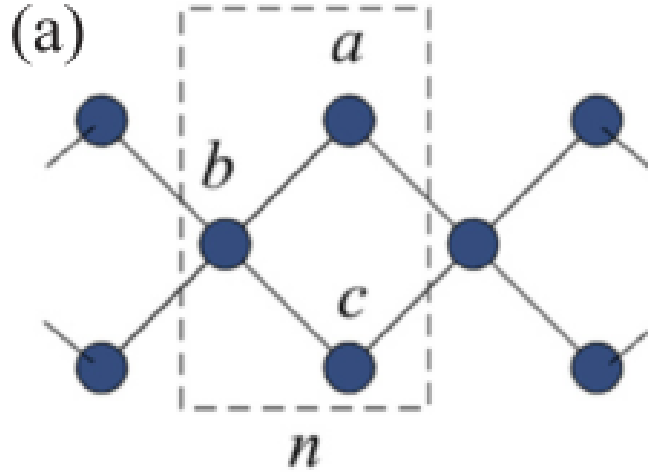


Figure 11: Diamond (rhombic) lattice showing different site labels. n is the unit cell. From Gligorić et al. (2016)

to node b , which is connected to the next nodes a and c . This leads to a system of discrete GPEs:

$$i \frac{da_n^+}{dt} + Ba_n^+ + b_n^+ + b_{n+1}^+ + \lambda(b_{n+1}^- + ib_n^-) + (\gamma|a_n^+|^2 + \zeta|a_n^-|)a_n^+ = 0, \quad (5.2)$$

$$i \frac{db_n^+}{dt} + Bb_n^+ + a_n^+ + a_{n-1}^+ + c_n^+ + c_{n-1}^+ + \lambda[c_n^- - a_{n-1}^- - i(a_n^- - c_{n-1}^-)] + (\gamma|b_n^+|^2 + \zeta|b_n^-|)b_n^+ = 0, \quad (5.3)$$

$$i \frac{dc_n^+}{dt} + Bc_n^+ + b_n^+ + b_{n+1}^+ - \lambda(b_n^- + ib_{n+1}^-) + (\gamma|c_n^+|^2 + \zeta|c_n^-|)c_n^+ = 0, \quad (5.4)$$

$$i \frac{da_n^-}{dt} - Ba_n^- + b_n^- + b_{n+1}^- - \lambda(b_{n+1}^+ - ib_n^+) + (\gamma|a_n^-|^2 + \zeta|a_n^+|)a_n^- = 0, \quad (5.5)$$

$$i \frac{db_n^-}{dt} - Bb_n^- + a_n^- + a_{n-1}^- + c_n^- + c_{n-1}^- - \lambda[c_n^+ - a_{n-1}^+ + i(a_n^+ - c_{n-1}^+)] + (\gamma|b_n^-|^2 + \zeta|b_n^+|)b_n^- = 0, \quad (5.6)$$

$$i \frac{dc_n^-}{dt} - Bc_n^- + b_n^- + b_{n+1}^- - \lambda(b_n^+ + ib_{n+1}^+) + (\gamma|c_n^-|^2 + \zeta|c_n^+|)c_n^- = 0, \quad (5.7)$$

where the i th unit cell has wavefunctions a_i^\pm , b_i^\pm and c_i^\pm and these wavefunctions are labelled + and - for the two different spinor components, for example, spin. B is an applied magnetic field (Zeeman term), λ is the spin-orbit interaction strength, and γ , γ_1 , and ζ are the nonlinear interaction strengths, which are determined by the inter-particle interactions on the same node. The prediction is that under SOC with non-zero interaction strengths the atoms will localise to a subset of a and c nodes and leave the b nodes empty. Fig. 12 shows CLSs on a diamond lattice. For each sub-figure the top row shows the spin up configuration and the bottom row shows the spin down configuration. It can be seen that the high density states are localised to one or a couple of nodes. We can see that to implement this proposal we need a BEC, a 2D trapping potential to confine the atoms in a single plane, an optical lattice in that plane, an applied magnetic field, and Raman kick lasers for SOC.

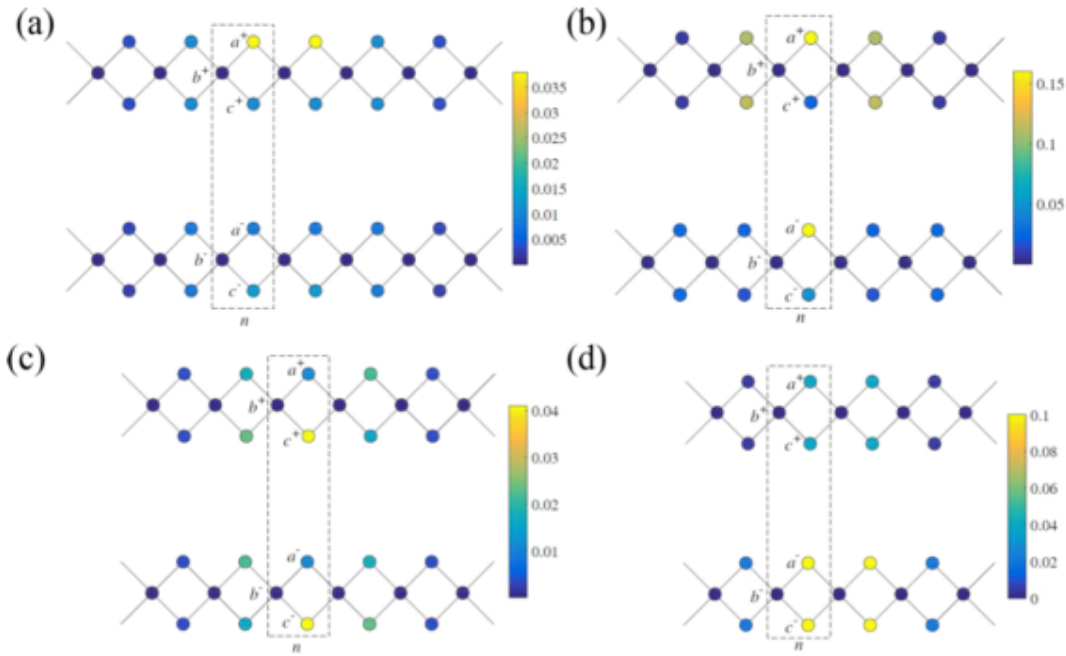


Figure 12: Diamond lattices with CLSs identified as localised high density states. From Gligorić et al. (2016)

Methodology

Ahmed and Omar

Cage the animal.

*Daily you pray to your god —
free the man to soar.*

Experiment

Following standard procedures we create a [BEC](#) of about $2 \cdot 10^4$ ^{87}Rb atoms in an all-optical trap. This requires collecting the atoms in a [MOT](#), laser cooling, and then evaporative cooling. At this point the atoms are at a temperature of less than 200 nK. The atoms are optically pumped into the $|F = 1, m_f = -1\rangle$ state with a short pulse of the optical pumping beam. The atoms are then transferred to a 2D pancake trap generated by two 1064 nm laser beams that intersect on a shallow angle. These lasers are far-red-detuned from resonance and thus create an attractive potential for the atoms. Once the atoms are in the 2D trap the optical lattice is ramped up. This potential is created by reflecting a 532 nm laser off a [SLM](#) and focusing it on the plane of the 2D trap. This light is far-blue-detuned from resonance and so creates a repulsive potential, thus the potential wells are created by an absence of light and the potential walls are created by the presence of 532 nm light. The [SLM](#) can generate arbitrary 2D images and thus can be used to imprint a lattice on the 2D trap (Haase et al., [2017](#)). This 2D trap and optical lattice were designed and installed by Donald White and Thomas Haase for their PhD projects (White, [2016](#)). After the 532 nm laser has been ramped to full power, the Raman kick lasers are pulsed to create a [SOC](#) interaction, as described in Dylan Brown's PhD thesis (Brown, [2019](#)). The effect of the kick laser is then imaged through [time of flight \(TOF\)](#) imaging to give a picture of the motion of the atoms. TOF imaging gives a picture of the atomic momentum by recording

the position of the atoms after they have ballistically expanded from a particular location in space.

The plan was to first achieve [SOC](#) in the dipole-trapped [BEC](#) without an optical lattice. Two coherent kick laser beams split by a polarising beam splitter and put through acousto-optical modulators are coupled to optical fibres on one table and sent to the main science chamber. The two kick laser beams enter the chamber from opposite sides and intersect at an angle of π radians.

The kick laser is red-detuned with the detuning, Δ , about 790 nm, which minimises the scalar light shift between the D_1 and D_2 lines. A magnetic Zeeman field of about 5 Gauss is applied in the z -direction to split the magnetic sublevels. This field will also produce a Zeeman shift to eliminate the $|F = 1, m_f = 1\rangle$ state. The magnetic field strength in combination with Δ , the kick laser intensity, and the detuning between the two kick lasers determine the Rabi frequency between the two pseudo-spin states as well as the small detuning from the magnetic sublevels. As mentioned above, one of the kick beams is circularly polarised and the other linearly polarised. The frequency offset between the two kick beams and the kick beam intensity is scanned to find the value that gives the greatest transition number into the other spin state. After each experimental shot the atoms are imaged through TOF and the atom numbers in the spin states counted. The spin states are identifiable because there is a momentum kick imparted on atoms in one spin state so that that state will be in a different position from the original un-kicked BEC. Each day the environmental effects had to be compensated for and so the combination of magnetic field strength and Raman detuning was scanned before the actual experiments. [Figure 13](#) shows an example of a daily scan of a Raman kick of a [BEC](#).

Next, an optical lattice was to be introduced. With respect to the lattice geometry, we are beginning with the diamond lattice described above. What was not reported in the theoretical treatment was the size of the nodes in the lattice and the spacing between them. The optical resolution of the SLM is about $1 \mu m$ thus the nodes will be a minimum diameter of $1 \mu m$. Initially we were to begin with the diagonal spacing between the nodes (at an angle of $\pi/2$ radians) of between 1 and $3 \mu m$. Images of lattices were to be loaded with the SLM and the time required to fill the nodes measured. Once this was achieved the loaded lattice, was to be illuminated with the kick beam and TOF images of the BEC examined to see whether there was the generation of [CLS](#).

The current [SLM](#) has limitations. For example it is not realistically possible to use greyscale images that result in variable potential energies across the image because of issues with the refresh rate. Also, the switching between images is not sufficiently responsive

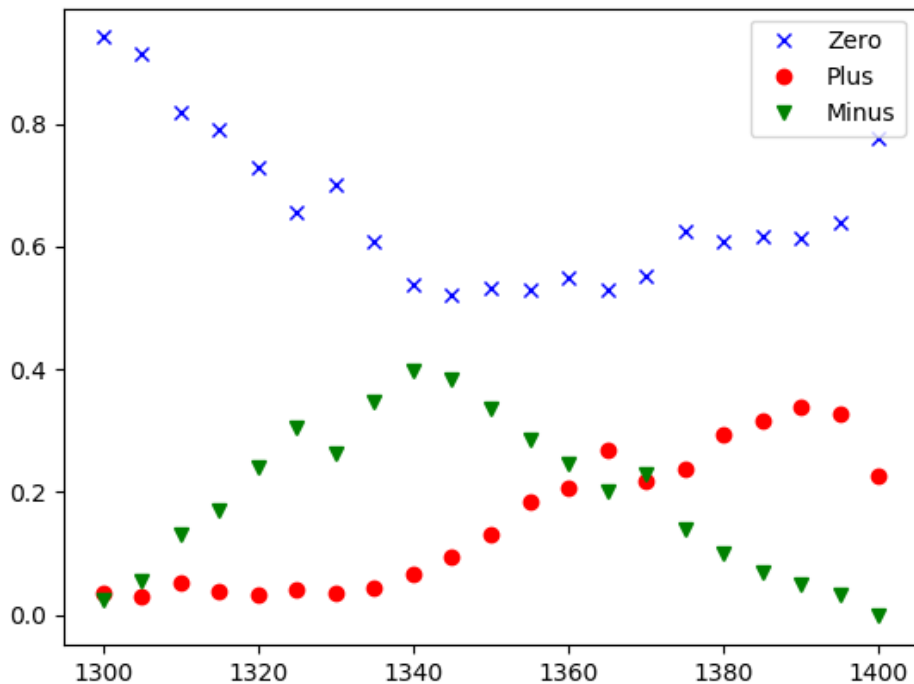


Figure 13: Scan of Raman detuning

for the experimental parameter regime in which we operate. To rectify this, we have a [digital micro-mirror device \(DMD\)](#) that we prepared. I designed and had the engineering department manufacture an adapter plate to mount the [DMD](#) face on a kinetic mount. I implemented a complete specification of the Visitech communication protocol and wrote a program to upload images to the [DMD](#) and run scripts, such as one that could scroll a diamond potential. This will replace the [SLM](#) and be able to produce greyscale images and rapidly swap between multiple images. As the [DMD](#) is a grid of mirrors that are either in the reflecting position or not, a greyscale image is produced by the successive swapping of many binary images to build up a layered potential. One advantage of the fast switching allowed by the [DMD](#) is to be able to initially load atoms into a subset of potential wells and then switch to the experimental regime where SOC can cause vacant nodes to be occupied.

New Apparatus

There was some difficulty in aligning the 2D pancake trap in such a way as to not introduce laser fringing. Currently, the experiments that have been run on the apparatus use a small tilt in the pancake trap to introduce a gravitational force to overcome the fringing. This was arrived at after months of manipulations of the experimental apparatus to try and get rid of the fringing. This work-around would not have been possible for the current study. One possible cause of the fringing is that the windows into the chamber are not anti-reflective coated for 1064 nm light, the wavelength of our pancake trap. A solution to this is to swap to our new, small, glass science cell, designed by my supervisor.

Using the glass cell as the target science chamber, I designed the apparatus and bread-board for a new setup. The system is a three chamber system with two initial MOTs and a variable focus telescope to move atoms cooled in a hybrid magnetic/optical trap in the second chamber to the science chamber.

With the new apparatus, I designed and partially implemented a control program in Python. The control program is unique in that the design of waveform generation to control experimental unit is modular. There can be a section for laser-cooling, a section for trap refocusing, a section for BEC creation, and a section for SOC manipulation. As part of the control program, I implemented a machine learning algorithm that uses a 6 layer MLP neural net to optimise BEC creation ¹

Further Experiments

One experiment that would be interesting to implement is to introduce SOC on an annulus. This circular potential is theorised to introduce a stripe phase in the distribution of pseudo-spin particles. What would be more interesting, however, is to design an experiment to test the mechanism behind Berry phase. On a plaquette, when a condensate travels around a minimal plaquette, it is supposed to gain a geometric phase. This is caused by the orbit about a pole in the complex space. An alternative explanation is that phase is advanced or retarded when a particle crosses a spatial barrier, such as the membrane of a quantum foam. In this case, traveling from A to B should gain the same phase as travelling from B to A , meaning it is not undone. Thus if phase is acquired even without a notion of rotation, then there is an alternative explanation for Berry phase.

¹As mentioned earlier, all this code is on Github

SOC Simulations

Valour

Hidden memory,

*Your presence my mind unfolds —
on my chest with you.*

As has been mentioned, ultracold atom experiments provide a clean and versatile workbench for examining analogies to other physical systems. One apparent drawback, however, is that the atoms used in the experiments do not carry an electric charge and thus it would appear that many areas of enquiry are not available. This is not the case, however. Synthetic gauge fields can be engineered to mimic electronic effects. The Coriolis force generated by rotating a condensate has been used to mimic a magnetic field, and use of laser fields has been used to mimic electric forces and spin-orbit coupling. The synthetic electromagnetic forces are introduced into the Hamiltonian as a vector potential term (See Appendix A). The effects of this term are carefully engineered to observe the desired behaviour in experiments. One way to derive the appropriate Hamiltonian is to express the laser and magnetic fields in terms of the vector potential and then crank through some tedious algebra.

In our experiment, SOC is achieved by coupling linear momentum to different magnetic states by having a detuning between counterpropagating laser beams that matches the energy gap and induces a Raman transition. As explained in Brown (2019), we choose an overall laser detuning that removes the scalar light shift. Our system uses ^{87}Rb and we choose the $F = 1$ manifold. The scalar light shift is voided at a detuning halfway between the D_1 and D_2 lines, so we shall have to consider both lines in our derivation. I had written down the Hamiltonian for the simulations and it matched the Hamiltonian later given to

me by Casper Groiseau, a student of my co-supervisor Scott Parkins, who had suggested I follow the technique in Masson (2019).

$$\hat{H} = \frac{p^2}{2m} + \omega_z \hat{S}_z - \frac{\Omega^2}{4} \cos(2k_\Delta y - 2\Delta\omega t) \hat{S}_x. \quad (7.1)$$

Following Pitaevskii and Stringari (2016) we make a unitary transform into a frame rotating at $2\Delta\omega$ and moving with momentum $2k_\Delta y$. We also flip the spin every rotation. So we apply the operator

$$\exp\left((2k_\Delta y - 2\Delta\omega)t \hat{S}_z\right). \quad (7.2)$$

The momentum component does not commute with the kinetic term in the Hamiltonian so we use the Hausdorff-Baker theorem to compute the action of the transform. We are left with the transformed Hamiltonian

$$\hat{H}_{\text{SOC}} = \frac{1}{2m} \left[(p_y - k_\Delta \hat{S}_z)^2 + p_\perp^2 \right] - \frac{\Omega^2}{4} \hat{S}_x + \frac{\delta}{2} \hat{S}_z, \quad (7.3)$$

where δ is the Zeeman detuning. Note that the $k_\Delta \hat{S}_z$ term is a manufactured synthetic electromagnetic field (See Appendix A), a synthetic gauge field that has resulted from transforming a Hamiltonian. In the frame of reference traveling in the cylindrical corkscrew of the unitary transformation, atoms of one spin will move in one direction, and atoms of the opposite spin will move in the opposite direction. This transformation obviously introduces an energy shift in the Hamiltonian, as explained in Chapter 3, and so this would bolster the evidence that condensates can exist above the ground state.

Spinor GPE Model

Taking the SOC Hamiltonian, we eliminated one of the spin states and only consider a pseudo-spin half system. Experimentally, this was achieved through adiabatic elimination of a spin state through the use of a static magnetic field sufficiently strong to bring a Zeeman shift into effect, here, we merely use a spinor system with 2×2 spin operators.

The lattice was implemented as a potential with circular wells of a particular depth in the diamond configuration. The depth of the wells was calculated from measurement of the SLM 532 nm laser power. The lattice is thus a static position-dependent potential that we can add to the Hamiltonian. In order for the potential to be static in the transformed frame of reference, it must be moving at k_Δ in the experimental frame of reference.

This Hamiltonian was implemented using the Quantum Optics package (Krämer et al., 2018) using natural units. Physical units were then calculated once the simulations had concluded.

Three unit cells were simulated. Equal densities were apportioned to the b nodes and the simulation was run. It can be seen from Figure 14 that the different spin populations

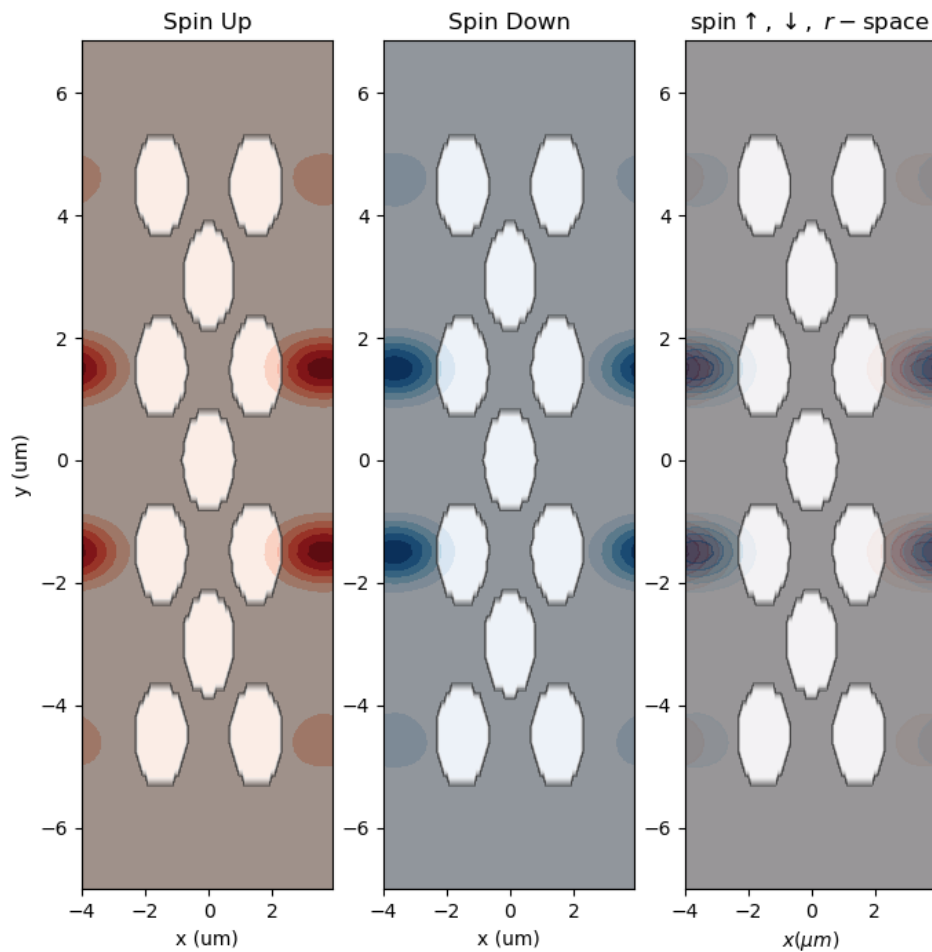


Figure 14: Spin populations of full spinor SOC Hamiltonian. The pump strength, Ω is 4 recoil units, the Zeeman splitting is 5.845 MHz, the radius of the wells is 0.8μ and the separation is $1.5 \mu\text{m}$. The SLM can resolve $0.8 \mu\text{m}$.

travel in different directions, that there is conversion from one spin population to another, and that there is tunneling between nodes. What is not present is any signature of CLSs.

The density movement is symmetric in space. Also, when the simulation is run further, the atoms travel outside the wells. There is a trade-off, if the wells are too deep, tunneling will not occur. As can be seen, the wells are not sufficiently deep to contain the atoms.

In order to attempt to remedy this problem, channels were added between the nodes. This was for the computer simulation, experimentally, the width of the channels are not resolvable. Figure 15 shows that the particles do follow the channels somewhat, but spill

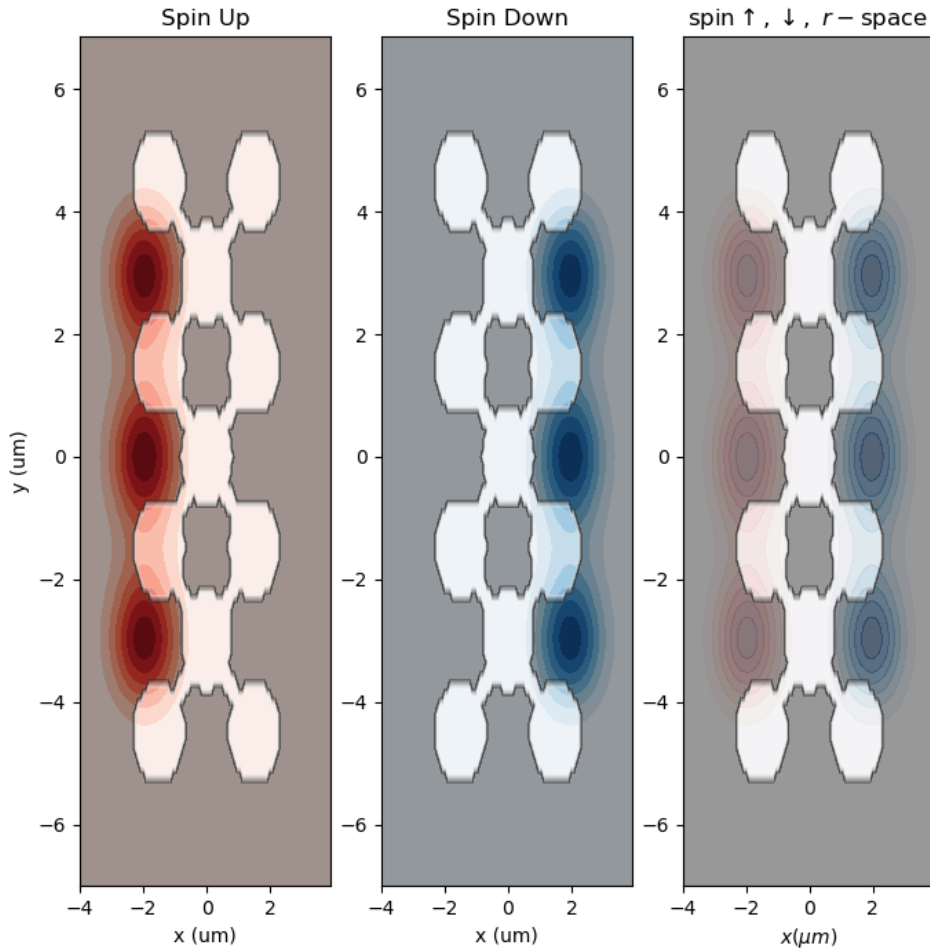


Figure 15: Spin populations of full spinor SOC Hamiltonian. The pump strength, Ω is 4 recoil units, the Zeeman splitting is 5.845 MHz, the radius of the wells is 0.8μ and the separation is $1.5 \mu\text{m}$. The SLM can resolve $0.8 \mu\text{m}$.

over the edges of the potential. What is not observed is the creation of CLSs, the atoms

separated symmetrically. This led to questioning the original model. While the argument appears sound, since we did not reproduce the results with the full GPE model, we wondered if there was some property of using discrete nodes that led to the observation of [CLSs](#).

Gligorić's Discrete GPE

The discrete model was implemented verbatim using the `DifferentialEquations` package of Julia (Bezanson et al., 2017). The same non-linearity parameters, $\gamma = \gamma_n = \zeta = 1$ were used, as well as a zero magnetic field, $B = 0$. The [SOC](#) parameter was $\lambda = 2$, exactly as in the figures of (Gligorić et al., 2016). Figure 16 shows the results of running the discrete model. With periodic boundary conditions, there was a symmetric distribution of densities between unit cells. Within unit cells, the distribution depended upon the spin state, but the b nodes were not all empty, as in the paper. Attempting to reproduce the uneven distribution, we looked at Dirichlet boundary conditions, in which the boundary values were locked to zero. The overall distribution was Gaussian, centred in the middle of the lattice and there was also separation of spin state, however, the distribution across unit cells still remains symmetrical. Figure 17 shows a time-series of one node.

We were unable to find [CLSs](#) using the discrete model. There was definitely separation of spin states, with the b node being occupied by one spin state and the a and c nodes being occupied by the opposite spin state. This is definitely different from the full GPE model. The difference lies in the fact that in the discrete model there is no way for atoms to spill over the node edges, and atoms can move backwards and forwards between the nodes. In the full GPE model the spin-flip operation was insufficiently strong to flip atoms quickly enough to then cause them to travel in the opposite direction. If we had used random initial conditions, with densities not uniformly spread over the b nodes, then it is likely that uneven distributions would arise. The theory behind the discrete model appears sound. Certain lattice configurations will generate flat bands that lead to localised position eigenstates. It seems that two factors have led to the inability of our two simulations to generate [CLSs](#). The full GPE model could not contain the atoms in the potential and the discrete model did not undergo symmetry-breaking.

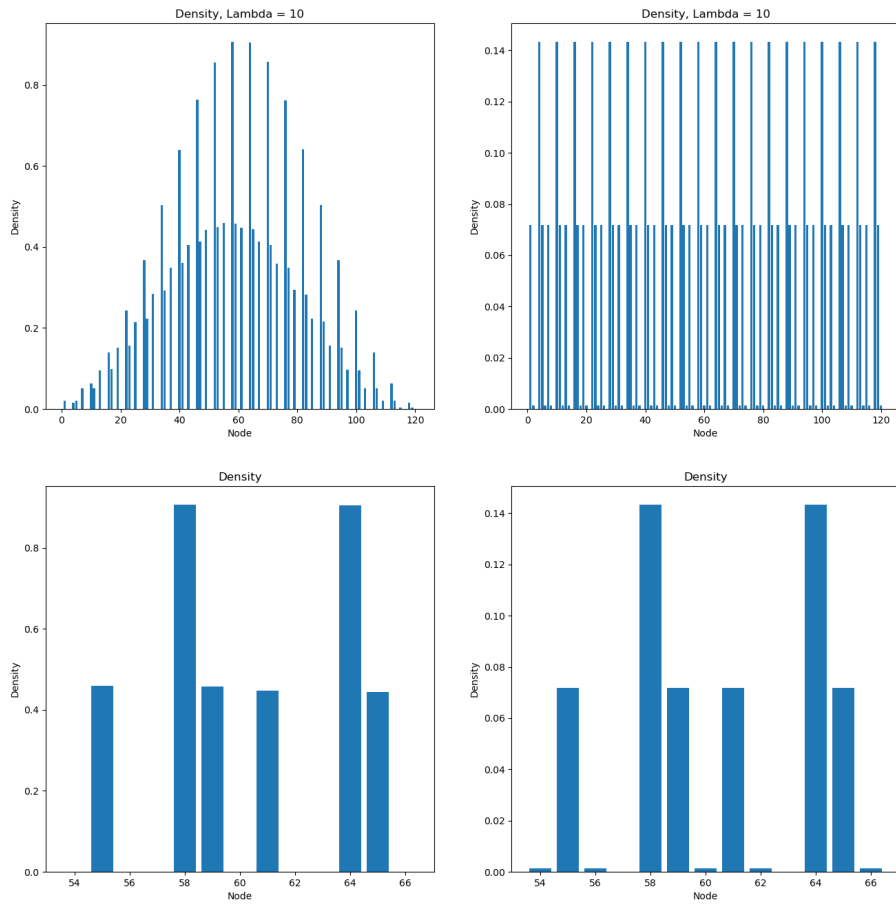
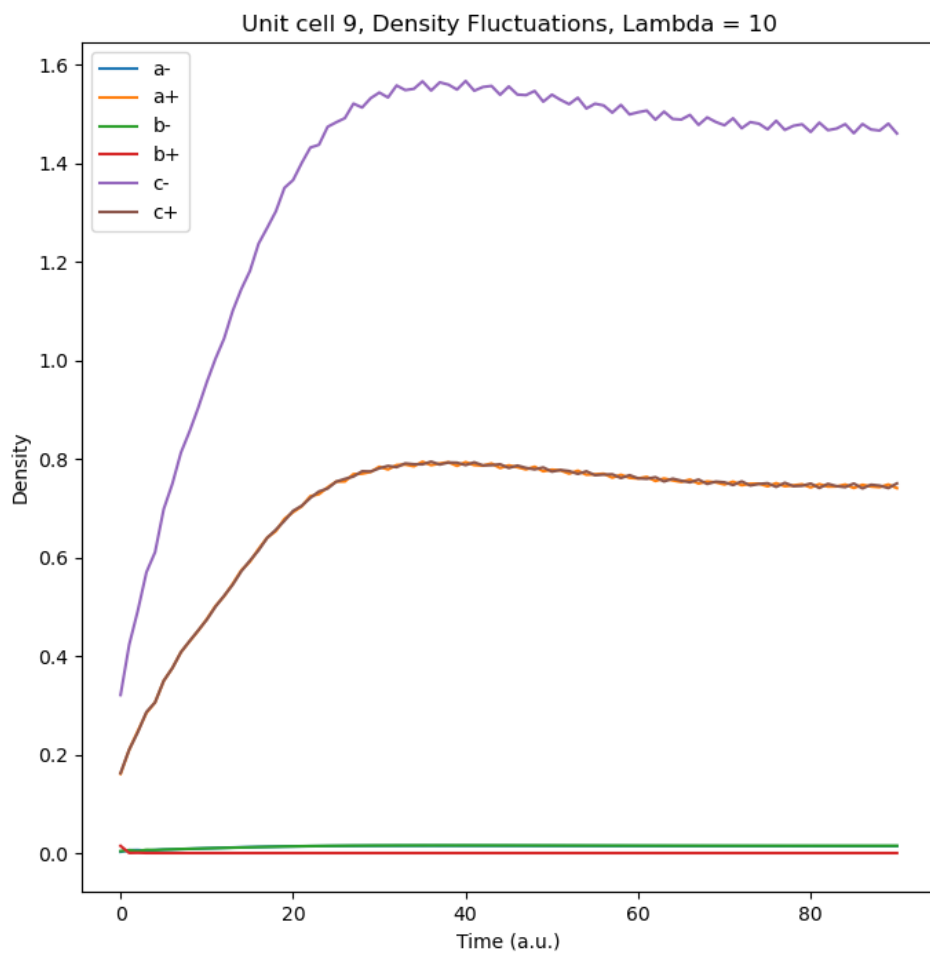


Figure 16: Left panels show Dirichlet boundary conditions and Right panels show periodic boundary conditions. Top panels are all twenty nodes and bottom panels show the central nodes. Each unit cell has 6 nodes, 3 spin up and 3 spin down. From left to right, the node order is $a^+, a^-, b^+, b^-, c^+, c^-$

Figure 17: Time series of node 9 for $\lambda = 10$

Conclusion

Form and Emptiness

*Body, supple and strong,
wind runs through my empty form —
All at once.*

How does the energy in a collective mode get transferred as useful work? Nonlinear crystals use wave mixing to stimulate electronic stimulation and emission. Can a breathing mode transfer collective energy? One possible mechanism by which collective oscillations generated by the action of the Na^+/K^+ pump could transfer energy is with the triggering of release of a membrane depolarisation.

One possible test to look for collective oscillations at the cellular level is to use a grid of electrodes to record the membrane signal of a *Xenopus laevis* oocyte *in vitro*. These frog eggs are large and are often used for patch-clamp neurophysiology experiments that examine the properties of transmembrane channels. The observations work by filling a micropipette with ionic fluid, trapping a single protein in the opening of the pipette, and measuring electrical changes with changes in treatment. What this method fails to reveal are the interactions between neighbouring proteins. By using a microelectrode array, such as that used with eCOG experiments with epileptic patients, the spatial variation in the field created by the Na^+/K^+ pump activity can be examined and searched for any collective behaviour. The ability of a condensate to exhibit superfluid *coherent* properties is a function of the interparticle force. So whether a condensate is a mesoscopic quantum object as a physical gestalt might best be left to philosophers.

As far as consciousness is concerned, is a condensate actually an addressable physical entity or is it merely a mathematical representation? Whether conscious awareness requires quantum phenomena might depend on whether one maintains that thought can be superposed or entangled. Perhaps this depends upon ideology. Even if condensates were related

to a mechanism behind a cohesive experience, they appear to be merely a mode of energy storage rather than a physical explanation for the reality of *qualia*¹. Perhaps the stretching of interstitial water molecules by membrane depolarisation induces nuclear contortions.

A condensate occurs when the interparticle spacing matches the matter wave extension. This implies that there is indeed some sort of shared reality and perhaps a physical unity arises. Certainly in certain representations, such as that of superposed number states, the representation implies a shared physical state.

If there is a shared physical state, then it seems that there should be some way to address the sum energy of the state and manipulate it to do useful work. Collision experiments between condensates show partial transparency and halos, which, while calculable in terms of the whole, can be explained by particle dynamics. Collective oscillations while interesting, need to be able to transfer energy. Quantum mechanically, wave mixing, where different energies of light join to create a packet of total energy, at the microscopic level works via electron excitation and de-excitation. What sort of mechanism could harness the sum energy of a condensate or collective oscillation and transfer it downstream?

When the de Broglie wavelength reaches the interparticle spacing, there is a need to represent the system of particles as an entangled superposition and thus each constituent is inseparable from the others, but is this merely a property of the signs we use to represent the reality? A label is a nifty means to attach a handle to a concept, but does that reification occur in the condensate system or in the mind of the researcher? But then, if a gestalt occurs in the mind, and we accept some sort of panprotopsychoist position, then that gestalt must have a material correlate, and is this a phenomenon such as a condensate?

If quantum mechanical phenomena are involved in consciousness, as mentioned in the introduction, then perhaps room temperature quasi-particles that hold their shape can be created by the brain. A likely location is the reticular formation of the thalamus, where those cells fire unless activated, and thus the activity highlights negative space. Memories are coordinated in the hippocampus, and various cortical columns, which represent a particular iota, are activated by the re-experiencing of a memory. The coordination likely occurs in the fronto-temporal region, where these iota are high-level representations. If a cortical column, as a collection of neurons, activates a particular pattern in the thalamus, and this pattern activates more experiential regions such as a pattern of visual cortex firing, then a sign of degradation of memory would be the inability of that column to activate a memory. Like a Hopfield network, that column would require a minimum pattern of connectivity. Furthermore, like Plato's aviary and a Hopfield network, memories require

¹A *quale* is an iota of felt experience

association. If an idea is subsequently contradicted, then there exists the danger that the iota connected with the contradicted idea become inaccessible. One clinical approach to ameliorating this decline would be to provide neurotrophic growth factors, such as in Olanzapine, in concert with auditory and visual re-stimulation and activation of networks that access those memories.

Examining the thermodynamic properties of a gas of bosons reduces the analysis to a spectrum of energy levels, and in this sense, all the particles in a condensate share a quantum state, however, in reality, particles have a massive nucleus, a position, and a momentum. The particles in a condensate do not all share the same position, even though their momenta might be close to identical, and so do indeed occupy a small volume of phase space. What quasi-particles lack is a massive nucleus, and so, a condensate of quasi-particles might indeed be closer to a mesoscopic quantum entity that can collectively transfer energy.

Light pulses have been stored in an atomic condensate cloud of Na atoms (R. Zhang, Garner, and Hau, 2009). The authors describe the light pulse as being imprinted on the collective wave function shared by all the atoms and then retrievable up to a second later. This interpretation, as opposed to the claim that the light pulse is transferring rapidly within the individual atoms in the cloud, certainly suggests that there is a collective quantum entity.

A condensate, be it ultracold alkali atoms, or quasi-particles, arises from a light-matter interaction. Electromagnetic energy interacts non-linearly with matter and leads to a non-dispersing collective packet of energy, that can breathe, that can propagate, that can interact, and that can represent state. Bose condensates provide a fascinating look into the world of the quantum, near the uncertainty limit and will provide a fertile ground for future investigation.

Light fields, specifically Raman two-photon transitions, can be used to couple the state of a condensate to its linear momentum. This introduces the equivalent of an electromagnetic force and thus, if it is possible to engineer CLSs then it is not inconceivable that a chemistry of condensates on lattices could be engineered. Using entanglement between condensates, a condensate molecule could be used to represent a unit in a quantum algebra that can be manipulated with algebraic operations.

Compact localised states result from there being a flat band in the momentum dispersion curve, so that there is a potential saddle in the distribution of atoms in position space, which would result in localisation. Another mechanism of localisation is Anderson localisation, which results from destructive interference in possible closed paths brought about by disorder in the potential.

Attempting to reproduce Gligorić's hypothesis theoretically was unsuccessful. The results might well have been reproduced in the experiment because of the natural disorder that might be present in an SLM image, thus leading to a symmetry breaking in space and a resultant appearance of [CLS](#).

We successfully conducted the experiment and provided the theoretical claim to prove that Einstein's assertion about the zero-kinetic energy requirement for condensation was false. We showed, using the de Broglie wavelength, that it is reasonable to expect room temperature quasi-particle condensates. I discussed phase coherence and collective oscillations, showing that the Na^+/K^+ pump meets Fröhlich's requirement for biological condensation. I have argued for the importance of a phase-alignment mechanism. Finally, I have discussed the theoretical claim that consciousness is quantum mechanical.

Appendices

Electromagnetic Fields

Lorentz Force Law

The derivation here is scattered throughout Cohen-Tannoudji, Diu, and Laloe (1977). In 1895 Lorentz derived his law that describes the force exerted on a moving, spin-less charged particle in an electric and a magnetic field,

$$\mathbf{F} = q(\mathbf{E} + \mathbf{v} \times \mathbf{B}), \quad (\text{A.1})$$

where q is the charge and \mathbf{v} is the velocity of the particle.

We start with Maxwell's equations,

$$\nabla \cdot \mathbf{E} = \frac{\rho}{\epsilon_0} \quad (\text{A.2})$$

$$\nabla \times \mathbf{E} = -\frac{\partial \mathbf{B}}{\partial t} \quad (\text{A.3})$$

$$\nabla \cdot \mathbf{B} = 0 \quad (\text{A.4})$$

$$\nabla \times \mathbf{B} = \mu_0 \mathbf{j} + \epsilon_0 \mu_0 \frac{\partial \mathbf{E}}{\partial t}, \quad (\text{A.5})$$

where ρ is the volume charge density and \mathbf{j} is the current density, which imply the existence of a vector potential \mathbf{A} and a scalar potential ϕ such that,

$$\mathbf{B}(\mathbf{r}, t) = \nabla \times \mathbf{A}(\mathbf{r}, t) \quad (\text{A.6})$$

$$\mathbf{E}(\mathbf{r}, t) = -\nabla \phi(\mathbf{r}, t) - \frac{\partial}{\partial t} \mathbf{A}(\mathbf{r}, t). \quad (\text{A.7})$$

We are working with electromagnetic fields in a vacuum (except for the actual target atoms), so we choose to work in the radiation (Coulomb) gauge, $\nabla \cdot \mathbf{E} = 0$. Rewriting Lorentz's force law,

$$m\ddot{\mathbf{r}} = q[\mathbf{E}(\mathbf{r}, t) + \dot{\mathbf{r}} \times \mathbf{B}(\mathbf{r}, t)]. \quad (\text{A.8})$$

Projecting onto an axis, in this case the x - axis, we have

$$m\ddot{x} = q[E_x + \dot{y}B_z - \dot{z}B_y] \quad (\text{A.9})$$

$$= q \left[-\frac{\partial\phi}{\partial x} - \frac{\partial A_x}{\partial t} + \dot{y} \left(\frac{\partial A_y}{\partial x} - \frac{\partial A_x}{\partial y} \right) - \dot{z} \left(\frac{\partial A_x}{\partial z} - \frac{\partial A_z}{\partial x} \right) \right] \quad (\text{A.10})$$

Guessing the Lagrangian

$$\mathcal{L}(\mathbf{r}, \dot{\mathbf{r}}, t) = \frac{1}{2}m\dot{\mathbf{r}}^2 + q\dot{\mathbf{r}} \cdot \mathbf{A}(\mathbf{r}, t) - q\phi(\mathbf{r}, t), \quad (\text{A.11})$$

we have,

$$\frac{\partial\mathcal{L}}{\partial\dot{x}} = m\dot{x} + qA_x(\mathbf{r}, t) \quad (\text{A.12})$$

$$\frac{\partial\mathcal{L}}{\partial x} = q\dot{\mathbf{r}} \cdot \frac{\partial}{\partial x} \mathbf{A}(\mathbf{r}, t) - q\frac{\partial}{\partial x} \phi(\mathbf{r}, t). \quad (\text{A.13})$$

From Lagrangian mechanics we know that

$$\frac{d}{dt} \frac{\partial\mathcal{L}}{\partial\dot{q}_i} - \frac{\partial\mathcal{L}}{\partial q} = 0, \quad (\text{A.14})$$

so,

$$\frac{d}{dt} [m\dot{x} + qA_x(\mathbf{r}, t)] - q\dot{\mathbf{r}} \cdot \frac{\partial}{\partial x} \mathbf{A}(\mathbf{r}, t) + q\frac{\partial}{\partial x} \phi(\mathbf{r}, t) = 0. \quad (\text{A.15})$$

Applying the time derivative we have,

$$m\ddot{x} + q \left[\frac{\partial A_x}{\partial t} + \dot{x} \frac{\partial A_x}{\partial x} + \dot{y} \frac{\partial A_x}{\partial y} + \dot{z} \frac{\partial A_x}{\partial z} \right] - q \left[\dot{x} \frac{\partial A_x}{\partial x} + \dot{y} \frac{\partial A_y}{\partial x} + \dot{z} \frac{\partial A_z}{\partial x} \right] + q \frac{\partial\phi}{\partial x} = 0, \quad (\text{A.16})$$

Thus,

$$m\ddot{x} = q \left[-\frac{\partial\phi}{\partial x} - \frac{\partial A_x}{\partial t} + \dot{y} \left(\frac{\partial A_y}{\partial x} - \frac{\partial A_x}{\partial y} \right) - \dot{z} \left(\frac{\partial A_x}{\partial z} - \frac{\partial A_z}{\partial x} \right) \right], \quad (\text{A.17})$$

which is exactly equation [A.10](#).

We can calculate the conjugate momentum, which is no longer the mechanical momentum $m\dot{\mathbf{r}}$, from the Lagrangian,

$$p_x = \frac{\partial \mathcal{L}}{\partial \dot{x}} = m\dot{x} + qA_x(\mathbf{r}, t), \quad (\text{A.18})$$

so,

$$\mathbf{p} = m\dot{\mathbf{r}} + q\mathbf{A}(\mathbf{r}, t), \quad (\text{A.19})$$

and

$$m\dot{\mathbf{r}} = \mathbf{p} - q\mathbf{A}(\mathbf{r}, t). \quad (\text{A.20})$$

We now convert to the Hamiltonian,

$$\mathcal{H}(\mathbf{r}, \mathbf{p}, t) = \mathbf{p} \cdot \dot{\mathbf{r}} - \mathcal{L}(\mathbf{r}, \dot{\mathbf{r}}, t) \quad (\text{A.21})$$

$$\begin{aligned} &= \mathbf{p} \cdot \frac{1}{m}(\mathbf{p} - q\mathbf{A}) - \frac{1}{2m}(\mathbf{p} - q\mathbf{A})^2 \\ &\quad - \frac{q}{m}(\mathbf{p} - q\mathbf{A}) \cdot \mathbf{A} + q\phi \end{aligned} \quad (\text{A.22})$$

$$= \frac{1}{2m}[\mathbf{p} - q\mathbf{A}(\mathbf{r}, t)]^2 + q\phi(\mathbf{r}, t), \quad (\text{A.23})$$

and since in the Coulomb gauge the scalar potential is zero, we are left with

$$\mathcal{H}(\mathbf{r}, \mathbf{p}, t) = \frac{1}{2m}[\mathbf{p} - q\mathbf{A}(\mathbf{r}, t)]^2. \quad (\text{A.24})$$

Thus, if a moving, spinless, charged particle is in an electromagnetic field, this is the single particle Hamiltonian.

Expanding the Hamiltonian We can expand the quadratic term in the Hamiltonian,

$$\hat{H}(t) = \frac{1}{2m}\mathbf{p}^2 - \frac{q}{2m}\mathbf{p} \cdot \mathbf{A}(\mathbf{r}, t) - \frac{q}{2m}\mathbf{A}(\mathbf{r}, t) \cdot \mathbf{p} + \frac{q^2}{2m}\mathbf{A}(\mathbf{r}, t)^2 \quad (\text{A.25})$$

We keep the vector potential classical and substitute the quantum mechanical momentum, $\mathbf{p} = -i\hbar\nabla$, so that we have the term

$$-\frac{q}{2m}\mathbf{p} \cdot \mathbf{A}(\mathbf{r}, t) - \frac{q}{2m}\mathbf{A}(\mathbf{r}, t) \cdot \mathbf{p} = -i\frac{q\hbar}{2m}(\nabla \cdot \mathbf{A} + \mathbf{A} \cdot \nabla). \quad (\text{A.26})$$

Since, by the chain rule, $\nabla \cdot \mathbf{A} = (\nabla \cdot \mathbf{A}) + \mathbf{A} \cdot \nabla$, and the first term is zero in the Coulomb gauge, we have

$$-\frac{q}{2m} \mathbf{p} \cdot \mathbf{A}(\mathbf{r}, t) - \frac{q}{2m} \mathbf{A}(\mathbf{r}, t) \cdot \mathbf{p} = i \frac{q\hbar}{m} \mathbf{A} \cdot \nabla = -\frac{q}{m} \mathbf{A}(\mathbf{r}, t) \cdot \mathbf{p}, \quad (\text{A.27})$$

and our Hamiltonian reads

$$\hat{H}(t) = \frac{1}{2m} \mathbf{p}^2 - \frac{q}{m} \mathbf{A}(\mathbf{r}, t) \cdot \mathbf{p} + \frac{q^2}{2m} \mathbf{A}(\mathbf{r}, t)^2 \quad (\text{A.28})$$

Zeeman Effect

In 1896, Zeeman discovered that a strong magnetic field would split lines in the emission spectrum of Sodium. The vector potential for a uniform magnetic field, \mathbf{B}_0 is

$$\mathbf{A}(\mathbf{r}, t) = -\frac{1}{2} \mathbf{r} \times \mathbf{B}_0. \quad (\text{A.29})$$

Using vector identities,

$$-\frac{q}{m} \mathbf{A}(\mathbf{r}, t) \cdot \mathbf{p} = \frac{q}{2m} (\mathbf{r} \times \mathbf{B}_0) \cdot \mathbf{p} = \frac{q}{2m} \mathbf{B}_0 \cdot (\mathbf{r} \times \mathbf{p}) \quad (\text{A.30})$$

$$= \frac{q}{2m} \mathbf{B}_0 \cdot \mathbf{L}, \quad (\text{A.31})$$

where \mathbf{L} is a generic angular momentum operator.

If we set a static magnetic field to be parallel to the z -axis, $\mathbf{B}_0 = B_z \mathbf{e}_z$, then we have

$$\mathbf{A}(\mathbf{r}, t) = \frac{1}{2} B_z (-y \mathbf{e}_x + x \mathbf{e}_y). \quad (\text{A.32})$$

We can see

$$\frac{q}{m} \mathbf{A}(\mathbf{r}, t) \cdot \mathbf{p} = \frac{q}{m} \frac{1}{2} B_z (-y \mathbf{e}_x + x \mathbf{e}_y) \cdot \mathbf{p} \quad (\text{A.33})$$

$$= \frac{q}{2m} B_z (-yp_x + xp_y), \quad (\text{A.34})$$

and the quantity $(xp_y - yp_x)$ is exactly the component of angular momentum in the z -direction, L_z . While this is a classical derivation from the notion of torque generated by a loop current, we can easily substitute quantum angular momentum operators for \mathbf{L} .

Looking at the term quadratic in $\mathbf{A}(\mathbf{r}, t)$, we have

$$\mathbf{A}(\mathbf{r}, t) \cdot \mathbf{A}(\mathbf{r}, t) = \frac{1}{2}B_z(-y\mathbf{e}_x + x\mathbf{e}_y) \cdot \frac{1}{2}B_z(-y\mathbf{e}_x + x\mathbf{e}_y) \quad (\text{A.35})$$

$$= \frac{1}{4}B_z^2(x^2 + y^2) \quad (\text{A.36})$$

This leads to the Hamiltonian

$$\hat{H} = \frac{1}{2m}\mathbf{p}^2 - \frac{q}{m}\mathbf{B}_0 \cdot \mathbf{L} + \frac{q^2}{8m}B_z^2(x^2 + y^2) \quad (\text{A.37})$$

The angular momentum operator L_z will choose m_ℓ energy levels, with energy difference,

$$\Delta E_{\text{lin}} = m_\ell \frac{q\hbar}{2m} B_z, \quad (\text{A.38})$$

This is the linear Zeeman effect and can be used to split the energy levels of different magnetic angular momentum states. The energy splitting attributable to the term quadratic in B_z gives rise to a small energy shift,

$$\Delta E_{\text{square}} = \frac{q^2}{8m}B_z^2(x^2 + y^2) \quad (\text{A.39})$$

When we looked at the angular momentum operator, that is in fact for a linear interaction. When we take into account the interactions between different shapes of the electron distribution, there can be higher-order interactions, such as between the s - and d - levels. Higher mass alkali atoms are not completely hydrogenic, as there are quantum defects and higher angular momentum quantum orbitals (ℓ), can be of lower energies than $\ell = 2$.

Spin and Magnetic Fields

The Stern-Gerlach experiment uncovered a previously unknown purely quantum mechanical feature of quantum particles, spin, which is an intrinsic angular momentum that is quantised (Gerlach and Stern, 1922). The existence of spin is contained in the spin-statistics theorem and the Pauli exclusion principle (Pauli, 1940).

The intrinsic magnetic moment $\boldsymbol{\mu}$ of a particle with spin angular momentum, $\mathbf{S} = \frac{\hbar}{2}\boldsymbol{\sigma}$, is

$$\boldsymbol{\mu} = \frac{g_s q}{2m} \frac{\hbar}{2} \boldsymbol{\sigma}, \quad (\text{A.40})$$

where g_s is the spin g -factor, which is about 2, and $\boldsymbol{\sigma}$ is the vector of Pauli spin matrices. These matrices for a spin-1 system can be derived from the spin-1/2 Pauli matrices and

can be decomposed into a one-dimensional singlet matrix and a three-dimensional triplet matrix,

$$\sigma_x = \frac{\hbar}{\sqrt{2}} \begin{bmatrix} 0 & 1 & 0 \\ 1 & 0 & 1 \\ 0 & 1 & 0 \end{bmatrix}, \quad (\text{A.41})$$

$$\sigma_y = \frac{\hbar}{\sqrt{2}} \begin{bmatrix} 0 & -i & 0 \\ i & 0 & -i \\ 0 & i & 0 \end{bmatrix}, \quad (\text{A.42})$$

$$\sigma_z = \frac{\hbar}{\sqrt{2}} \begin{bmatrix} 1 & 0 & 0 \\ 0 & 0 & 0 \\ 0 & 0 & -1 \end{bmatrix}. \quad (\text{A.43})$$

The force felt by a particle with spin in a magnetic field is

$$\mathbf{F} = -\nabla(\boldsymbol{\mu} \cdot \mathbf{B}), \quad (\text{A.44})$$

and so the potential is

$$U = -\frac{q\hbar}{2m} \boldsymbol{\sigma} \cdot \mathbf{B}. \quad (\text{A.45})$$

$$= -\frac{q\hbar}{2m} \boldsymbol{\sigma} \cdot \nabla \times \mathbf{A}(\mathbf{r}, t) \quad (\text{A.46})$$

Multiple Electromagnetic Potentials

If we have two electromagnetic potentials, for example, one for a laser field, \mathbf{A}_L , and one for a magnetic field, \mathbf{A}_M , then we can treat them separately as the dot product distributes over addition and the gradient operator also distributes over addition,

$$\mathbf{A} \cdot \mathbf{p} = (\mathbf{A}_L + \mathbf{A}_M) \cdot \mathbf{p} = (\mathbf{A}_L \cdot \mathbf{p}) + (\mathbf{A}_M \cdot \mathbf{p}) \quad (\text{A.47})$$

$$\nabla \times \mathbf{A} = \nabla \times (\mathbf{A}_L + \mathbf{A}_M) = (\nabla \times \mathbf{A}_L) + (\nabla \times \mathbf{A}_M) \quad (\text{A.48})$$

Anomalous Zeeman Effect

Spin-Momentum Hamiltonian

We derived the Hamiltonian for an atom in an electromagnetic field, in this case we have two fields, the laser fields and the static magnetic field,

$$\hat{H}_{EM} = \frac{1}{2m} (\mathbf{p} - \mathbf{A}(\mathbf{r}, t))^2. \quad (\text{B.1})$$

The electromagnetic fields can be separated,

$$\mathbf{A}(\mathbf{r}, t) = \mathbf{A}_L(\mathbf{r}, t) + \mathbf{A}_M(\mathbf{r}, t). \quad (\text{B.2})$$

Leading to,

$$\hat{H}_{EM} = \frac{1}{2m} [\mathbf{p}^2 - 2q(\mathbf{A}_L(\mathbf{r}, t) + \mathbf{A}_M(\mathbf{r}, t)) \cdot \mathbf{p} + q^2(\mathbf{A}_L(\mathbf{r}, t) + \mathbf{A}_M(\mathbf{r}, t))^2] \quad (\text{B.3})$$

The kinetic energy term can be taken out and we may include a static, scalar potential, such as a harmonic trap, $U(\mathbf{r}, t) = -k\mathbf{r}^2$, leading to the atomic term,

$$\hat{H}_0 = \frac{1}{2m} \mathbf{p}^2 + U(\mathbf{r}). \quad (\text{B.4})$$

We can break down the remaining terms into interaction terms and quadratic terms,

$$\hat{H}_I = -\frac{q}{m} (\mathbf{A}_L(\mathbf{r}, t) + \mathbf{A}_M(\mathbf{r}, t)) \cdot \mathbf{p} \quad (\text{B.5})$$

$$\hat{H}_Q = \frac{q^2}{2m} (\mathbf{A}_L(\mathbf{r}, t)^2 + \mathbf{A}_L(\mathbf{r}, t) \cdot \mathbf{A}_M(\mathbf{r}, t) + \mathbf{A}_M(\mathbf{r}, t)^2). \quad (\text{B.6})$$

In the interaction term, the potentials are separable, leading to two terms, one the recognisable interaction term normally reduced to the electric dipole interaction, and the other the term that expresses the interaction of an atom with a static electromagnetic field,

$$\hat{H}_I = -\frac{q}{m}\mathbf{A}_L(\mathbf{r}, t) \cdot \mathbf{p} - \frac{q}{m}\mathbf{B}_0 \cdot \mathbf{L}. \quad (\text{B.7})$$

In the quadratic term we have first a laser term, the intensity for which required is too high an energy beam achievable only by a short-pulse, the interaction of the laser field and the static magnetic field, which may couple via the atom, and finally, the magnetic field term. The first of these terms may be discarded. For the second term, the diameter of an atom is around 10^{-10} m, whereas the wavelength of the laser we used in our experiment is around 10^{-6} m, so the atom, to first approximation, neglecting the wavevector dependence, sees a constant electromagnetic field. From equation A.39, we can see that the energy shift of the second term in B.6 above is not asymmetrical and thus *would not lead to the ability to adiabatically eliminate a spin state*, what is more, this term increases the energy of all spin states equally in the same direction, leaving us free to ignore this term when relying on relative energy gaps between sub-states — this term may be gauged away. Thus, we may ignore all three quadratic terms.

We must point out that the quadratic interaction term involves an oscillating field and a static magnetic field, both of which are nearly resonant with the atom, one with the hyperfine splitting and the other with the spin moments. This would be manifest as slow wave breathing if at all possible.

So we have a perturbation to the Hamiltonian. In the case we are modelling, we have the following perturbation to the single particle Hamiltonian,

$$\hat{V} = -\frac{q^2}{2m}\mathbf{A}_L(\mathbf{r}, t) \cdot \mathbf{p} - \frac{q^2}{m}\mathbf{B}_0 \cdot \mathbf{L}, \quad (\text{B.8})$$

leading to our Hamiltonian,

$$\hat{H} = \hat{H}_0 + \hat{V}. \quad (\text{B.9})$$

Counter-propagating beams

Here we draw from Goldman (2014) and Pitaevskii (2016). We orient our coordinate system so that the axis of quantisation, the direction of the static magnetic field, is the vertical z -axis, and our laser beams propagate along the y -axis. The vector potential of a single

monochromatic source propagating in the y direction with angular frequency, ω , and with wavevector $k = \frac{\omega}{c}$, is

$$\begin{aligned}\mathbf{A}_L(\mathbf{r}, t) &= -A_0 \exp i(ky - \omega t)\mathbf{e}_x - A_0^* \exp -i(ky - \omega t)\mathbf{e}_x^* \\ &= -A_0 \exp i(ky - \omega t)\mathbf{e}_x + \text{complex conjugate}\end{aligned}\quad (\text{B.10})$$

We choose A_0 to be pure imaginary. Eliding the complex conjugate for the moment, if we have two counterpropagating beams, A, B , of orthogonal linear polarisation sourced from the same laser, directed through a linear polariser, and split with a polarising beam-splitter, thus locking the phase,

$$\mathbf{A}_L(\mathbf{r}, t) = \mathbf{A}_L(\mathbf{r}, t)_A + \mathbf{A}_L(\mathbf{r}, t)_B \quad (\text{B.11})$$

$$\begin{aligned}&= -A_0 \exp i(k_A y - \omega_A t)\mathbf{e}_x \\ &\quad + A_0 \exp -i(k_B y - \omega_B t)\mathbf{e}_z.\end{aligned}\quad (\text{B.12})$$

Using the definitions with a frequency offset of $2\omega_\Delta$, so that

$$k_A = k + k_\Delta \quad (\text{B.13})$$

$$k_B = k - k_\Delta \quad (\text{B.14})$$

$$\omega_A = \omega + \omega_\Delta \quad (\text{B.15})$$

$$\omega_B = \omega - \omega_\Delta, \quad (\text{B.16})$$

and the abbreviations

$$e^{\pm A} = \exp \pm i(k_A y - \omega_A t) \quad (\text{B.17})$$

$$e^{\pm B} = \exp \pm i(k_B y - \omega_B t) \quad (\text{B.18})$$

$$e^\pm = \exp \pm i(ky - \omega t) \quad (\text{B.19})$$

$$e^{\pm \Delta} = \exp \pm i(k_\Delta y - \omega_\Delta t), \quad (\text{B.20})$$

we have

$$\mathbf{A}_L(\mathbf{r}, t) = -A_0[e^A \mathbf{e}_x - e^{-B} \mathbf{e}_z] \quad (\text{B.21})$$

$$= -A_0 e^\Delta [e^+ \mathbf{e}_x - e^- \mathbf{e}_z]. \quad (\text{B.22})$$

Then,

$$\mathbf{B}_L(\mathbf{r}, t) = \nabla \times \mathbf{A}_L(\mathbf{r}, t) \quad (\text{B.23})$$

$$= -iA_0[k_B e^{-B} \mathbf{e}_x - k_A e^A \mathbf{e}_z] \quad (\text{B.24})$$

$$= -iA_0 e^\Delta [k_B e^- \mathbf{e}_x - k_A e^+ \mathbf{e}_z] \quad (\text{B.25})$$

Using the identities for right- and left- circular polarised light,

$$\mathbf{e}_+ = \frac{1}{\sqrt{2}}(\mathbf{e}_x + i\mathbf{e}_z) \quad (\text{B.26})$$

$$\mathbf{e}_- = \frac{1}{\sqrt{2}}(\mathbf{e}_x - i\mathbf{e}_z), \quad (\text{B.27})$$

we have for x- and z- linearly polarised light,

$$\mathbf{e}_x = \frac{1}{\sqrt{2}}(\mathbf{e}_+ + \mathbf{e}_-) \quad (\text{B.28})$$

$$\mathbf{e}_z = -i\frac{1}{\sqrt{2}}(\mathbf{e}_+ - \mathbf{e}_-). \quad (\text{B.29})$$

Substituting these in we have,

$$\mathbf{A}_L(\mathbf{r}, t) = -A_0 e^\Delta [e^+ \frac{1}{\sqrt{2}}(\mathbf{e}_+ + \mathbf{e}_-) - e^- (-i) \frac{1}{\sqrt{2}}(\mathbf{e}_+ - \mathbf{e}_-)] \quad (\text{B.30})$$

$$= -A_0 e^\Delta \frac{1}{\sqrt{2}} [e^+ \mathbf{e}_+ + e^+ \mathbf{e}_- + ie^- \mathbf{e}_+ - ie^- \mathbf{e}_-] \quad (\text{B.31})$$

$$= -A_0 e^\Delta \frac{1}{\sqrt{2}} [(e^+ + ie^-) \mathbf{e}_+ + (e^+ - ie^-) \mathbf{e}_-] \quad (\text{B.32})$$

and

$$\mathbf{B}_L(\mathbf{r}, t) = -iA_0 e^\Delta [k_B e^- \frac{1}{\sqrt{2}}(\mathbf{e}_+ + \mathbf{e}_-) - k_A e^+ (-i) \frac{1}{\sqrt{2}}(\mathbf{e}_+ - \mathbf{e}_-)] \quad (\text{B.33})$$

$$= -iA_0 e^\Delta \frac{1}{\sqrt{2}} [k_B e^- \mathbf{e}_+ + k_B e^- \mathbf{e}_- + ik_A e^+ \mathbf{e}_+ - ik_A e^+ \mathbf{e}_-] \quad (\text{B.34})$$

$$= -iA_0 e^\Delta \frac{1}{\sqrt{2}} [(k - k_\Delta) e^- \mathbf{e}_+ + (k - k_\Delta) e^- \mathbf{e}_- + i(k + k_\Delta) e^+ \mathbf{e}_+ - i(k + k_\Delta) e^+ \mathbf{e}_-] \quad (\text{B.35})$$

$$= -iA_0 e^\Delta \frac{1}{\sqrt{2}} [(k(e^- + ie^+) - k_\Delta(e^- - ie^+)) \mathbf{e}_+ + (k(e^- - ie^+) - k_\Delta(e^- + ie^+)) \mathbf{e}_-]. \quad (\text{B.36})$$

Using the identities

$$e^\theta + ie^{-\theta} = \sqrt{2}e^{i\frac{\pi}{4}} \cdot \sin\left(\theta + \frac{\pi}{4}\right) \quad (\text{B.37})$$

$$e^\theta - ie^{-\theta} = \sqrt{2}e^{-i\frac{\pi}{4}} \cdot \cos\left(\theta + \frac{\pi}{4}\right) \quad (\text{B.38})$$

$$e^{-\theta} + ie^\theta = \sqrt{2}e^{i\frac{\pi}{4}} \cdot \cos\left(\theta + \frac{\pi}{4}\right) \quad (\text{B.39})$$

$$e^{-\theta} - ie^\theta = \sqrt{2}e^{-i\frac{\pi}{4}} \cdot \sin\left(\theta + \frac{\pi}{4}\right), \quad (\text{B.40})$$

Setting $\theta = ky - \omega t + \frac{\pi}{4}$, we have

$$\mathbf{A}_L(\mathbf{r}, t) = -A_0 e^\Delta \frac{1}{\sqrt{2}} \left[\sqrt{2}e^{i\frac{\pi}{4}} \sin\theta \mathbf{e}_+ + \sqrt{2}e^{-i\frac{\pi}{4}} \cos\theta \mathbf{e}_- \right] \quad (\text{B.41})$$

$$= -A_0 e^\Delta e^{i\frac{\pi}{4}} [\sin\theta \mathbf{e}_+ - i \cos\theta \mathbf{e}_-] \quad (\text{B.42})$$

and

$$\begin{aligned} \mathbf{B}_L(\mathbf{r}, t) &= -iA_0 e^\Delta \frac{1}{\sqrt{2}} \left[\left(k\sqrt{2}e^{i\frac{\pi}{4}} \cos\theta - k_\Delta \sqrt{2}e^{-i\frac{\pi}{4}} \sin\theta \right) \mathbf{e}_+ \right. \\ &\quad \left. + \left(k\sqrt{2}e^{-i\frac{\pi}{4}} \sin\theta - k_\Delta \sqrt{2}e^{i\frac{\pi}{4}} \cos\theta \right) \mathbf{e}_- \right] \end{aligned} \quad (\text{B.43})$$

$$\begin{aligned} &= -iA_0 e^\Delta e^{i\frac{\pi}{4}} [(k \cos\theta + ik_\Delta \sin\theta) \mathbf{e}_+ \\ &\quad + (ik \sin\theta + k_\Delta \cos\theta) \mathbf{e}_-]. \end{aligned} \quad (\text{B.44})$$

Now, recalling that $\mathbf{e}_+^* = \mathbf{e}_-$, we write the complex conjugate,

$$\begin{aligned} \mathbf{A}_L(\mathbf{r}, t) &= -A_0 e^\Delta e^{i\frac{\pi}{4}} [\sin\theta \mathbf{e}_+ - i \cos\theta \mathbf{e}_-] \\ &\quad + A_0 e^{-\Delta} e^{-i\frac{\pi}{4}} [\sin\theta \mathbf{e}_+^* + i \cos\theta \mathbf{e}_-^*] \end{aligned} \quad (\text{B.45})$$

and

$$\begin{aligned} \mathbf{B}_L(\mathbf{r}, t) &= -iA_0 e^\Delta e^{i\frac{\pi}{4}} [(k \cos\theta + ik_\Delta \sin\theta) \mathbf{e}_+ \\ &\quad + (ik \sin\theta + k_\Delta \cos\theta) \mathbf{e}_-] \\ &\quad - iA_0 e^{-\Delta} e^{-i\frac{\pi}{4}} [(k \cos\theta - ik_\Delta \sin\theta) \mathbf{e}_+^* \\ &\quad - (ik \sin\theta - k_\Delta \cos\theta) \mathbf{e}_-^*]. \end{aligned} \quad (\text{B.46})$$

Unitary Transform We now digress. If we want to make a canonical transform of coordinates accompanied by a unitary transform of the Hamiltonian, the wavefunction changes

$$\psi \rightarrow \psi' = U\psi \quad (\text{B.47})$$

and the Hamiltonian changes

$$\hat{H} \rightarrow \hat{H}' = U\hat{H}U^\dagger + i\hbar\dot{U}U^\dagger. \quad (\text{B.48})$$

We are going to perform a combined rotation and spin flip, so that our transformation is

$$U = \exp -i(k_\Delta y - \omega_\Delta t) \cdot \sigma_x, \quad (\text{B.49})$$

This will act to rotate the cylindrically polarised unit vectors,

$$\mathbf{e}_+ \rightarrow \exp -i \left(k_\Delta y - \omega_\Delta t + \frac{\pi}{4} \right) \cdot \sigma_x \mathbf{e}_+ \quad (\text{B.50})$$

$$\mathbf{e}_- \rightarrow \exp -i \left(k_\Delta y - \omega_\Delta t + \frac{\pi}{4} \right) \cdot \sigma_x \mathbf{e}_- \quad (\text{B.51})$$

$$\mathbf{e}_+^* \rightarrow \exp i \left(k_\Delta y - \omega_\Delta t + \frac{\pi}{4} \right) \cdot \sigma_x \mathbf{e}_- \quad (\text{B.52})$$

$$\mathbf{e}_-^* \rightarrow \exp i \left(k_\Delta y - \omega_\Delta t + \frac{\pi}{4} \right) \cdot \sigma_x \mathbf{e}_+, \quad (\text{B.53})$$

So, delaying applying the transform to the Hamiltonian, we change our basis vectors, and the slowly moving Δ wave is transformed away,

$$\begin{aligned} \mathbf{A}_L(\mathbf{r}, t) &= -A_0 \exp \sigma_x [\sin \theta \mathbf{e}_+ - i \cos \theta \mathbf{e}_-] \\ &\quad + A_0 \exp \sigma_x [\sin \theta \mathbf{e}_- + i \cos \theta \mathbf{e}_+] \\ &= iA_0 e^{\sigma_x} [e^{i\theta} \mathbf{e}_+ + e^{-i\theta} \mathbf{e}_-] \end{aligned} \quad (\text{B.54})$$

and

$$\begin{aligned} \mathbf{B}_L(\mathbf{r}, t) &= -iA_0 \exp \sigma_x [(k \cos \theta + ik_\Delta \sin \theta) \mathbf{e}_+ \\ &\quad + (ik \sin \theta + k_\Delta \cos \theta) \mathbf{e}_-] \\ &\quad - iA_0 \exp \sigma_x [(k \cos \theta - ik_\Delta \sin \theta) \mathbf{e}_- \\ &\quad - (ik \sin \theta - k_\Delta \cos \theta) \mathbf{e}_+] \end{aligned} \quad (\text{B.55})$$

$$= -iA_0 e^{\sigma_x} [k(e^{-i\theta} \mathbf{e}_+ + e^{i\theta} \mathbf{e}_-) + k_\Delta(e^{i\theta} \mathbf{e}_+ + e^{-i\theta} \mathbf{e}_-)]. \quad (\text{B.56})$$

If we look at the exponential terms and only consider first order interactions, then the following approximation holds,

$$e^{\mp i(ky - \omega t)} = e^{\mp iky} e^{\pm i\omega t} = e^{\pm i\omega t} \cdot [1 \pm iky - \frac{1}{2}k^2 y^2 + \dots] = e^{\pm i\omega t}, \quad (\text{B.57})$$

and so the energy shift is symmetric. Only when moments higher than the quadrupole term are considered will there be an adiabatic elimination because of the energy difference between paramagnetically and diamagnetically aligned spin moments in the static magnetic field and also the powers of i introduce a directional asymmetry.

Comparison with Masson

I attempted to follow the derivation of Masson, but needed to include both upper manifolds, because in the experiment the lasers were detuned at the wavelength that minimises the scalar light shift, have, setting $\Omega_+ = \Omega_- = \Omega_{\pm} = \frac{1}{2}\Omega$, the detunings, where we consider $\omega_A = \omega_B = \omega$ for the detunings and $\Delta_2 = \omega - \omega_2$ and $\Delta_1 = \omega - \omega_2$, the Hamiltonian has a prefactor,

$$-\frac{1}{48}A_0^2\Omega_{\pm}^2 \quad (\text{B.58})$$

and his method leads to

$$\begin{aligned} \hat{H} = & \left(32 \frac{1}{\Delta_2} + 16 \frac{1}{\Delta_1} \right) \mathbf{1} \\ & - \begin{bmatrix} 0 & e^{-i\omega t} & 0 \\ e^{i\omega t} & 0 & e^{-i\omega t} \\ 0 & e^{i\omega t} & 0 \end{bmatrix} 8\sqrt{2} \left(\frac{1}{\Delta_2} - \frac{1}{\Delta_1} \right) \cos((k_A - k_B)y - (\omega_A - \omega_B)t) \\ & + \begin{bmatrix} 0 & 0 & e^{-i\omega t} \\ 0 & 0 & 0 \\ e^{i\omega t} & 0 & 0 \end{bmatrix} \left(5 \frac{1}{\Delta_2} + \frac{1}{\Delta_1} \right). \quad (\text{B.59}) \end{aligned}$$

This does not match the Hamiltonian I wrote down for my simulations and also does not match the Hamiltonian matching mine that Caspar Groiseau derived for me. This method only took account of the linear interactions. And, I must point out that when the detunings match, the cos term is multiplied by a factor of 0.

Wigner-Eckhart Theorem

The Wigner-Eckhart Theorem shows that when operating to modify the angular momentum of a state, the transition between any two specific states is proportional to the Clebsch-Gordon coefficients, which are symmetric, and have no dependence upon magnetic substates.

Group Theory

The state of a valence electron is in the group $SO(3, \mathbb{C}) \otimes SU(2, \mathbb{C})$, representing the three magnetic sublevels, $\ell = 2, m = -0, \pm 1$, and the two spin states of the electron, $s = \pm \frac{1}{2}$. The group $SO(3, \mathbb{R})$ is the Euclidean rotation group, which is not simply connected, however, the Hilbert space is a complex space, and, fortunately, $SO(3, \mathbb{C})$, which represents a Lie group, is simply connected. The irreducible dimension of the above tensor product is $4 \otimes 2$, which is not what is achieved in classical spherical tensor operations. Complex position space might be representable as the three directions plus the potential of the electromagnetic field and the spin space is represented by two orientations. There appears to be no symmetry-breaking possible in the complex position space. The group is Abelian, and to make a transition from one state to another via an intermediary that is unbalanced would require a different operation for the reverse transition, but an Abelian group is commutative.

The two spin states have different energy levels in a magnetic field because of the difference between paramagnetic and diamagnetic alignment. This can lead to symmetry breaking and could explain the mechanism behind uneven energy shifts in a Raman optical transition in the presence of a medium strength magnetic field.

Postscript

If consciousness is quantum mechanical, and if dharma can exist as solitons, then the memory of Princess Diana lives on.

Works cited

- Alexander, J. C. (1986). “Patterns at primary hopf bifurcations of a plexus of identical oscillators”. In: *SIAM Journal on Applied Mathematics* 46 (2), pp. 199–221. ISSN: 00361399. DOI: [10.1137/0146015](https://doi.org/10.1137/0146015). URL: <https://epubs.siam.org/page/terms> (cit. on p. 21).
- Anderson, B. P. and Kasevich, M. A. (1998). “Macroscopic Quantum Interference from Atomic Tunnel Arrays”. In: *Science* 282 (5394), pp. 1686–1689. ISSN: 1095-9203. DOI: [10.1126/science.282.5394.1686](https://doi.org/10.1126/science.282.5394.1686). URL: <http://www.sciencemag.org/cgi/doi/10.1126/science.282.5394.1686> (cit. on p. 38).
- Anderson, M. H., Ensher, J. R., Matthews, M. R., Wieman, C. E., and Cornell, E. A. (July 1995a). “Observation of Bose-Einstein condensation in a dilute atomic vapor”. In: *Science* 269 (5221), pp. 198–201. ISSN: 00368075. DOI: [10.1126/science.269.5221.198](https://doi.org/10.1126/science.269.5221.198). URL: <http://www.ncbi.nlm.nih.gov/pubmed/17789847> (cit. on p. 1).
- Anderson, M. H., Ensher, J. R., Matthews, M. R., Wieman, C. E., and Cornell, E. A. (1995b). “Observation of Bose-Einstein Condensation in a Dilute Atomic Vapor”. In: *Science* 269 (5221) (cit. on p. 35).
- Anderson, P. W. (1958). “Absence of diffusion in certain random lattices”. In: *Physical Review* 109 (5), pp. 1492–1505. ISSN: 0031899X. DOI: [10.1103/PhysRev.109.1492](https://doi.org/10.1103/PhysRev.109.1492) (cit. on p. 42).
- Aoki, H., Ando, M., and Matsumura, H. (1996). “Hofstadter butterflies for flat bands”. In: *Physical Review B - Condensed Matter and Materials Physics* 54 (24), R17296–R17299. ISSN: 1550235X. DOI: [10.1103/PhysRevB.54.R17296](https://doi.org/10.1103/PhysRevB.54.R17296) (cit. on p. 41).
- Atala, M., Aidelsburger, M., Lohse, M., Barreiro, J. T., Paredes, B., and Bloch, I. (2014). “Observation of chiral currents with ultracold atoms in bosonic ladders”. In: *Nature Physics* 10 (8), pp. 588–593. ISSN: 17452481. DOI: [10.1038/nphys2998](https://doi.org/10.1038/nphys2998) (cit. on p. 39).
- Becker, D., Lachmann, M. D., Seidel, S. T., Ahlers, H., Dinkelaker, A. N., Grosse, J., Hellmig, O., Müntinga, H., Schkolnik, V., Wendrich, T., Wenzlawski, A., Weps, B., Corgier, R., Franz, T., Gaaloul, N., Herr, W., Lüdtke, D., Popp, M., Amri, S., Duncker, H., Erbe, M., Kohfeldt, A., Kubelka-Lange, A., Braxmaier, C., Charron, E., Ertmer,

- W., Krutzik, M., Lämmerzahl, C., Peters, A., Schleich, W. P., Sengstock, K., Walser, R., Wicht, A., Windpassinger, P., and Rasel, E. M. (2018). “Space-borne Bose–Einstein condensation for precision interferometry”. In: *Nature* 562 (7727), pp. 391–395. ISSN: 14764687. DOI: [10.1038/s41586-018-0605-1](https://doi.org/10.1038/s41586-018-0605-1). URL: <http://dx.doi.org/10.1038/s41586-018-0605-1> (cit. on p. 17).
- Beličev, P. P., Gligorić, G., Petrovic, J., Maluckov, A., Hadžievski, L., and Malomed, B. A. (Mar. 2015). “Composite localized modes in discretized spin-orbit-coupled Bose-Einstein condensates”. In: *Journal of Physics B: Atomic, Molecular and Optical Physics* 48 (6), p. 065301. ISSN: 13616455. DOI: [10.1088/0953-4075/48/6/065301](https://doi.org/10.1088/0953-4075/48/6/065301). URL: <http://stacks.iop.org/0953-4075/48/i=6/a=065301?key=crossref.a96f42d4a4f5b25cc4729047b0781421> (cit. on p. 44).
- Beugeling, W., Goldman, N., and Smith, C. M. (Aug. 2012). “Topological phases in a two-dimensional lattice: Magnetic field versus spin-orbit coupling”. In: *Physical Review B* 86 (7), p. 075118. ISSN: 1098-0121. DOI: [10.1103/PhysRevB.86.075118](https://doi.org/10.1103/PhysRevB.86.075118). URL: <https://link.aps.org/doi/10.1103/PhysRevB.86.075118> (cit. on p. 38).
- Bezanson, J., Edelman, A., Karpinski, S., and Shah, V. B. (2017). “Julia: A fresh approach to numerical computing”. In: *SIAM Review* 59 (1), pp. 65–98. ISSN: 00361445. DOI: [10.1137/141000671](https://doi.org/10.1137/141000671) (cit. on p. 55).
- Blakie, P. B., Bradley, A. S., Davis, M. J., Ballagh, R. J., and Gardiner, C. W. (2008). “Dynamics and statistical mechanics of ultra-cold Bose gases using c-field techniques”. In: *Advances in Physics* 57 (5), pp. 363–455. ISSN: 1460-6976. DOI: [10.1080/00018730802564254](https://doi.org/10.1080/00018730802564254). URL: <https://www.tandfonline.com/action/journalInformation?journalCode=tadp20> (cit. on p. 12).
- Bloch, I., Dalibard, J., and Nascimbène, S. (Apr. 2012). “Quantum simulations with ultracold quantum gases”. In: *Nature Physics* 8 (4), pp. 267–276. ISSN: 1745-2473. DOI: [10.1038/nphys2259](https://doi.org/10.1038/nphys2259). URL: <http://www.nature.com/articles/nphys2259> (cit. on p. 35).
- Bodyfelt, J. D., Leykam, D., Danieli, C., Yu, X., and Flach, S. (2014). “Flatbands under correlated perturbations”. In: *Physical Review Letters* 113 (23), pp. 1–5. ISSN: 10797114. DOI: [10.1103/PhysRevLett.113.236403](https://doi.org/10.1103/PhysRevLett.113.236403) (cit. on p. 44).
- Bose, S. N. (1924). “Planck’s Law and Light Quantum Hypothesis.” In: *Zeitschrift für Physik* 26 (Received), pp. 1–4. ISSN: 1434-6001. DOI: [10.1007/BF01327326](https://doi.org/10.1007/BF01327326) (cit. on p. 5).
- Brown, D. J., McPhail, A. V. H., White, D. H., Baillie, D., Ruddell, S. K., and Hoogerland, M. D. (2018). “Thermalization, condensate growth, and defect formation in an out-of-equilibrium Bose gas”. In: *Physical Review A* 98 (1), pp. 1–6. ISSN: 24699934. DOI: [10.1103/PhysRevA.98.013606](https://doi.org/10.1103/PhysRevA.98.013606) (cit. on pp. xix, 2, 12, 14).

- Brown, D. J. (2014). “Raman Processes and Synthetic Gauge Fields in Bose-Einstein Condensates”. University of Auckland (cit. on p. 40).
- Brown, D. J. (2019). “Non-Equilibrium Dynamics of Bose-Einstein Condensates”. University of Auckland (cit. on pp. 47, 51).
- Buluta, I. and Nori, F. (2009). “Quantum Simulators”. In: *Science* 326 (1), pp. 108–111 (cit. on p. 35).
- Buzsáki, G., Anastassiou, C. A., and Koch, C. (June 2012). “The origin of extracellular fields and currents-EEG, ECoG, LFP and spikes”. In: *Nature Reviews Neuroscience* 13 (6), pp. 407–420. ISSN: 1471003X. DOI: [10.1038/nrn3241](https://doi.org/10.1038/nrn3241). URL: <https://www.nature.com/articles/nrn3241> (cit. on p. 24).
- Bychkov, Y. A. and Rashba, E. I. (1984). “Oscillatory effects and the magnetic susceptibility of carriers in inversion layers”. In: *Journal of Physics C: Solid State Physics* 17 (33), pp. 6039–6045. ISSN: 00223719. DOI: [10.1088/0022-3719/17/33/015](https://doi.org/10.1088/0022-3719/17/33/015) (cit. on p. 39).
- Cairns-Smith, A. G. (G. (1998). *Evolving the mind : on the nature of matter and the origin of consciousness*. Cambridge University Press, p. 329. ISBN: 978-0521637558 (cit. on p. 1).
- Campbell, D. K., Flach, S., and Kivshar, Y. S. (2004). “Localizing energy through non-linearity and discreteness”. In: *Physics Today* 57 (1), pp. 43–49. ISSN: 00319228. DOI: [10.1063/1.1650069](https://doi.org/10.1063/1.1650069) (cit. on p. 42).
- Cheuk, L. W., Sommer, A. T., Hadzibabic, Z., Yefsah, T., Bakr, W. S., and Zwierlein, M. W. (2012). “Spin-injection spectroscopy of a spin-orbit coupled Fermi gas”. In: *Physical Review Letters* 109 (9), pp. 1–5. ISSN: 00319007. DOI: [10.1103/PhysRevLett.109.095302](https://doi.org/10.1103/PhysRevLett.109.095302) (cit. on p. 43).
- Chevy, F., Madison, K. W., and Dalibard, J. (2000). “Measurement of the angular momentum of a rotating Bose-Einstein condensate”. In: *Physical Review Letters* 85 (11), pp. 2223–2227. ISSN: 00319007. DOI: [10.1103/PhysRevLett.85.2223](https://doi.org/10.1103/PhysRevLett.85.2223) (cit. on p. 14).
- Cohen-Tannoudji, C. N. (1998). “Nobel Lecture: Manipulating atoms with photons”. In: *Reviews of Modern Physics* 70 (3), pp. 707–719. ISSN: 0034-6861. DOI: [10.1103/RevModPhys.70.707](https://doi.org/10.1103/RevModPhys.70.707). URL: <https://link.aps.org/doi/10.1103/RevModPhys.70.707> (cit. on p. 36).
- Cohen-Tannoudji, C. N., Diu, B., and Laloe, F. (1977). *Quantum Mechanics*. John Wiley and Sons, Ltd (cit. on p. 65).
- Dalfovo, F., Giorgini, S., Pitaevskii, L. P., and Stringari, S. (1998). “Theory of Bose-Einstein condensation in trapped gases”. In: *Reviews of Modern Physics* 71 (3), pp. 463–512.

- ISSN: 0034-6861. DOI: [10.1103/RevModPhys.71.463](https://doi.org/10.1103/RevModPhys.71.463). URL: <http://arxiv.org/abs/cond-mat/9806038><http://dx.doi.org/10.1103/RevModPhys.71.463> (cit. on p. 35).
- Davis, K. B., Mewes, M. O., Andrews, M. R., Druten, N. J. V., Durfee, D. S., Kurn, D. M., and Ketterle, W. (1995). “Bose-Einstein condensation in a gas of sodium atoms”. In: *Physical Review Letters* 75 (22), pp. 3969–3973. ISSN: 00319007. DOI: [10.1103/PhysRevLett.75.3969](https://doi.org/10.1103/PhysRevLett.75.3969) (cit. on pp. 1, 35).
- Denschlag, J. (2000). “Generating solitons by phase engineering of a Bose-Einstein condensate”. In: *Science* 287 (5450), pp. 97–101. ISSN: 00368075. DOI: [10.1126/science.287.5450.97](https://doi.org/10.1126/science.287.5450.97) (cit. on p. 14).
- Descartes, R. (1641). *Meditations on First Philosophy* (cit. on p. 1).
- Dresselhaus, G. (1955). “Spin-Orbit Coupling Effects in Zinc Blende Structures”. In: *Phys.Rev.* 100 (2), pp. 580–586. ISSN: 0031-899X. DOI: [10.1103/PhysRev.100.580](https://doi.org/10.1103/PhysRev.100.580). URL: <http://dx.doi.org/10.1103/PhysRev.100.580><http://arxiv.org/abs/cond-mat/9806038> (cit. on p. 39).
- Einstein, A. (1925a). “Quantentheorie des einatomigen idealen Gases”. In: *Sitzungsberichte der Preussischen Akademie der Wissenschaften* XXII. DOI: <https://doi.org/10.1002/3527608958.ch27> (cit. on p. 5).
- Einstein, A. (1925b). “Quantentheorie des einatomigen idealen Gases - Zweite Abhandlung”. In: *Sitzungsberichte der Preussischen Akademie der Wissenschaften* S, pp. 3–10. DOI: <https://doi.org/10.1002/3527608958.ch28> (cit. on pp. 1, 6).
- Einstein, A. (2015). *On the Quantum Theory of the Ideal Gas*. Ed. by D. K. Buchwald, I. József, R. Ze’ev, T. Sauer, and O. Moses (cit. on p. 13).
- Fabbri, N., Clément, D., Fallani, L., Fort, C., Modugno, M., Stam, K. M. V. D., and Inguscio, M. (2009). “Excitations of Bose-Einstein condensates in a one-dimensional periodic potential”. In: *Physical Review A - Atomic, Molecular, and Optical Physics* 79 (4). ISSN: 10502947. DOI: [10.1103/PhysRevA.79.043623](https://doi.org/10.1103/PhysRevA.79.043623) (cit. on p. 14).
- Feynman, R. P. (1982). “Simulating physics with computers”. In: *International Journal of Theoretical Physics* 21 (6-7), pp. 467–488. ISSN: 00207748. DOI: [10.1007/BF02650179](https://doi.org/10.1007/BF02650179) (cit. on p. 35).
- Fisher, M. P., Weichman, P. B., Grinstein, G., and Fisher, D. S. (1989a). “Boson localization and the superfluid-insulator transition”. In: *Physical Review B* 40 (1), pp. 546–570. ISSN: 01631829. DOI: [10.1103/PhysRevB.40.546](https://doi.org/10.1103/PhysRevB.40.546) (cit. on p. 30).
- Fisher, M. P., Weichman, P. B., Grinstein, G., and Fisher, D. S. (1989b). “Boson localization and the superfluid-insulator transition”. In: *Physical Review B* 40 (1), pp. 546–570. ISSN: 01631829. DOI: [10.1103/PhysRevB.40.546](https://doi.org/10.1103/PhysRevB.40.546) (cit. on p. 38).

- Fröhlich, H. (1968a). “Bose condensation of strongly excited longitudinal electric modes”. In: *Physics Letters A* 26 (9), pp. 402–403. ISSN: 03759601. DOI: [10.1016/0375-9601\(68\)90242-9](https://doi.org/10.1016/0375-9601(68)90242-9) (cit. on pp. 18, 21).
- Fröhlich, H. (1968b). “Long-range coherence and energy storage in biological systems”. In: *International Journal of Quantum Chemistry* 2 (5), pp. 641–649. ISSN: 1097461X. DOI: [10.1002/qua.560020505](https://doi.org/10.1002/qua.560020505) (cit. on pp. xxi, 1, 18, 21).
- Gardiner, C. W., Anglin, J. R., and Fudge, T. I. A. (2002). “The stochastic Gross-Pitaevskii equation”. In: *Journal of Physics B: Atomic, Molecular and Optical Physics J. Phys. B: At. Mol. Opt. Phys* 35, pp. 1555–1582 (cit. on p. 12).
- Gardiner, C. W. and Davis, M. J. (2003). “The stochastic Gross-Pitaevskii equation: II”. In: *J. Phys. B: At. Mol. Opt. Phys* 36, pp. 4731–4753 (cit. on p. 12).
- Gardiner, C. W., Zoller, P., Ballagh, R. J., and Davis, M. J. (1997). “Kinetics of bose-einstein condensation in a trap”. In: *Physical Review Letters* 79 (10), pp. 1793–1796. ISSN: 10797114. DOI: [10.1103/PhysRevLett.79.1793](https://doi.org/10.1103/PhysRevLett.79.1793) (cit. on p. 8).
- Gerlach, W. and Stern, O. (1922). “Der experimentelle Nachweis der Richtungsquantelung im Magnetfeld”. In: *Zeitschrift für Physik* 9 (1), pp. 349–352. ISSN: 14346001. DOI: [10.1007/BF01326983](https://doi.org/10.1007/BF01326983) (cit. on p. 69).
- Giamarchi, T., Rüegg, C., and Tchernyshyov, O. (2008). “Bose-Einstein condensation in magnetic insulators”. In: *Nature Physics* 4 (3), pp. 198–204. ISSN: 17452473. DOI: [10.1038/nphys893](https://doi.org/10.1038/nphys893) (cit. on p. 19).
- Gligorić, G., Maluckov, A., Hadžievski, L., Flach, S., and Malomed, B. A. (2016). “Nonlinear localized flat-band modes with spin-orbit coupling”. In: *Physical Review B* 94 (14), pp. 1–8. ISSN: 24699969. DOI: [10.1103/PhysRevB.94.144302](https://doi.org/10.1103/PhysRevB.94.144302) (cit. on pp. xxi, 2, 44, 45, 46, 55).
- Goldman, N., Juzeliunas, G., Öhberg, P., and Spielman, I. B. (2014). “Light-induced gauge fields for ultracold atoms”. In: *Reports on Progress in Physics* 77 (12). ISSN: 00344885. DOI: [10.1088/0034-4885/77/12/126401](https://doi.org/10.1088/0034-4885/77/12/126401) (cit. on p. 39).
- Goldman, N., Kubasiak, A., Bermudez, A., Gaspard, P., Lewenstein, M., and Martin-Delgado, M. A. (2009). “Non-Abelian Optical Lattices: Anomalous Quantum Hall Effect and Dirac Fermions”. In: *Physical Review Letters* 103 (3), pp. 2–5. ISSN: 00319007. DOI: [10.1103/PhysRevLett.103.035301](https://doi.org/10.1103/PhysRevLett.103.035301) (cit. on p. 35).
- Gopalsamy, K. and Rai, B. (1988). “Stability Analysis of Synchronous Oscillations in a Weakly Coupled Integrodifferential System”. In: *Journal of Mathematical Analysis and Applications* 136, pp. 369–382 (cit. on p. 26).

- Greentree, A. D., Tahan, C., Cole, J. H., and Hollenberg, L. C. (Nov. 2006). “Quantum phase transitions of light”. In: *Nature Physics* 2 (12), pp. 856–861. ISSN: 17452481. DOI: [10.1038/nphys466](https://doi.org/10.1038/nphys466). URL: <https://www.nature.com/articles/nphys466> (cit. on p. 30).
- Greiner, M., Mandel, O., Esslinger, T., Hansch, T. W., and Bloch, I. (2002). “Quantum phase transition from a superfluid to a Mott insulator in a gas of ultracold atoms”. In: *Nature* 415, p. 39 (cit. on pp. 30, 35, 38).
- Grusdt, F., Li, T., Bloch, I., and Demler, E. (2017). “Tunable spin-orbit coupling for ultracold atoms in two-dimensional optical lattices”. In: *Physical Review A* 95 (6), pp. 1–10. ISSN: 24699934. DOI: [10.1103/PhysRevA.95.063617](https://doi.org/10.1103/PhysRevA.95.063617) (cit. on p. 38).
- Haase, T. A., White, D. H., Brown, D. J., Herrera, I., and Hoogerland, M. D. (Nov. 2017). “A versatile apparatus for two-dimensional atomtronic quantum simulation”. In: *Review of Scientific Instruments* 88 (11), p. 113102. ISSN: 10897623. DOI: [10.1063/1.5009584](https://doi.org/10.1063/1.5009584). URL: <http://aip.scitation.org/doi/10.1063/1.5009584> (cit. on p. 47).
- Haljan, P. C., Coddington, I., Engels, P., and Cornell, E. A. (2001). “Driving bose-einstein-condensate vorticity with a rotating normal cloud”. In: *Physical Review Letters* 87 (21), pp. 210403-1-210403-4. ISSN: 10797114. DOI: [10.1103/PhysRevLett.87.210403](https://doi.org/10.1103/PhysRevLett.87.210403) (cit. on p. 14).
- Hasan, M. Z. and Kane, C. L. (2010). “Colloquium: Topological insulators”. In: *Reviews of Modern Physics* 82 (4), pp. 3045–3067. ISSN: 00346861. DOI: [10.1103/RevModPhys.82.3045](https://doi.org/10.1103/RevModPhys.82.3045) (cit. on p. 35).
- Hootman, S. R. and Ernst, S. A. (1988). *Estimation of Na,K-Pump Numbers and Turnover in Intact Cells with [^3H]Ouabain* (cit. on p. 24).
- Huber, S. D. and Altman, E. (2010). “Bose condensation in flat bands”. In: *Physical Review B - Condensed Matter and Materials Physics* 82 (18), pp. 1–16. ISSN: 10980121. DOI: [10.1103/PhysRevB.82.184502](https://doi.org/10.1103/PhysRevB.82.184502) (cit. on p. 43).
- Inguscio, M., S. Stringari, and C. E. Wieman, eds. (1998). *Bose-Einstein Condensation in Atomic Gases, Proceedings of the International School of Physics “Enrico Fermi”*. IOS Press. ISBN: 9780967335551. URL: <https://books.google.de/books?id=OJH1SU0n4dgC> (cit. on p. 35).
- Jaksch, D., Bruder, C., Cirac, J. I., Gardiner, C. W., and Zoller, P. (1998). “Cold bosonic atoms in optical lattices”. In: *Physical Review Letters* 81 (15), pp. 3108–3111. ISSN: 10797114. DOI: [10.1103/PhysRevLett.81.3108](https://doi.org/10.1103/PhysRevLett.81.3108) (cit. on pp. 28, 29).
- Jessen, P. S., Gerz, C., Lett, P. D., Phillips, W. D., Rolston, S. L., Spreew, R. J. C., and Westbrook, C. I. (1992). “Observation of Quantized Motion of Rb Atoms in an Optical Field”. In: *Physical Review Letters* 69 (1), pp. 49–52 (cit. on p. 37).

- Ji, A. C., Liu, W. M., Song, J. L., and Zhou, F. (2008). “Dynamical creation of fractionalized vortices and vortex lattices”. In: *Physical Review Letters* 101 (1), pp. 2–5. ISSN: 00319007. DOI: [10.1103/PhysRevLett.101.010402](https://doi.org/10.1103/PhysRevLett.101.010402) (cit. on p. 14).
- Jin, D. S., Ensher, J. R., Matthews, M. R., Wieman, C. E., and Cornell, E. A. (1996). “Collective excitations of a Bose-Einstein condensate in a dilute gas”. In: *Physical Review Letters* 77 (3), p. 420. DOI: [10.1142/9789812813787_0063](https://doi.org/10.1142/9789812813787_0063) (cit. on p. 22).
- Jo, G.-B., Guzman, J., Thomas, C. K., Hosur, P., Vishwanath, A., and Stamper-Kurn, D. M. (2011). “Ultracold Atoms in a Tunable Optical Kagome Lattice”. In: *Physical Review Letters* 045305 (January), pp. 1–5. ISSN: 0031-9007. DOI: [10.1103/PhysRevLett.108.045305](https://doi.org/10.1103/PhysRevLett.108.045305). URL: <http://arxiv.org/abs/1109.1591> <http://dx.doi.org/10.1103/PhysRevLett.108.045305> (cit. on p. 38).
- Kartashov, Y. V., Konotop, V. V., Zezyulin, D. A., and Torner, L. (2016). “Dynamic localization in optical and Zeeman lattices in the presence of spin-orbit coupling”. In: *Physical Review A* 94 (6), pp. 1–6. ISSN: 24699934. DOI: [10.1103/PhysRevA.94.063606](https://doi.org/10.1103/PhysRevA.94.063606) (cit. on p. 38).
- Kastrup, H. A. (2006). “Quantization of the canonically conjugate pair angle and orbital angular momentum”. In: *Physical Review A - Atomic, Molecular, and Optical Physics* 73 (5). ISSN: 10502947. DOI: [10.1103/PhysRevA.73.052104](https://doi.org/10.1103/PhysRevA.73.052104) (cit. on p. 30).
- Ketterle, W., Durfee, D., and Stamper-Kurn, D. (1999). *Making, Probing and understanding Bose-Einstein condensates*. Ed. by M. Inguscio, S. Stringari, and C. E. Wieman (cit. on p. 8).
- Klaers, J., Schmitt, J., Vewinger, F., and Weitz, M. (2010). “Bose-Einstein condensation of photons in an optical microcavity”. In: *Nature* 468 (7323), pp. 545–548. ISSN: 00280836. DOI: [10.1038/nature09567](https://doi.org/10.1038/nature09567) (cit. on p. 19).
- Krämer, S., Plankensteiner, D., Ostermann, L., and Ritsch, H. (2018). “QuantumOptics.jl: A Julia framework for simulating open quantum systems”. In: *Computer Physics Communications* 227, pp. 109–116. DOI: [10.17632/3696r5jhm4.1](https://doi.org/10.17632/3696r5jhm4.1). URL: <http://dx.doi.org/10.17632/3696r5jhm4.1> (cit. on pp. 30, 53).
- Kuramoto, Y. and Nakao, H. (2019). “On the concept of dynamical reduction: The case of coupled oscillators”. In: *Philosophical Transactions of the Royal Society A: Mathematical, Physical and Engineering Sciences* 377 (2160). ISSN: 1364503X. DOI: [10.1098/rsta.2019.0041](https://doi.org/10.1098/rsta.2019.0041) (cit. on p. 21).
- Larson, J., Martikainen, J.-P., Collin, A., and Sjöqvist, E. (Oct. 2010). “Spin-orbit-coupled Bose-Einstein condensate in a tilted optical lattice”. In: *Physical Review A* 82 (4),

- p. 043620. ISSN: 1050-2947. DOI: [10.1103/PhysRevA.82.043620](https://doi.org/10.1103/PhysRevA.82.043620). URL: <https://link.aps.org/doi/10.1103/PhysRevA.82.043620> (cit. on p. 38).
- Leggett, A. J. (2001). “Bose-Einstein condensation in the alkali gases: Some fundamental concepts”. In: *Reviews of Modern Physics* 73 (2), pp. 307–356. ISSN: 00346861. DOI: [10.1103/RevModPhys.73.307](https://doi.org/10.1103/RevModPhys.73.307) (cit. on p. 35).
- Lewenstein, M., Sanpera, A., Ahufinger, V., Damski, B., Sen, A., and Sen, U. (2007). “Ultracold atomic gases in optical lattices: Mimicking condensed matter physics and beyond”. In: *Advances in Physics* 56 (2), pp. 243–379. ISSN: 00018732. DOI: [10.1080/00018730701223200](https://doi.org/10.1080/00018730701223200) (cit. on pp. 37, 38).
- Leykam, D., Flach, S., Bahat-Treidel, O., and Desyatnikov, A. S. (2013). “Flat band states: Disorder and nonlinearity”. In: *Physical Review B - Condensed Matter and Materials Physics* 88 (22), pp. 26–28. ISSN: 10980121. DOI: [10.1103/PhysRevB.88.224203](https://doi.org/10.1103/PhysRevB.88.224203) (cit. on p. 44).
- Li, L., Li, Z., Malomed, B. A., Mihalache, D., and Liu, W. M. (2005). “Exact soliton solutions and nonlinear modulation instability in spinor Bose-Einstein condensates”. In: *Physical Review A - Atomic, Molecular, and Optical Physics* 72 (3), pp. 1–11. ISSN: 10502947. DOI: [10.1103/PhysRevA.72.033611](https://doi.org/10.1103/PhysRevA.72.033611) (cit. on p. 18).
- Liang, M., Tian, J., Liu, L., Pierre, S., Liu, J., Shapiro, J., and Xie, Z. J. (Apr. 2007). “Identification of a pool of non-pumping Na/K-ATPase”. In: *The Journal of biological chemistry* 282 (14), pp. 10585–10593. ISSN: 0021-9258. DOI: [10.1074/JBC.M609181200](https://doi.org/10.1074/JBC.M609181200). URL: <https://pubmed.ncbi.nlm.nih.gov/17296611/> (cit. on p. 24).
- Liang, Z. X., Zhang, Z. D., and Liu, W. M. (2005). “Dynamics of a bright soliton in Bose-Einstein condensates with time-dependent atomic scattering length in an expulsive parabolic potential”. In: *Physical Review Letters* 94 (5), pp. 18–21. ISSN: 00319007. DOI: [10.1103/PhysRevLett.94.050402](https://doi.org/10.1103/PhysRevLett.94.050402) (cit. on p. 14).
- Lieb, E. H. (1989). “Two theorems on the Hubbard model”. In: *Physical Review Letters* 62 (10), pp. 1201–1204. ISSN: 00319007. DOI: [10.1103/PhysRevLett.62.1201](https://doi.org/10.1103/PhysRevLett.62.1201) (cit. on p. 41).
- Lin, Y. J., Compton, R. L., Jiménez-García, K., Phillips, W. D., Porto, J. V., and Spielman, I. B. (2011). “A synthetic electric force acting on neutral atoms”. In: *Nature Physics* 7 (7), pp. 531–534. ISSN: 17452473. DOI: [10.1038/nphys1954](https://doi.org/10.1038/nphys1954). URL: <http://dx.doi.org/10.1038/nphys1954> (cit. on p. 39).
- Lin, Y. J., Jiménez-García, K., and Spielman, I. B. (2011). “Spin-orbit-coupled Bose-Einstein condensates”. In: *Nature* 471 (7336), pp. 83–86. ISSN: 00280836. DOI: [10.1038/nature09887](https://doi.org/10.1038/nature09887) (cit. on p. 39).

- Liu, X. J., Borunda, M. F., Liu, X., and Sinova, J. (2009). “Effect of induced spin-orbit coupling for atoms via laser fields”. In: *Physical Review Letters* 102 (4), pp. 1–4. ISSN: 00319007. DOI: [10.1103/PhysRevLett.102.046402](https://doi.org/10.1103/PhysRevLett.102.046402) (cit. on p. 39).
- Maimaiti, W., Andreanov, A., Park, H. C., Gendelman, O., and Flach, S. (2017). “Compact localized states and flat-band generators in one dimension”. In: *Physical Review B* 95 (11), pp. 1–8. ISSN: 24699969. DOI: [10.1103/PhysRevB.95.115135](https://doi.org/10.1103/PhysRevB.95.115135) (cit. on p. 44).
- Masson, S. (2019). “Many-body cavity QED”. University of Auckland (cit. on p. 52).
- Matthews, M. R., Anderson, B. P., Haljan, P. C., Hall, D. S., Wieman, C. E., and Cornell, E. A. (1999). “Vortices in a Bose-Einstein condensate”. In: *Physical Review Letters* 83 (13), p. 2498. DOI: [10.1142/9789812813787_0077](https://doi.org/10.1142/9789812813787_0077) (cit. on p. 22).
- McFadden, J. and Al-Khalili, J. (2018). “The origins of quantum biology”. In: *Proceedings of the Royal Society A: Mathematical, Physical and Engineering Sciences* 474, p. 20180674. DOI: [10.1098/rspa.2018.0674](https://doi.org/10.1098/rspa.2018.0674) (cit. on pp. 1, 18).
- McPhail, A. V. H. and Hoogerland, M. D. (Oct. 2021). “A Bose–Einstein condensate is a Bose condensate in the laboratory ground state”. In: *Proceedings of the Royal Society A: Mathematical, Physical and Engineering Sciences* 477 (2254). ISSN: 1364-5021. DOI: [10.1098/rspa.2021.0465](https://doi.org/10.1098/rspa.2021.0465). URL: <https://royalsocietypublishing.org/doi/abs/10.1098/rspa.2021.0465> (cit. on p. xix).
- McPhail, A. V. H. (2009). *From a classical neuroscience towards a quantum theory of mind and consciousness*. DOI: [10.51669/NatPhil-002-1](https://doi.org/10.51669/NatPhil-002-1) (cit. on p. 2).
- Mielke, A. (1991). “Ferromagnetism in the Hubbard-Model on Line Graphs and Further Considerations”. In: *Journal of Physics a-Mathematical and General* 24 (14), pp. 3311–3321 (cit. on p. 41).
- Miesner, H. (1998). “Bosonic Stimulation in the Formation of a Bose-Einstein Condensate”. In: *Science* 279 (5353), pp. 1005–1007. ISSN: 00368075. DOI: [10.1126/science.279.5353.1005](https://doi.org/10.1126/science.279.5353.1005) (cit. on pp. 8, 14, 18, 30, 32).
- Morsch, O. and Oberthaler, M. (2006). “Dynamics of Bose-Einstein condensates in optical lattices”. In: *Reviews of Modern Physics* 78 (1), pp. 179–215. ISSN: 00346861. DOI: [10.1103/RevModPhys.78.179](https://doi.org/10.1103/RevModPhys.78.179) (cit. on pp. 38, 42).
- Mukherjee, S., Spracklen, A., Choudhury, D., Goldman, N., Öhberg, P., Andersson, E., and Thomson, R. R. (2015). “Observation of a Localized Flat-Band State in a Photonic Lieb Lattice”. In: *Physical Review Letters* 114 (24), pp. 1–5. ISSN: 10797114. DOI: [10.1103/PhysRevLett.114.245504](https://doi.org/10.1103/PhysRevLett.114.245504) (cit. on p. 44).
- Mukherjee, S. and Thomson, R. R. (2015). “Observation of localized flat-band modes in a quasi-one-dimensional photonic rhombic lattice”. In: *Optics Letters* 40 (23), pp. 5443–

5446. ISSN: 15394794. DOI: [10.1364/OL.40.005443](https://doi.org/10.1364/OL.40.005443). URL: <http://arxiv.org/abs/1509.08445><http://dx.doi.org/10.1364/OL.40.005443> (cit. on p. 44).
- Nakao, H. (2016). “Phase reduction approach to synchronisation of nonlinear oscillators”. In: *Contemporary Physics* 57 (2), pp. 188–214. ISSN: 13665812. DOI: [10.1080/00107514.2015.1094987](https://doi.org/10.1080/00107514.2015.1094987) (cit. on p. 26).
- New, G. (2011). *Introduction to nonlinear optics*. Vol. 9780521877. Cambridge University Press, pp. 1–257. ISBN: 9780511975851. DOI: [10.1017/CBO9780511975851](https://doi.org/10.1017/CBO9780511975851) (cit. on p. 1).
- Osterloh, K., Baig, M., Santos, L., Zoller, P., and Lewenstein, M. (2005). “Cold atoms in non-abelian gauge potentials: From the hofstadter "moth" to lattice gauge theory”. In: *Physical Review Letters* 95 (1), pp. 1–4. ISSN: 00319007. DOI: [10.1103/PhysRevLett.95.010403](https://doi.org/10.1103/PhysRevLett.95.010403) (cit. on p. 39).
- Ostrovskaya, E. A. and Kivshar, Y. S. (2003). “Matter-Wave Gap Solitons in Atomic Band-Gap Structures”. In: *Physical Review Letters* 90 (16), p. 4. ISSN: 10797114. DOI: [10.1103/PhysRevLett.90.160407](https://doi.org/10.1103/PhysRevLett.90.160407) (cit. on p. 42).
- Pan, J. S., Zhang, W., Yi, W., and Guo, G. C. (2016). “Bose-Einstein condensate in an optical lattice with Raman-assisted two-dimensional spin-orbit coupling”. In: *Physical Review A* 94 (4). ISSN: 24699934. DOI: [10.1103/PhysRevA.94.043619](https://doi.org/10.1103/PhysRevA.94.043619) (cit. on p. 38).
- Parameswaran, S. A., Roy, R., and Sondhi, S. L. (2013). “Fractional quantum Hall physics in topological flat bands”. In: *Comptes Rendus Physique* 14 (9-10), pp. 816–839. ISSN: 16310705. DOI: [10.1016/j.crhy.2013.04.003](https://doi.org/10.1016/j.crhy.2013.04.003). URL: <http://dx.doi.org/10.1016/j.crhy.2013.04.003> (cit. on p. 43).
- Pauli, W. (1940). “The connection between spin and statistics”. In: *Physical Review* 58 (8), pp. 716–722. ISSN: 0031899X. DOI: [10.1103/PhysRev.58.716](https://doi.org/10.1103/PhysRev.58.716) (cit. on pp. 3, 18, 69).
- Pegg, D. T. and Barnett, S. M. (1989). “Phase properties of the quantized single-mode electromagnetic field”. In: *Physical Review A* 39 (4), p. 1665 (cit. on p. 30).
- Pethick, C. J. and Smith, H. (2008). *Bose-Einstein condensation in dilute gases*. Vol. 9780521846, pp. 1–569. ISBN: 9780511802850. DOI: [10.1017/CBO9780511802850](https://doi.org/10.1017/CBO9780511802850) (cit. on pp. 7, 8, 10, 35).
- Pitaevskii, L. and Stringari, S. (2016). *Quantum Mixtures and Spinor Gases*. DOI: [10.1093/acprof:oso/9780198758884.001.0001](https://doi.org/10.1093/acprof:oso/9780198758884.001.0001). URL: <https://oxford-universitypressscholarship-com/view/10.1093/acprof:oso/9780198758884.001.0001/acprof-9780198758884-chapter-21> (cit. on p. 52).
- Pitaevskii, L. and Stringari, S. (2003). *Bose-Einstein Condensation*. Vol. 116. Clarendon Press, p. 492. ISBN: 0198507194 (cit. on pp. 1, 7, 18, 35).

- Raithel, G., Birkel, G., Kastberg, A., Phillips, W. D., and Rolston, S. L. (1997). “Cooling and localization dynamics in optical lattices”. In: *Physical Review Letters* 78 (4), pp. 630–633. ISSN: 10797114. DOI: [10.1103/PhysRevLett.78.630](https://doi.org/10.1103/PhysRevLett.78.630) (cit. on p. 38).
- Ramírez, C. and Wang, C. (2009). “Bosonic nature of collective Cooper pairs”. In: *Physics Letters, Section A: General, Atomic and Solid State Physics* 373 (2), pp. 269–271. ISSN: 03759601. DOI: [10.1016/j.physleta.2008.11.006](https://doi.org/10.1016/j.physleta.2008.11.006) (cit. on p. 19).
- Röntgen, M., Morfonios, C. V., and Schmelcher, P. (2018). “Compact localized states and flat bands from local symmetry partitioning”. In: *Physical Review B* 97 (3), pp. 1–12. ISSN: 24699969. DOI: [10.1103/PhysRevB.97.035161](https://doi.org/10.1103/PhysRevB.97.035161) (cit. on p. 44).
- Ruostekoski, J. (2009). “Optical kagome lattice for ultracold atoms with nearest neighbor interactions”. In: *Physical Review Letters* 103 (8), pp. 1–4. ISSN: 00319007. DOI: [10.1103/PhysRevLett.103.080406](https://doi.org/10.1103/PhysRevLett.103.080406) (cit. on p. 38).
- Ruseckas, J., Juzeliunas, G., Öhberg, P., and Fleischhauer, M. (2005). “Non-abelian gauge potentials for ultracold atoms with degenerate dark states”. In: *Physical Review Letters* 95 (1), pp. 1–4. ISSN: 00319007. DOI: [10.1103/PhysRevLett.95.010404](https://doi.org/10.1103/PhysRevLett.95.010404) (cit. on p. 39).
- Sievers, A. J. and Takeno, S. (1988). “Intrinsic localized modes in anharmonic crystals”. In: *Physical Review Letters* 61 (8), pp. 970–973. ISSN: 00319007. DOI: [10.1103/PhysRevLett.61.970](https://doi.org/10.1103/PhysRevLett.61.970) (cit. on p. 42).
- Slot, M. R., Gardenier, T. S., Jacobse, P. H., Miert, G. C. V., Kempkes, S. N., Zevenhuizen, S. J., Smith, C. M., Vanmaekelbergh, D., and Swart, I. (2017). “Experimental realization and characterization of an electronic Lieb lattice”. In: *Nature Physics* 13 (7), pp. 672–676. ISSN: 17452481. DOI: [10.1038/nphys4105](https://doi.org/10.1038/nphys4105) (cit. on p. 38).
- Sørensen, A. S., Demler, E., and Lukin, M. D. (2005). “Fractional quantum hall states of atoms in optical lattices”. In: *Physical Review Letters* 94 (8), pp. 1–4. ISSN: 00319007. DOI: [10.1103/PhysRevLett.94.086803](https://doi.org/10.1103/PhysRevLett.94.086803) (cit. on p. 35).
- Spielman, I. B. (2009). “Raman processes and effective gauge potentials”. In: *Physical Review A - Atomic, Molecular, and Optical Physics* 79 (6), pp. 1–7. ISSN: 10502947. DOI: [10.1103/PhysRevA.79.063613](https://doi.org/10.1103/PhysRevA.79.063613) (cit. on p. 39).
- Stamper-Kurn, D. M., Miesner, H. J., Inouye, S., Andrews, M. R., and Ketterle, W. (1998). “Collisionless and hydrodynamic excitations of a Bose-Einstein condensate”. In: *Physical Review Letters* 81 (3), p. 500. ISSN: 0031-9007. DOI: [10.1103/PhysRevLett.81.500](https://doi.org/10.1103/PhysRevLett.81.500) (cit. on p. 14).
- Stanescu, T. D., Anderson, B., and Galitski, V. (2008). “Spin-orbit coupled Bose-Einstein condensates”. In: *Physical Review A - Atomic, Molecular, and Optical Physics* 78 (2), pp. 1–10. ISSN: 10502947. DOI: [10.1103/PhysRevA.78.023616](https://doi.org/10.1103/PhysRevA.78.023616) (cit. on p. 39).

- Stanescu, T. D., Zhang, C., and Galitski, V. (2007). “Nonequilibrium spin dynamics in a trapped fermi gas with effective spin-orbit interactions”. In: *Physical Review Letters* 99 (11), pp. 1–4. ISSN: 00319007. DOI: [10.1103/PhysRevLett.99.110403](https://doi.org/10.1103/PhysRevLett.99.110403) (cit. on p. 39).
- Steel, M. J., Olsen, M. K., Plimak, L. I., Drummond, P. D., Tan, S. M., Collett, M. J., Walls, D. F., and Graham, R. (1998). “Dynamical quantum noise in trapped Bose-Einstein condensates”. In: *Physical Review A - Atomic, Molecular, and Optical Physics* 58 (6), pp. 4824–4835. ISSN: 10941622. DOI: [10.1103/PhysRevA.58.4824](https://doi.org/10.1103/PhysRevA.58.4824) (cit. on p. 11).
- Strawson, G. (2010). *Mental reality*. MIT Press, p. 373. ISBN: 9780262193528 (cit. on p. 1).
- Strecker, K. E., Partridge, G. B., Truscott, A. G., and Hulet, R. G. (2002). “Formation and propagation of matter-wave soliton trains”. In: *Nature* 417 (6885), pp. 150–153. ISSN: 00280836. DOI: [10.1038/nature747](https://doi.org/10.1038/nature747) (cit. on p. 14).
- Struck, J., Olschläger, C., Weinberg, M., Hauke, P., Simonet, J., Eckardt, A., Lewenstein, M., Sengstock, K., and Windpassinger, P. (2012). “Tunable gauge potential for neutral and spinless particles in driven optical lattices”. In: *Physical Review Letters* 108 (22), pp. 1–5. ISSN: 00319007. DOI: [10.1103/PhysRevLett.108.225304](https://doi.org/10.1103/PhysRevLett.108.225304) (cit. on p. 38).
- Sun, K., Gu, Z., Katsura, H., and Sarma, S. D. (2011). “Nearly flatbands with nontrivial topology”. In: *Physical Review Letters* 106 (23), pp. 1–4. ISSN: 00319007. DOI: [10.1103/PhysRevLett.106.236803](https://doi.org/10.1103/PhysRevLett.106.236803) (cit. on p. 43).
- Susskind, L. and Glogower, J. (1964). “Quantum mechanical phase and time operator”. In: *Physics* 1 (1), pp. 49–61. ISSN: 0554-128X. DOI: [10.1103/physicsphysiquefizika.1.49](https://doi.org/10.1103/physicsphysiquefizika.1.49) (cit. on p. 30).
- Sutherland, B. (1986). “Localization of electronic wave functions due to local topology”. In: *Physical Review B* 34 (8), pp. 5208–5211. ISSN: 01631829. DOI: [10.1103/PhysRevB.34.5208](https://doi.org/10.1103/PhysRevB.34.5208) (cit. on p. 41).
- T. W. Hemmerich, A. H. (1993). “Two-Dimensional Atomic Crystal Bound by Light”. In: *Physical Review Letters* 70 (4), pp. 410–413 (cit. on p. 37).
- Taie, S., Ozawa, H., Ichinose, T., Nishio, T., Nakajima, S., and Takahashi, Y. (2015). “Matter-Wave Localization and Delocalization of Ultracold Bosons in an Optical Lieb Lattice”. In: *Science Advances* 8502 (November), 1e1500854. ISSN: 2375-2548. DOI: [10.1126/sciadv.1500854](https://doi.org/10.1126/sciadv.1500854) (cit. on pp. 38, 44).
- Tasaki, H. (1992). “Ferromagnetism in the Hubbard models with degenerate single-electron ground states”. In: *Physical Review Letters* 69 (10), pp. 1608–1611. ISSN: 00319007. DOI: [10.1103/PhysRevLett.69.1608](https://doi.org/10.1103/PhysRevLett.69.1608) (cit. on p. 41).
- Ueda, M. (2010). *Fundamentals and New Frontiers of Bose-Einstein Condensation*. World Scientific (cit. on pp. 1, 4, 6).

- Verkerk, P., Lounis, B., Salomon, C., Cohen-Tannoudji, C., Courtois, J. Y., and Grynberg, G. (1992). “Dynamics and spatial order of cold cesium atoms in a periodic optical potential”. In: *Physical Review Letters* 68 (26), pp. 3861–3864. ISSN: 00319007. DOI: [10.1103/PhysRevLett.68.3861](https://doi.org/10.1103/PhysRevLett.68.3861) (cit. on p. 37).
- Vicencio, R. A., Cantillano, C., Morales-Inostroza, L., Real, B., Mejía-Cortés, C., Weimann, S., Szameit, A., and Molina, M. I. (2015). “Observation of Localized States in Lieb Photonic Lattices”. In: *Physical Review Letters* 114 (24), pp. 1–5. ISSN: 10797114. DOI: [10.1103/PhysRevLett.114.245503](https://doi.org/10.1103/PhysRevLett.114.245503) (cit. on p. 44).
- Walraven, J. T. M. (2019). *Elastic collisions in ultracold atomic gases - lectures* (cit. on p. 31).
- Weill, R., Bekker, A., Levit, B., and Fischer, B. (2019). “Bose–Einstein condensation of photons in an erbium–ytterbium co-doped fiber cavity”. In: *Nature Communications* 10 (1). ISSN: 20411723. DOI: [10.1038/s41467-019-08527-0](https://doi.org/10.1038/s41467-019-08527-0) (cit. on p. 19).
- Wen, L., Li, L., Li, Z. D., Song, S. W., Zhang, X. F., and Liu, W. M. (2011). “Matter rogue wave in Bose-Einstein condensates with attractive atomic interaction”. In: *European Physical Journal D* 64 (2-3), pp. 473–478. ISSN: 14346060. DOI: [10.1140/epjd/e2011-20485-4](https://doi.org/10.1140/epjd/e2011-20485-4) (cit. on p. 14).
- White, D. (2016). “Quantum Transport Experiments with Ultracold Atoms”. University of Auckland (cit. on p. 47).
- Witthaut, D. and Timme, M. (2014). “Kuramoto dynamics in Hamiltonian systems”. In: *Physical Review E - Statistical, Nonlinear, and Soft Matter Physics* 90 (3), p. 32917. ISSN: 15502376. DOI: [10.1103/PhysRevE.90.032917](https://doi.org/10.1103/PhysRevE.90.032917) (cit. on p. 28).
- Wu, C., Bergman, D., Balents, L., and Sarma, S. D. (2007). “Flat bands and wigner crystallization in the honeycomb optical lattice”. In: *Physical Review Letters* 99 (7), pp. 1–4. ISSN: 00319007. DOI: [10.1103/PhysRevLett.99.070401](https://doi.org/10.1103/PhysRevLett.99.070401) (cit. on p. 43).
- Wu, T. M. and Austin, S. J. (1981). “Fröhlich’s model of bose condensation in biological systems”. In: *Journal of Biological Physics* 9 (2), pp. 97–107. ISSN: 00920606. DOI: [10.1007/BF01987286](https://doi.org/10.1007/BF01987286) (cit. on p. 18).
- Wu, Z., Zhang, L., Sun, W., Xu, X. T., Wang, B. Z., Ji, S. C., Deng, Y., Chen, S., Liu, X. J., and Pan, J. W. (2016). “Realization of two-dimensional spin-orbit coupling for Bose-Einstein condensates”. In: *Science* 354 (6308), pp. 83–88. ISSN: 10959203. DOI: [10.1126/science.aaf6689](https://doi.org/10.1126/science.aaf6689) (cit. on p. 39).
- Yao, N. Y., Laumann, C. R., Gorshkov, A. V., Bennett, S. D., Demler, E., Zoller, P., and Lukin, M. D. (2012). “Topological flat bands from dipolar spin systems”. In: *Physical*

- Review Letters* 109 (26), pp. 1–5. ISSN: 00319007. DOI: [10.1103/PhysRevLett.109.266804](https://doi.org/10.1103/PhysRevLett.109.266804) (cit. on p. 43).
- Zeng, T. S., Zhu, W., and Sheng, D. N. (2017). “Two-component quantum Hall effects in topological flat bands”. In: *Physical Review B* 95 (12), pp. 1–8. ISSN: 24699969. DOI: [10.1103/PhysRevB.95.125134](https://doi.org/10.1103/PhysRevB.95.125134) (cit. on p. 44).
- Zhang, R., Garner, S. R., and Hau, L. V. (Dec. 2009). “Creation of long-term coherent optical memory via controlled nonlinear interactions in bose-einstein condensates”. In: *Physical Review Letters* 103 (23). ISSN: 00319007. DOI: [10.1103/PhysRevLett.103.233602](https://doi.org/10.1103/PhysRevLett.103.233602) (cit. on p. 61).
- Zhang, T. and Jo, G. B. (2015). “One-dimensional sawtooth and zigzag lattices for ultracold atoms”. In: *Scientific Reports* 5, pp. 1–7. ISSN: 20452322. DOI: [10.1038/srep16044](https://doi.org/10.1038/srep16044). URL: <http://dx.doi.org/10.1038/srep16044> (cit. on p. 38).
- Zhang, Y. and Zhang, C. (Feb. 2013). “Bose-Einstein condensates in spin-orbit-coupled optical lattices: Flat bands and superfluidity”. In: *PHYSICAL REVIEW A* 87 (2), pp. 2–6. ISSN: 1050-2947. DOI: [10.1103/PhysRevA.87.023611](https://doi.org/10.1103/PhysRevA.87.023611) (cit. on p. 43).
- Zinner, N. T. and Thøgersen, M. (2009). “Stability of a Bose-Einstein condensate with higher-order interactions near a Feshbach resonance”. In: *Physical Review A - Atomic, Molecular, and Optical Physics* 80 (2). ISSN: 10502947. DOI: [10.1103/PhysRevA.80.023607](https://doi.org/10.1103/PhysRevA.80.023607) (cit. on p. 18).